TEST-CASE: HPP Bannwil, Switzerland

Prepared by Ismail Albayrak[1,1], Stephan Kammerer[1], David Vetsch[1], Robert Boes[1], Armin Peter[2], Jeffry Tuhtan[3], Ulli Stoltz[4] and Carl Robert Kriewitz-Byun[5]

[1]VAW, ETH Zurich, [2]FCO, [3]TUT, [4]VOITH and [5]BKW

[1,1]Responsible person: albayrak@vaw.baug.ethz.ch

Updated on 30.10.2020.

Table of Contents

List of Figures

List of Tables

1. Description of the Test-Case

1.1. Description of the water bodies related to the HPP

The hydropower plant (HPP) Bannwil is located on river Aare in the community of Bannwil, some 46 km downstream of Lake of Biel. There are two upstream HPPs on the Aare River below Lake Biel, HPP Brügg at the lake outflow and HPP Flumenthal about 12 km from Bannwil (Figure 1). The river Aare is a 291 km long tributary of the Rhine and the longest river totally within Switzerland. The next HPP downstream is Wynau about 5.5 km from HPP Bannwil. There are in total 10 hydropower plants between Lake Biel and the junction with the Rhine river. The altitude of the lowest and highest points of this river reach are ca. 312 m asl and 429 m asl, respectively. The average altitude of the whole catchment amounts to 1060 m asl and the whole catchment area is 17687 km^2 (Fig. 1), of which 1.4 % are covered by glaciers. The Aare River passes through three major lakes: Lake of Brienz, Lake of Thun and Lake of Biel.

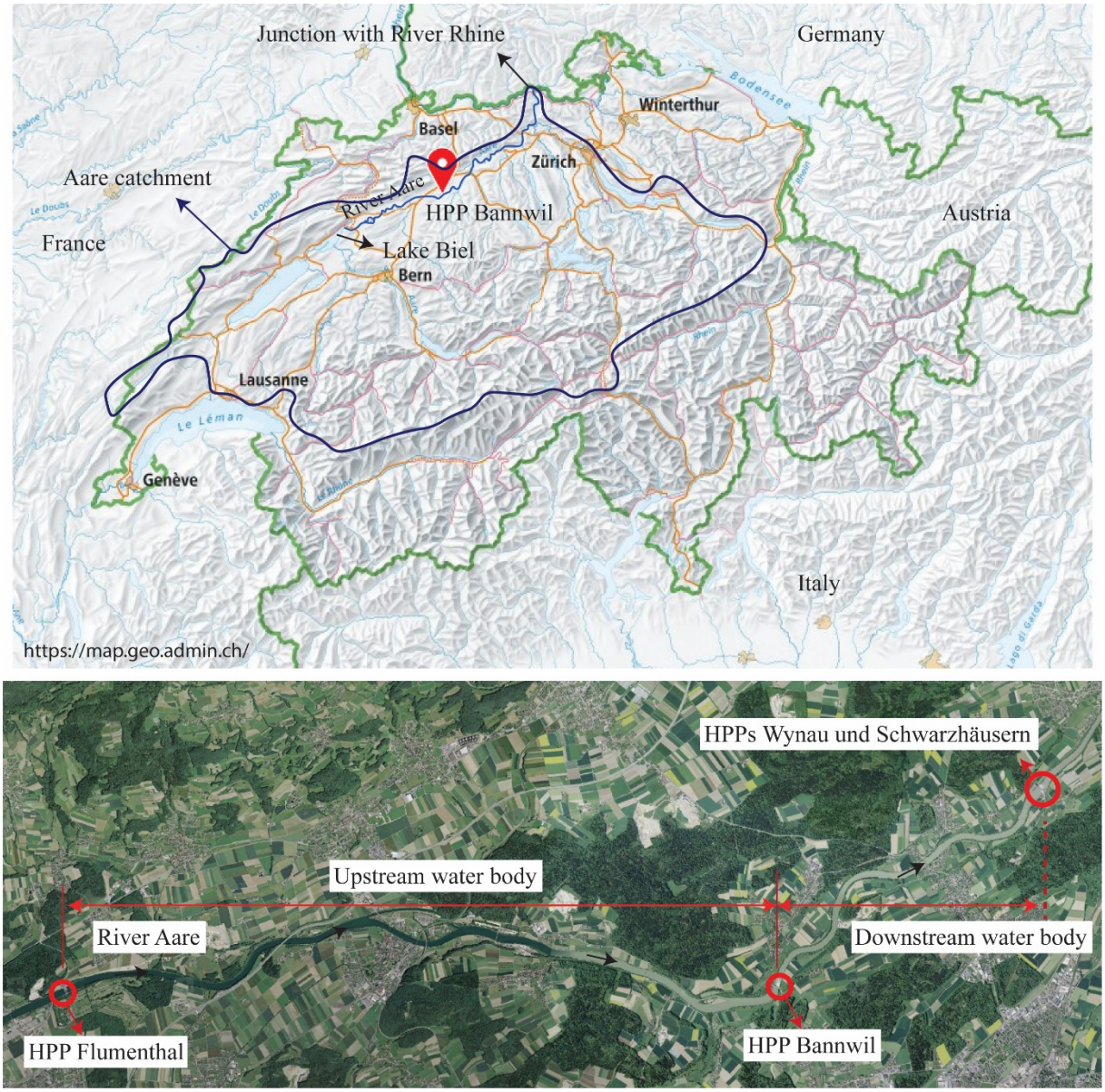

Figure 1: Water bodies related to the HPP Bannwil.

1.1.1. Hydrology of River Aare

On river Aare, the mean monthly discharge increases from February to June and then decreases from July to October (Fig. 2). The multi-year annual mean discharge amounts to 286 m^3/s (Fig. 2). The design discharge of HPP Bannwil of 450 m^3/s is exceeded on average for about 42 days a year (Fig. 3).

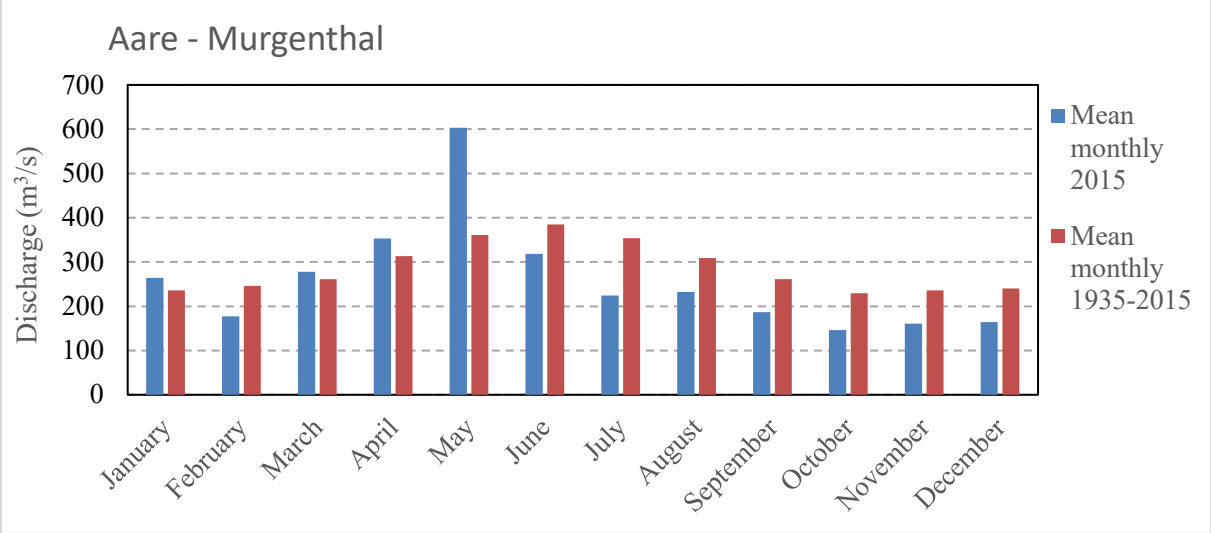

Figure 2: Mean monthly discharge of river Aare at Murgenthal (AG) (source: https://www.hydrodaten.admin.ch).

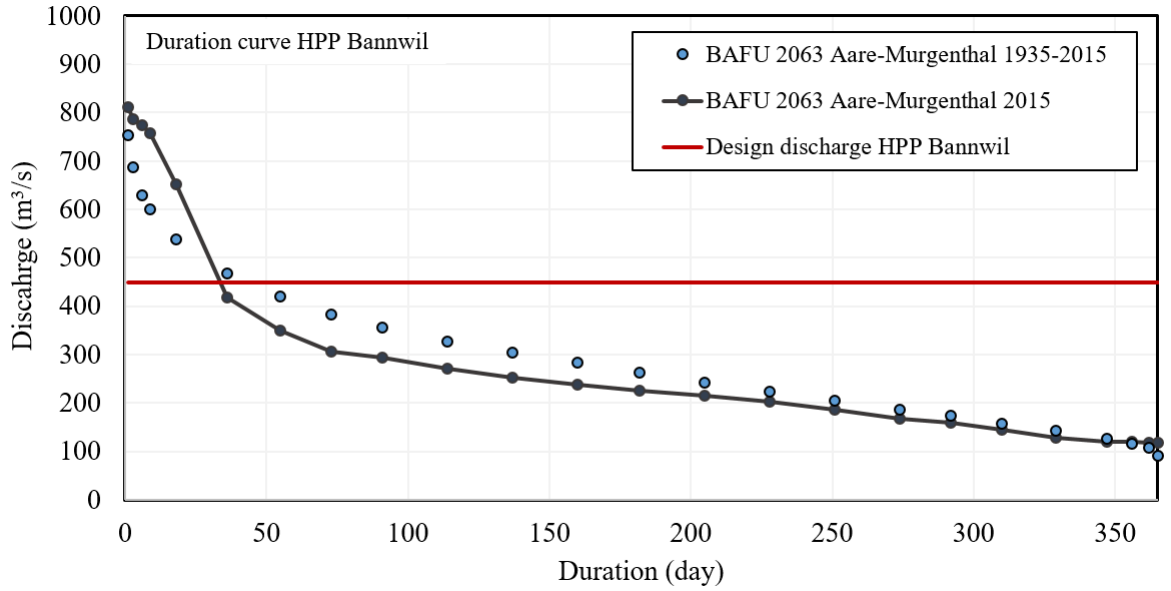

Figure 3: Discharge – duration curve of the river Aare at Murgenthal (AG) (data source https://www.hydrodaten.admin.ch).

1.1.2. Main pressures

River Aare is located in the Rhine river catchment, which was historically one of the most important Atlantic salmon rivers in Europe. The upstream migration of Salmons (*Salmo Salar*) in the Rhine catchment became almost impossible after hydropower plant constructions. This includes River Aare.

All of the occurring fish species present in the Aare river (total of 44 fish species) face potentially high mortality during downstream migration, or difficulties during upstream migration. Some important species of the fish fauna are:

- Eel (*Anguilla anguilla*)
- Brown trout (*Salmo trutta*)
- chub
- grayling
- spirlin
- Common barbel (*Barbus Barbus*)

Furthermore, the river Aare is highly influenced by hydropower and considered as a heavily modified water body. Further, there are three nuclear power plants on the Aare River, two of them putting back the used cooling water, which induces an increase of the river water temperature. The river has a moderate ecological potential. Measures for sediment control, fish migration, flow changes, habitat in-channel and morphology off-channel have been implemented in the water body. In particular, measures like gravel replenishment to restore the bed load regime have been implemented. Mitigation measures in the River Basin Management Plan, which are not yet implemented, include the restoration of upstream fish migration facilities along all HPPs in the Aare river and the planning and implementation of downstream fish migration measures.

1.2. Presentation of the HPP

Figure 4 shows the location and the close-up photo of HPP Bannwil. Its characteristics are listed in Table 1.

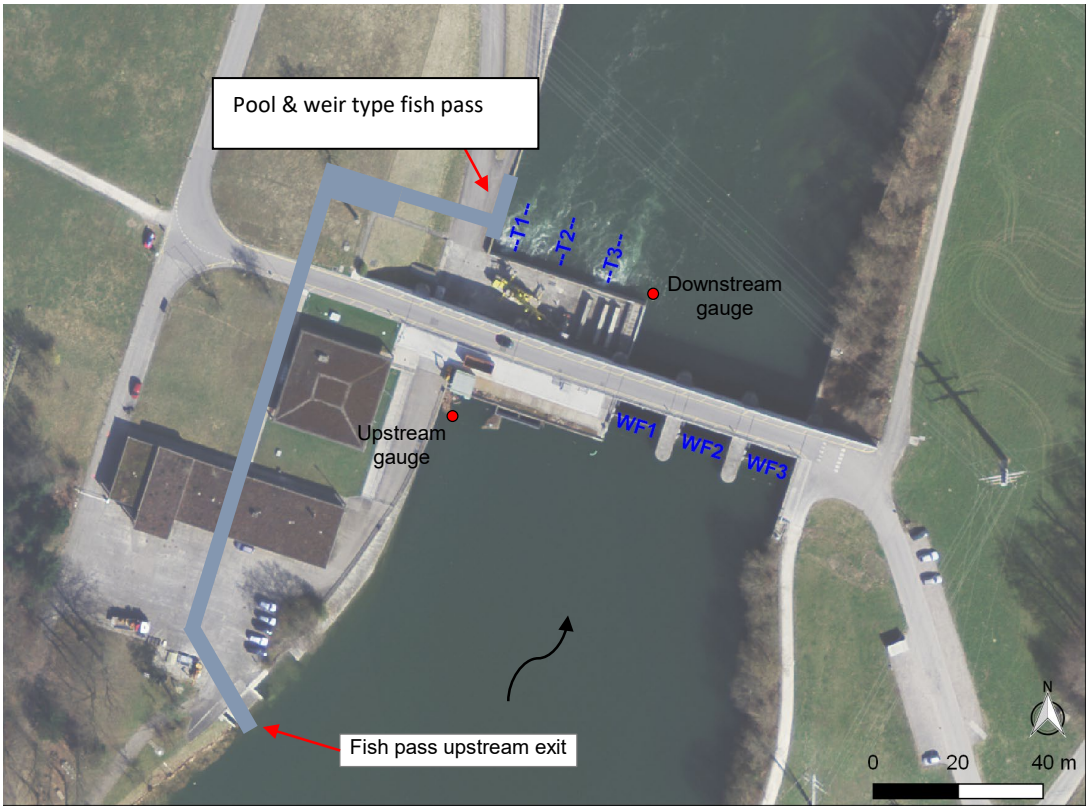

Figure 4: HPP Bannwil overview (background image: © 2018 swisstopo (JD 100041)), where "T" stands for turbine and "WF" for weir bay.

Table 1: Main characteristics of the HPP Bannwil

Watercourse	Aare
Location :	Bannwil
Mean annual discharge (1935-2015)	286 m^3/s
Design discharge	450 m^3/s
Head	5.5 – 8.5 m
Power	28.5 MW, 150 GWh (3 bulb turbines)
Species concerned :	25 to 35 fish species known; target species: barbel and large salmonids (e.g. Salmon and trout). Salmon expected in the next 10 - 20 years.

1.2.1. E-flow

E-flow is not a concern at HPP Bannwil because it is a block-type HPP where upcoming flow passes through the turbines and/or weir (during flood events) to the downstream river reach and there is no residual flow section.

1.2.2. Downstream migration devices

There is no specific measures implemented at HPP Bannwil. Fish can only pass through the turbines and/or over the weirs when they are in operation. Weir discharge occurs on average (1935-2015) for about 42 days per year (see Figure 3).

1.2.3. Upstream migration devices

The current fish pass is pool and weir type pass with bottom and top openings (Figure 5). The entrance is located on the left shore of the river shortly downstream of the powerhouse (Figure 4). The bottom slope of this technical fish pass is on average 6 %. Most of the head difference is accomplished in the first half of the fishway. It consists of chamber with a spiral fish way. The upper part of the fishway consists of near horizontal canal that lead to the exit roughly 100 m upstream of the HPP. The mean discharge in the fishway amounts to 350 l/s. The fish pass needs to be restructured to accommodate larger fish in the near future. Current plans include replacing the lower part with a vertical fish pass design and the upper part with a nature like open channel.

Figure 5: Pool and weir type fish pass with top and bottom openings at HPP Bannwil.

2. Objectives of this Test Case

Downstream fish migration

Downstream fish migration measures are investigated by means of field and numerical studies. The current situation and the efficiency of spill flow or water release as an operational measure at the HPP Bannwil have been investigated through field monitoring and 3-D numerical modelling in the area near the powerhouse and the weir. The monitoring comprises:

- characterization of the flow field using ADCP
- 3D numerical simulations
- survey of the fish downstream movements using ARIS Sonar and radiotelemetry techniques

Preliminary 3D numerical simulations were considered in the planning of the monitoring. After the monitoring campaign, the 3D hydraulic model has been refined and validated using the ADCP data. Applying this model to different structural and/or operational scenarios allows to come up with solutions to improve fish migration at reduced energy losses. For the former, the innovative fish guidance structures (FGS) further developed in WP3, Task 3.5 (by etho-hydraulic modelling in the VAW laboratory) is used as a basis. The hydraulic conditions at potential locations of the FGS including bypass have been studied with the numerical model.

Turbine passage

Dynamic pressure fluctuations experienced by fish during the turbine and spillway passages will be studied at HPP Bannwil using a Barotrauma Detection System (BDS) developed at TUT (Figure 6). Flow scenarios will be full and half loads of the turbines, and the sensors should be injected at heights corresponding to the upper blade tip, bulb center and lower blade tip, respectively. The data will consist of pressure and inertial measurement unit time series as comma delimited text files. The raw data will be analyzed and the results will be provided to Voith (WP2) for BioPA modelling by TUT. Voith will build a CFD model of the turbine flows at HPP Bannwil, run the model and compare the model results with the BDS results. The results will be used for WP 3.3. Furthermore, Voith will use the same CFD-models and focus on different operating modes to evaluate the possibility of adapting the operation for certain time periods. Finally, the results from TUT and VOITH will be provided to TUM for fish turbine mortality assessment. SJE might help TUT for the field measurements and is responsible for the analysis of the BDS data.

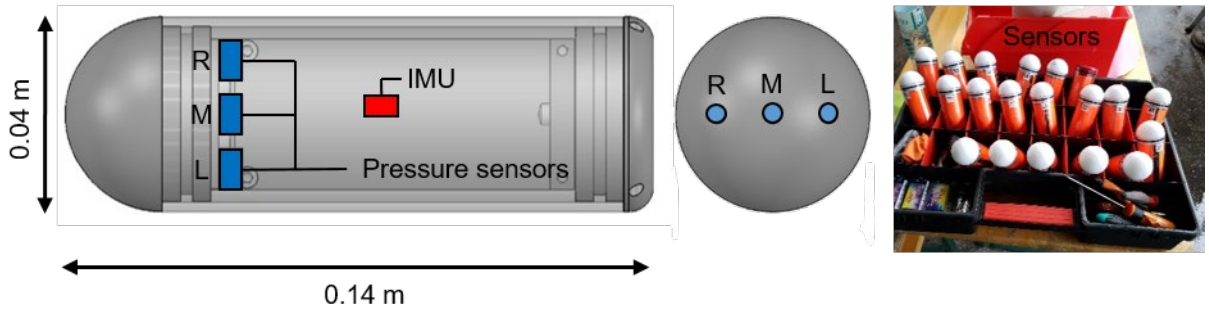

Figure 6: Schematic and dimensions of the BDS, showing the locations of the three pressure transducers and the Inertial Measurement Unit (IMU). Left: side-view of sensor. Right: top-view facing the cap showing the left (L), middle (M) and right (R) pressure ports.

Why are we planning this on this Test case?

The test case site of HPP Bannwil is the only representative large HPP within the FIThydro test cases where downstream fish migration needs to be improved. As this HPP has no downstream fish passage facility, conceptual investigations for downstream fish passage as well as turbine passage are needed.

What are we expecting?

We expect from this test case to (I) determine hydraulic conditions at the HPPs under various operational conditions including weir operations, (II) advance in our understanding of the effect of turbine operation on fish passage, (III) evaluate fish passage through the turbines and over the weirs (as an operational measure for downstream fish passage), (IV) contribute to the development of the BiaPA model as well as turbine mortality assessment using BDS, and (V) consolidate the design recommendation for fish-friendly water intakes at reduced energy losses.

Relevance in FIThydro?

We will respond to some objectives of the project and WP2 such as application of the existing and newly developed SMTDs on a test case, and will have feedbacks on their use and application ranges.

3. Presentation and results of activities in FIThydro

3.1. Downstream fish migration measures (ETHZ, FCO, BKW)

The current situation is documented through field monitoring and 3D numerical modelling in the area near the powerhouse and the weir. The monitoring comprises the characterization of the flow field with velocity measurements using Acoustic Doppler Current Profiler (ADCP) and a survey of the fish movements. The latter is made with Aris Sonar and radiotelemetry techniques.

Spill flow or water release may be the simplest means of transporting fish past HPP obstacles, which can be also cost-effective when the downstream migration period of the target species is short or migration occurs during high river flows. This option and the effect of the HPP operation on the flow field and fish migration for different load cases, e.g. with and without spillway flow, is investigated by measuring flow velocities as well as monitoring fish movements. The obtained hydraulic data is used to calibrate and validate the numerical model.

Applying this model to different structural and/or operational scenarios allows to come up with solutions to improve fish migration at reduced energy losses. For the former, the innovative fish guidance structures (FGS) further developed in WP3, Task 3.5 (by etho-hydraulic modelling in the VAW laboratory) is used as a basis. The hydraulic conditions at potential locations of FGS including bypass are studied with the numerical model.

3.1.1. Data

Data are collected from the field campaigns, the HPP operator and literature.

3.1.2. Methodology

- Velocity and bathymetry measurements near the HPP using ADCP
- Survey of the fish movements using ARIS Sonar and radiotelemetry techniques with fixed installations at the HP and mobile tracking upstream and downstream of the HP
- 3D numerical modelling using the software *FLOW-3D*

3.1.2.1. ADCP measurements

High-resolution 3D velocity as well as bathymetry measurements were conducted using an ADCP mounted on a remote-controlled Q-Boat from *Teledyne Marine*. The River Pro 1200 kHz ADCP including piston style four-beam transducer with a 5th, independent 600 kHz vertical beam was used (Figure 7). In addition to the ADCP probe, the boat is also equipped with a differential GSP system (Hemisphere AtlasLink) with a position accuracy of about 0.1 m. The application range for the ADCP device range from 0 to 5 m/s as well as flow depths between 0.5 and 25 m.

Figure 7: Teledyne Marine Q-boat of VAW equipped with ADCP probe and GPS antenna.

In the scope of this project, two field campaigns were conducted at HHP Bannwil. The first campaign took place at a river discharge of 402 m^3/s on 23 April 2018. The main goal was to acquire additional cross sections of the riverbed to complete the 3D bathymetry for the numerical model. Furthermore, cross sectional flow velocities were measured for model validation. Generally, at one location (cross section) several ADCP transects are acquired, whereby one transect corresponds to one crossing of the river approximately perpendicular to the main flow direction. Depending on the width of the river (at HPP Bannwil about 120 m in the upstream and 90 m in the downstream reaches) it may take up to 10 min to record a single transect. For comparison with the steady state flow field resulting from the numerical model, an average of several ADCP transects is needed. The main goal of the second campaign on 19 September 2018 (discharge 143 m^3/s) was to conduct repeated transect measurements for an in-depth analysis of transect averaging. The post processing was done according to the workflow sketched in Figure 8 using the software WinRiver II[1] and VMT[2].

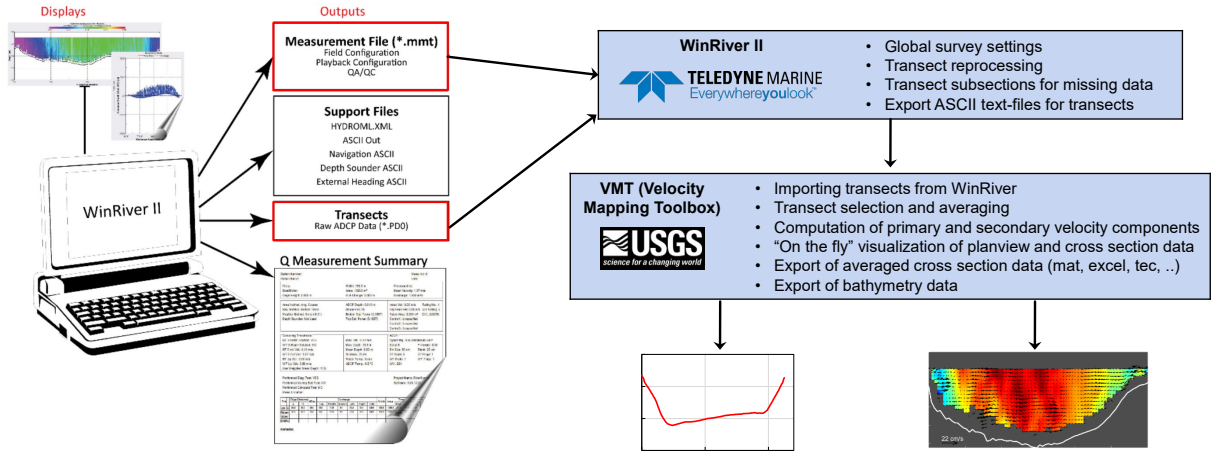

Figure 8: Workflow used for post-processing of ADCP data (modified from [1]).

[1] Data collection and post processing software provided by U.S. Geological Survey
[2] Matlab based software for processing and visualizing ADCP data provided by U.S. Geological Survey

3.1.2.2. Numerical modelling

General model theory

The 3-dimensional motion of fluid can be mathematically described by the *Navier-Stokes* equations considering conservation of mass and momentum. The software *FLOW-3D* is used, numerically solving the *Reynolds*-averaged *Navier-Stokes* (RANS) equations within the computational domain. The domain is subdivided into several mesh blocks containing rectangular grid cells (structured mesh). Fluid velocities and pressures are located at staggered mesh locations as shown for a typical grid cell in Figure 9.

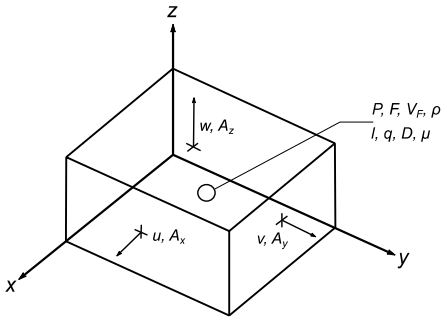

Figure 9: Location of variables in *FLOW-3D* computational mesh [2].

The numerical model involves the following variables: u velocities and fractional areas A_x at the centers of cell-faces normal to the x-direction, v velocities and fractional areas A_y at the centers of cell-faces normal to the y-direction and w velocities and fractional areas A_z at the centers of cell-faces normal to the z-direction, pressures (P), fluid fractions (F), fractional volumes (V_F), densities (ρ), internal energy (I), turbulence quantities for energy (q), dissipation (D) and viscosity (μ) are located at cell centres [2].

Wall boundaries and other solid geometrical structures like the weir body and the powerhouse are embedded in the mesh by the so called FAVOR^{TM} method defining the fractional face areas and fractional volumes of the cells that are open to fluid flow. In order to properly capture the free-surface dynamics, the *Volume of Fluid* (*VOF*) method is applied in *FLOW-3D* [2]. Because of computer memory and processing time limitations, the full spectrum of turbulent fluctuations cannot be resolved by the equations of mass and momentum conservation. Hence turbulence models are required to close the RANS equations. For this study, the Renormalized-Group k-ε (RNG) turbulence model is used.

Model setup

The topographic data used to set up the Aare river bathymetry are shown in Figure 10. The modelled Aare river reach covers about 500 m upstream and 250 m downstream of the weir in order to minimize the effects of boundary conditions. This is of particular importance with regard to flow deviation by the river bend upstream of the HPP. In addition to the GEWISS profiles[3] that have a rather coarse resolution in streamwise direction (cross sectional data every 100 to 300 m), intermediate cross sections were acquired by means of the ADCP measurements. In order to capture the river curvature accurately, further cross sections were interpolated. Together with break-lines defined at the toe of

[3] River cross sections from official survey of the Swiss Federal Office for the Environment (FOEN)

the bank and other significant slope transitions, the riverbed topography was triangulated using GIS and AutoCAD software. The weir is used as a reference for the local coordinate system of the 3D model (Figure 10 and Figure 11).

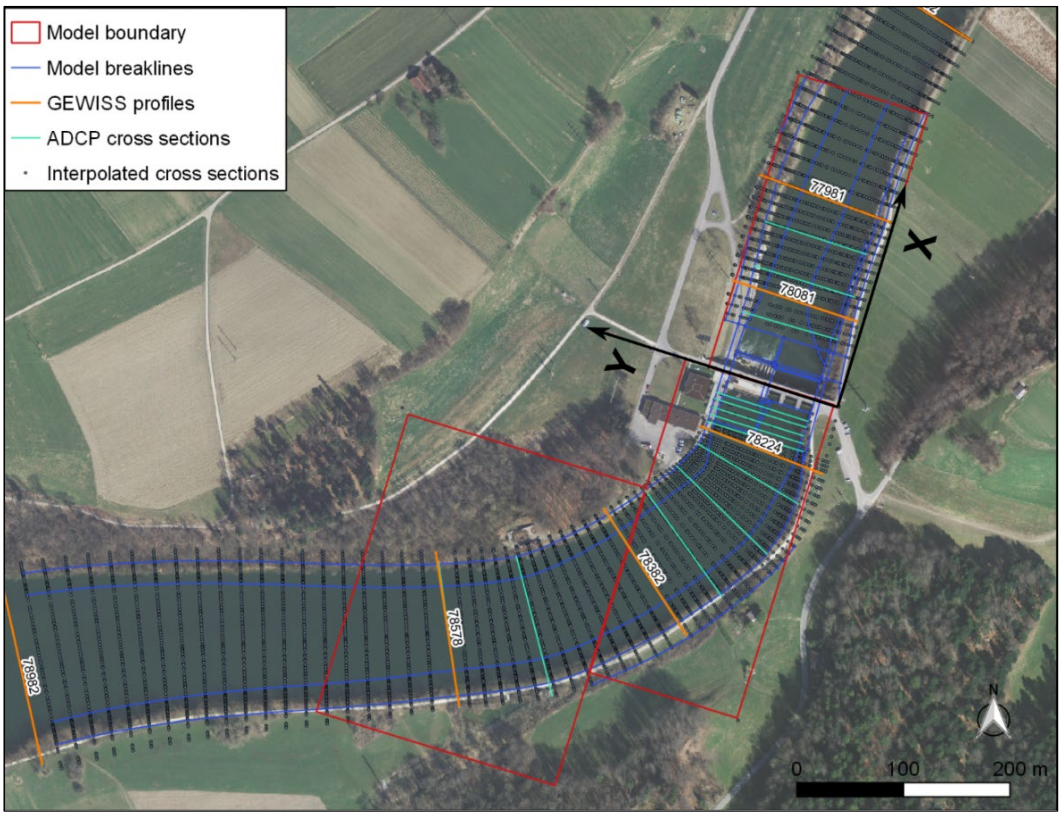

Figure 10: Model domain (within model boundary) and topographic data used to set up the numerical 3D model (background image: © 2018 swisstopo (JD 100041)).

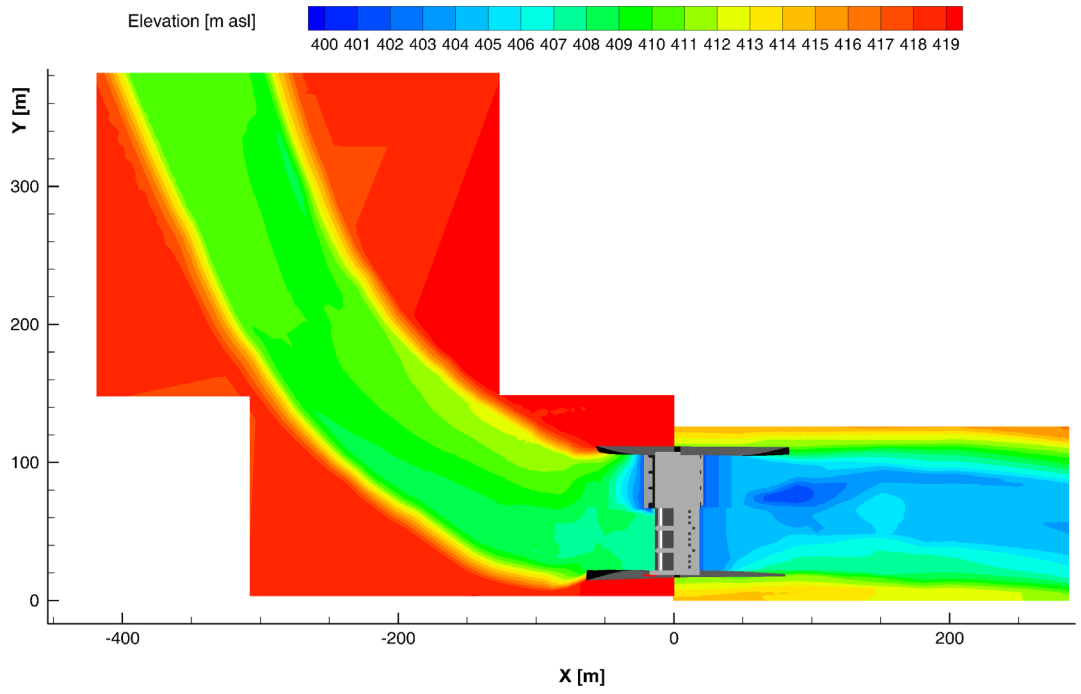

Figure 11: Riverbed bathymetry in coordinate system of the 3D model.

Construction plans provided by the operator were used to model the 3D hydraulic structures like the powerhouse, the weir body and the gates. Such solid structures were designed using CAD software tools and imported into *FLOW-3D* in the form of stereolithographic files (STL). For the purpose of simplification, the three radial gates with flaps were replaced by simple sluice gates (see Figure 12). Furthermore, turbine runners, flow distributors and trash racks are not geometrically resolved in the model. So-called baffles were used to account for flow resistance of these structural elements. In *FLOW-3D* baffles represent surfaces and therefore do not affect the volume fraction. The baffle geometry snaps to the cell faces of the mesh (see Figure 9), leading to a stair-stepped shape of an originally curved baffle geometry [2]. The user can define different properties such as porosity and linear or quadratic loss coefficients for each baffle. For the current model, the baffles loss coefficients were calibrated in order to match water surface elevations and the discharge distributions between turbines and weir with the measurement data.

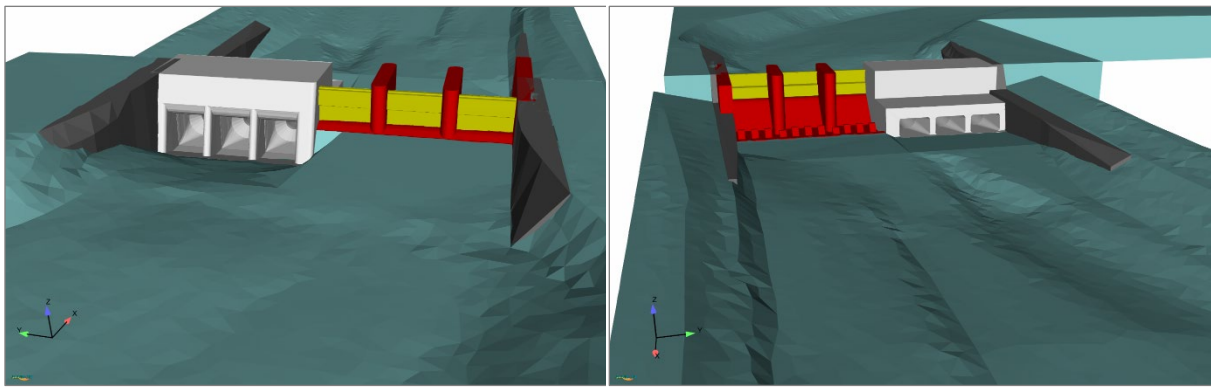

Figure 12: Power plant components represented in the 3D model, view from upstream (left) and downstream (right).

The structured computational mesh of *FLOW-3D* may consist of an arbitrary number of single mesh blocks to cover the model domain. The spatial grid resolution in Cartesian coordinate directions may differ for each mesh block. At first, simulations for the entire model domain were performed. An upstream boundary condition of type volume flow rate (VFR) was used at mesh block 1 (see Figure 13). By specifying the water surface elevation hydrostatic pressure (P) was defined as downstream boundary condition for mesh block 7. The closer to the area of interest, the higher the spatial mesh resolution is. To resolve the power plant structure accurately, a conforming mesh with a resolution of 0.25 m (*x*, *y* and *z*) was specified for mesh block 5. In *FLOW-3D* "conforming mesh" means that the transition between solid and void or solid and fluid is resolved with a nested finer mesh within a defined overlap length compared to the surrounding block. After a steady state solution is reached for the full domain, this solution can be used as restart information for a smaller subdomain model with a finer mesh resolution (bottom of Figure 13). As upstream boundary condition for the restart simulation, a so-called "grid overlay" (G) can be applied. Thus, restart data from the original simulation are used to set flow parameters upstream of mesh block 1. The concept of restart simulations for smaller domains allows for more detailed modelling of particular regions of interest, for example close to the turbine inlets or the stilling basin downstream of the weir. The computational grids consist of roughly 4 to 6 Mio active fluid cells depending on the scenario.

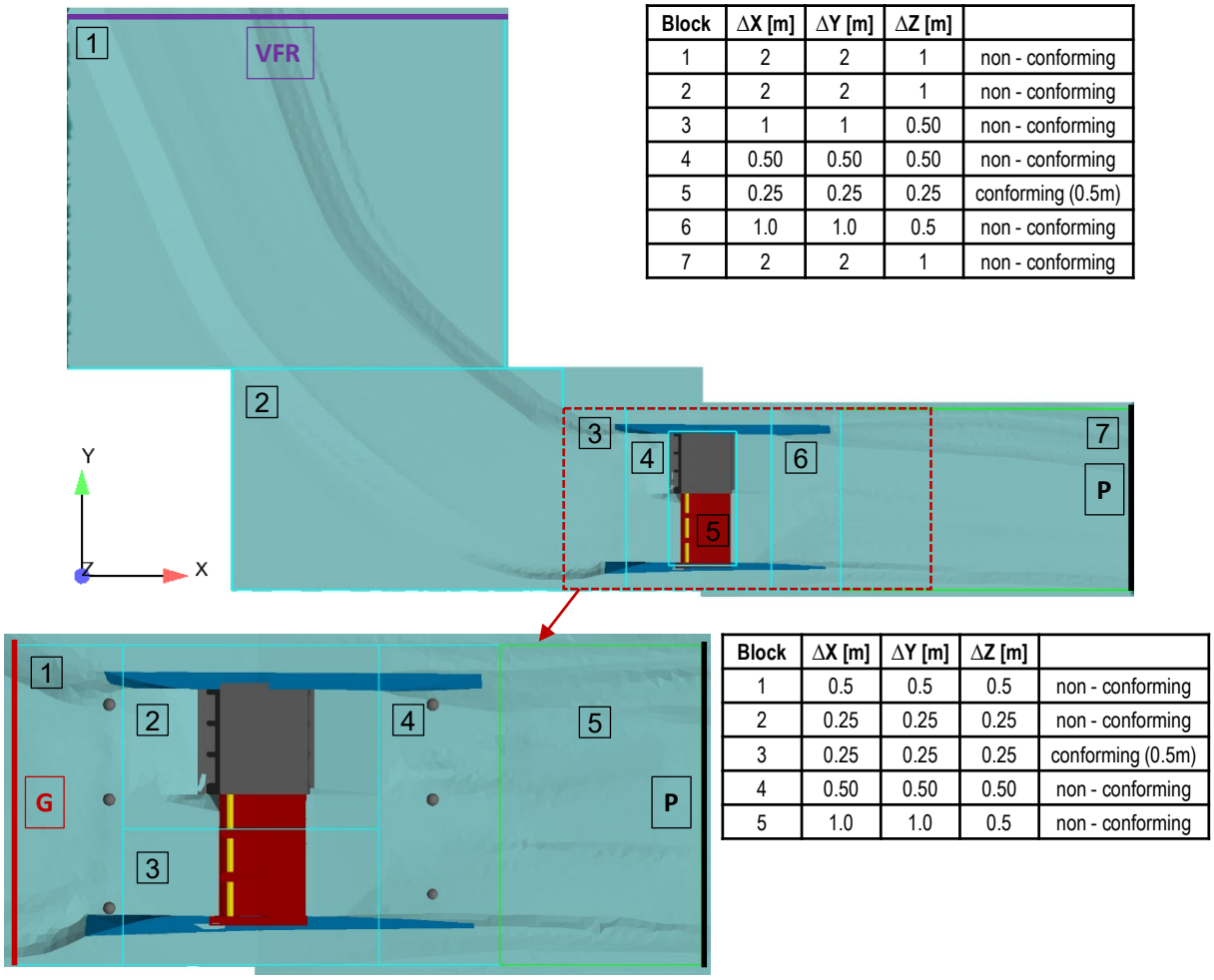

Block	ΔX [m]	ΔY [m]	ΔZ [m]	
1	2	2	1	non - conforming
2	2	2	1	non - conforming
3	1	1	0.50	non - conforming
4	0.50	0.50	0.50	non - conforming
5	0.25	0.25	0.25	conforming (0.5m)
6	1.0	1.0	0.5	non - conforming
7	2	2	1	non - conforming

Block	ΔX [m]	ΔY [m]	ΔZ [m]	
1	0.5	0.5	0.5	non - conforming
2	0.25	0.25	0.25	non - conforming
3	0.25	0.25	0.25	conforming (0.5m)
4	0.50	0.50	0.50	non - conforming
5	1.0	1.0	0.5	non - conforming

Figure 13: Grid resolution of the 3D model with full domain (on top) and exemplary grid refinement for restart simulations of a particular subdomain (at bottom).

Simulation scenarios

In the scope of the numerical investigations, four different flow conditions were simulated (Table 2). The discharges simulated for scenario 1a and 1b correspond to the hydraulic conditions observed during the ADCP measurement campaigns (see chapter 3.1.3.1) and were used for model validation. The total and turbine discharges are termed Q_{tot} and Q_T, respectively. For scenario 2a, 231 m^3/s are diverted over the weir as gate flow (Q_{LG}), while the turbine flow is at full load (Q_T =454 m^3/s). During scenario 2b, both gate flow (Q_{LG}) and overflow (Q_{UG}) occur and the total weir discharge (Q_W=Q_{UG}+Q_{LG}) amounts to 106 m^3/s), while the turbine flow is again at quasi full load. For all scenarios, discharge and water surface elevation measurements were provided by the HPP operator.

Table 2: Scenarios simulated with the numerical 3D model.

	Scenario	Q_T [m^3/s]	Q_W [m^3/s]	Q_{UG} [m^3/s]	Q_{LG} [m^3/s]	Q_{tot} [m^3/s]	Exceedance duration of total flow [d/a]
1. Turbine discharge	1a	402	0	0	0	402	57
	1b	143	0	0	0	143	338
2. Combined discharge	2a	454	231	0	231	685	4
	2b	448	106	75	31	553	20

3.1.2.3. Fish monitoring

Hydro-acoustic analysis

From June 19 -21, 2018 a hydro-acoustic investigation of fish behaviour was carried out at HPP Bannwil. The aim of the study was to detect fish in front of the trash rack and to evaluate their position and behaviour in order to gain basic knowledge of their horizontal and vertical distribution and to support the development of measures for fish protection. To this end, a downward-directed imaging sonar recorded video-like data at six different positions along the trash rack (Figure 14). Overall, five runs were conducted within 3 days: for the first four runs data were recorded for 15 min at each position, whereas during the last run the sampling interval was set to 1 hour. Figure 15 gives an overview of the experimental setup in front of the trash rack. As it became apparent during the field campaign that very low numbers of fish were present, the sonar was left to record data at position VI in between the runs (continuous data). Data processing was carried out with the post-processing software package sonar5 professional and ARISFish.

The data were analysed by measuring the body length of each individual and localizing its first and last appearance in the beam. The spatial distributions as well as swimming directions were derived from these data. Independently, the paths of six individuals were tracked in order to evaluate the smoothness of motion and behaviour in detail. Figure 15 shows the set-up of the ARIS explorer sonar mounted on an arm of the Palfinger trash rack cleaning system at HPP in Bannwil.

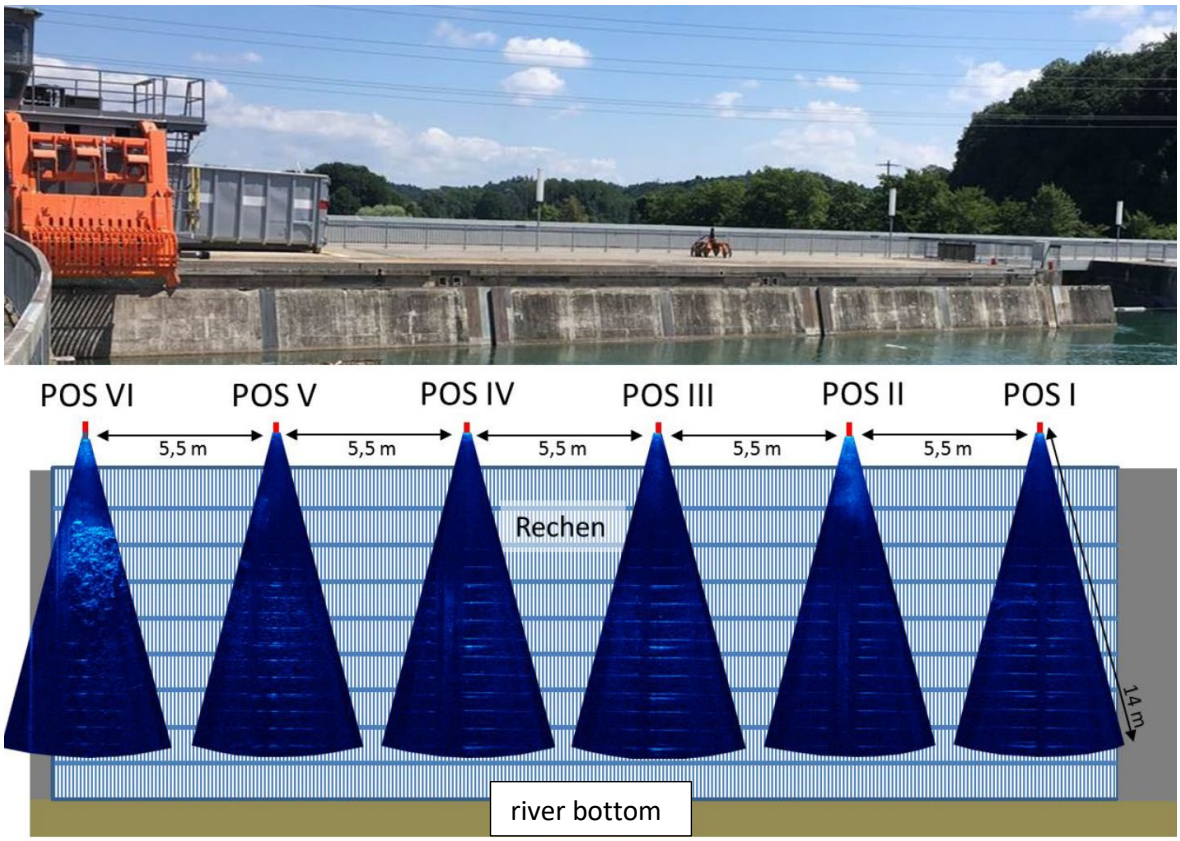

Figure 14: Hydro-acoustic imaging setup with DIDSON and ARIS sonar systems in front of the trash rack. 6 different positions were covering the area in front of the trash rack. View in flow direction.

Figure 15: ARIS sonar system at HPP Bannwil. Left: ARIS explorer sonar mounted on an arm of the Palfinger trash rack cleaner. Right: lowered arm with ARIS system in data recording status

Radio telemetry Analysis

Catch and tagging of fishes

57 barbels (*Barbus barbus*) were radio tagged in April 2019 (10 individuals) and December 2019 (47 individuals). The rheophilic European barbel is a common fish encountered in the middle reaches of rivers and is abundant in the Aare River. They were caught in the fish ladder which was used by barbels as an overwinter refuge. Pools in the fish ladder were fenced in order to prevent the escapement of the barbels. Then they were caught with a dip net. Prior to tagging, fish were anaesthetized by immersion in an aqueous solution of 0.28 mg/l 2-Phenoxyethanol. This anaesthetic is prescribed by the Swiss Federal authority responsible for animal experiments. Fishes were placed ventral side up onto a U-shaped surgery table. By means of a scalpel a 2-3 cm long single cut incision was made on the ventral midline surface posterior to the pelvic girdle. The radio transmitter and a 23 mm PIT-Tag were placed into the body cavity through the incision. The antenna of the transmitter was threaded through a cannula passed through the body wall. After the transmitter has been placed in the coelom, it was positioned away from the incision to prevent pressure necrosis close to the wound [3]. Dependent on the length of the incision 2-3 independent silk sutures (Ethicon) were made to close the incision. The barbels were several times sprayed with water during the surgery which took about 2-3 minutes. After each incision, surgical equipment was rinsed in 100 % ethanol. Three different radio transmitters were used: nano tags NTFD-6-2 with a mass in air of 3 g and with pulse rates of 2-3 sec, MCFT2 series mass in air 8 g with pulse rates of 2-3 sec, MCFT3 series with temperature and pressure loggers and pulse rate of 5 sec, a logging feature at 25 seconds, mass in air 12 g. The manufacturer of the tags is Lotek Wireless Inc. Canada with the operating frequency of 148.340 MHz. All transmitters were equipped with trailing whip antennas.

The tag/body mass ratio of 2 % was not exceeded. All transmitters were individually coded and had life times between 287 days (nano tags) and 306-378 days. We used 23 mm PIT-Tags from Oregon RFID, manufacturer Texas Instruments, ISO 11784/11785. After tagging the recovery of the fish was monitored. Before release the condition and behavior was observed. After 1-3 hours of recovery fish were released 1.07 km upstream of the hydropower plant.

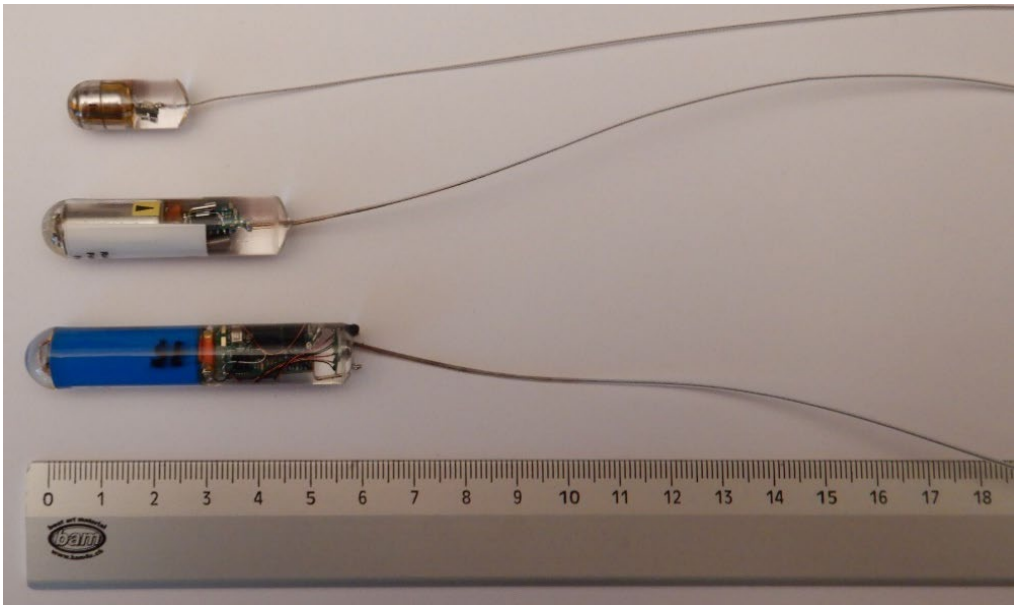

Figure 16: The used telemetry transmitters with trailing whip antenna. Top to bottom: nano tag with 3 g, MCFT2 tag with 8 g, MCFT3 sensor tag (pressure and temperature) with 12 g. Tag manufacturer LOTEK Wireless Inc., Canada.

Installation of radio telemetry equipment and hand tracking

The radio telemetry equipment was installed by end of November 2019 at the hydropower plant (Figure 17). Presence and absence test tracking was carried out with the different tag types among overlapping antennas reception cells prior to the tagging of the barbels. In the forebay 3 telemetry antennas were installed (one underwater antenna). Over each spillway a separate Yagi antenna was placed. In addition 2 downstream Yagi antennas and 3 underwater antennas (one at each turbine exit) were installed. In the fish pass 2 additional underwater antenna were placed, combined with 2 PIT-Tag antennas in the middle section of the ladder. 1-3 antennas were connected to a SRX 800 receiver (Lotek Wireless Inc., Canada). The receiver supported coded multi-sensor tags (temperature and pressure). Data were downloaded approximately every 14 days in order to prevent a blockage of the memory of the receiver. The two consecutive handmade PIT-Tag antennas were place in two pools of the fish ladder and were connected to single readers (Oregon RFID, Portland, USA). All telemetry receivers and PIT-Tagging readers were equipped with GPS position acquisition to ensure the GPS clock remains precise and functional. Fixed radiotelemetry arrays were programmed in order to optimize performance. Data analysis was carried out using R statistical software [4].

Manual tracking (by walking or cycling along the river) was carried out 22 times between April 2019 and September 2020 (Figure 18). Data were mainly collected between Olten (22.3 km downstream of Bannwil) and Solothurn (16.7 km upstream of Bannwil). The tracking results show spatial distribution, migration patterns and rates, home ranges, habitat use and survival of fishes. QGIS was used to analyze

fish migration over time. The manual tracking was carried out with a three-element YAGI antenna connected to a SRX 800 receiver equipped with a GPS antenna.

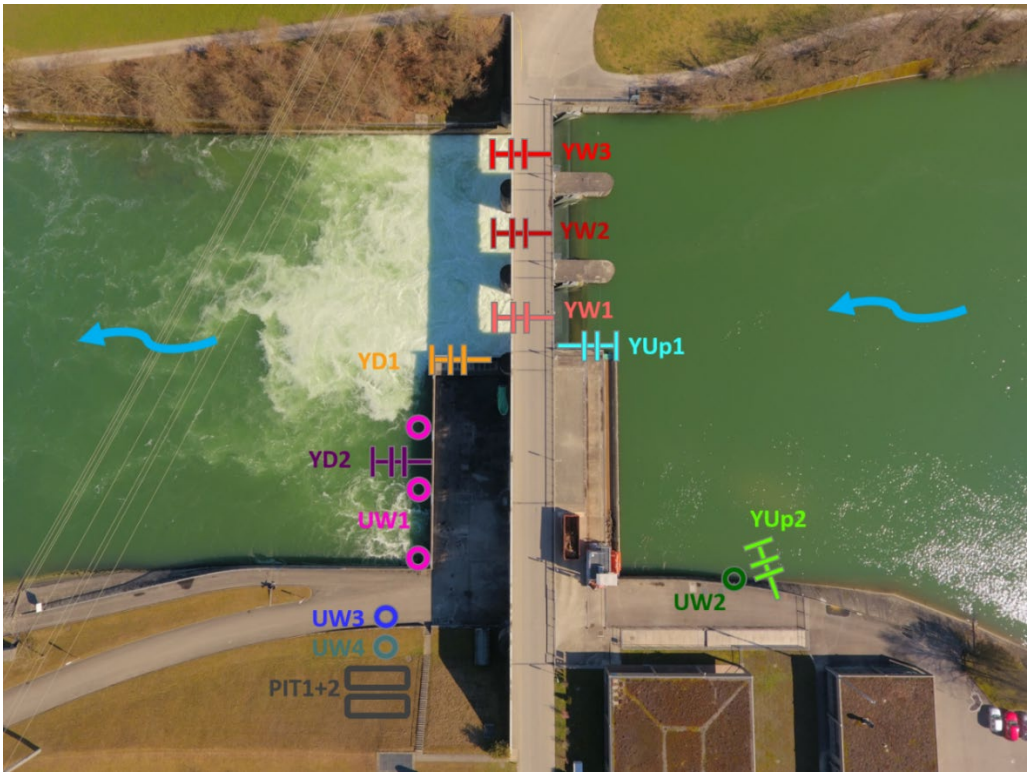

Figure 17: Overview of the installation of the fixed telemetry and PIT-Tagging stations at the hydropower plant Bannwil. 13 fixed-telemetry antennas were placed in the forebay and the tailwater, including the fish ladder, in which also two PIT-Tagging antennas were placed. The fish ladder is situated underground.

Figure 18: Manual tracking at the hydropower plant Bannwil using a three-element YAGI-antenna and SRX800 receiver connected to a GPS antenna.

3.1.3 Results

3.1.3.1 ADCP measurements

Field campaign 1: Q = 402 m^3/s

Selected results of the first ADCP campaign are shown in Figures 19 and 20. For the given discharge of 402 m^3/s, the depth-averaged velocities upstream of the HPP are in a range from about 0.7 m/s to 1.1 m/s, depending on the distance from the turbine inlets. The effect of the turbines is clearly visible as the current is concentrated in the left half of the river and towards the inlets. Close to the weir, the flow is almost parallel to the weir axis and a return flow occurs at the right bank.

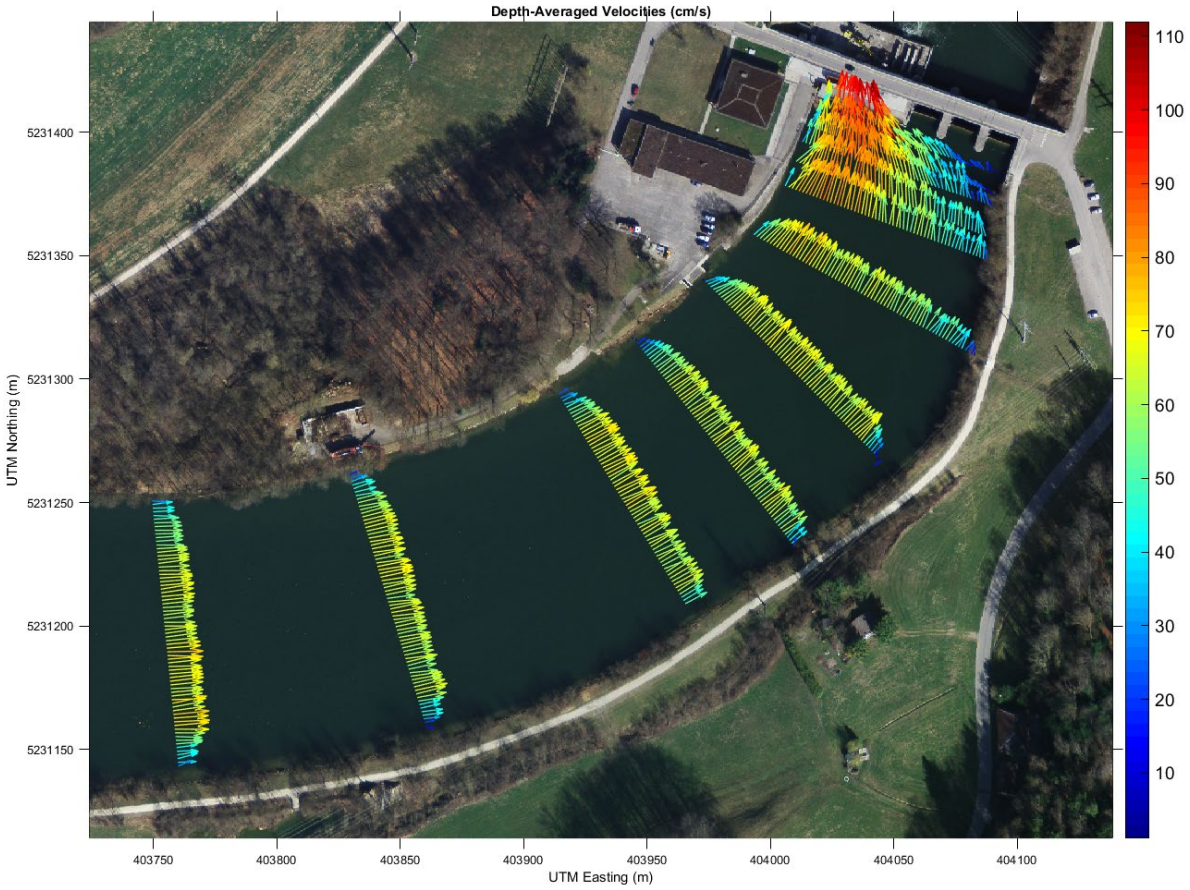

Figure 19: Depth-averaged flow velocities [cm/s] upstream of HPP Bannwil measured with boat-mounted ADCP at a discharge of 402 m^3/s (background image: © 2018 swisstopo (JD 100041)).

The cross section closest to the turbines was recorded about 6 m upstream of the trash rack (see Figure 20). The maximum approach flow velocities in streamwise direction reach up to 1.4 m/s and are located about 3 m above the bottom in front of the inlet of turbine 1 (left turbine). Even slight backwards flow can be observed about 43 m from the left bank in front of the pillar between the powerhouse and the weir. Transversal flow velocities point towards the turbine inlets and reach about 0.5 to 1 m/s. As can be observed in Figure 20, the lower most 2 m of the cross section cannot be captured with the ADCP probe due to so-called side lobe interference. This interference of the acoustic beams is caused by reflections from the bottom and may lead to a loss of vertical profiling range of up to 15 % of the total flow depth [5].

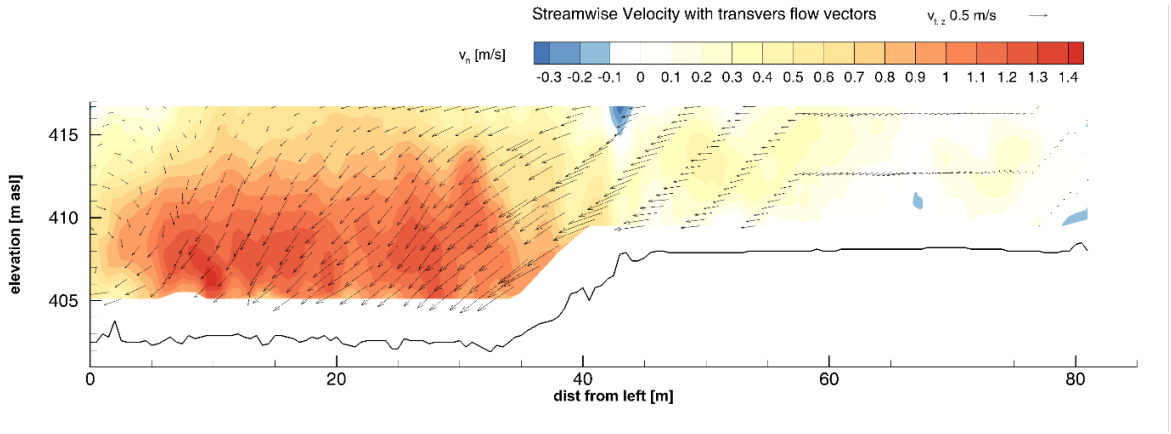

Figure 20: Contour plot of streamwise flow velocities about 6 m upstream of turbine inlets for Q_T = 402 m³/s (view in flow direction).

Campaign 2: Q = 143 m³/s

Due to the very dry weather conditions in summer 2018, the discharge of the Aare River decreased significantly to only 143 m³/s on the day of the second campaign in September 2018. Only turbines 1 and 2 (left and central) were in operation then. Transects were repeatedly recorded downstream of the HPP as shown in Figure 21.

The highest velocities of about 1.4 m/s are observed close to the left riverbank. Due to the turbine outflow similar to a jet flow, a clockwise backward circulation occurs downstream of the HPP which leads to negative streamwise velocities of up to 0.5 m/s towards the right riverbank. When analysing one single ADCP transect, one can observe quite high velocities gradients and generally high fluctuations (Figure 21a). The more transects are being averaged, the more homogeneous the flow velocities become. Averaging the values of up to 8 transects at one cross section leads to robust and smooth results, i.e. no major changes of the flow quantities result for more than 8 transects. Therefore, it is recommend to acquire a minimum of 8 transects at each cross-section. Such averaged flow field over 8 transects can be used for comparison with the results of the numerical model.

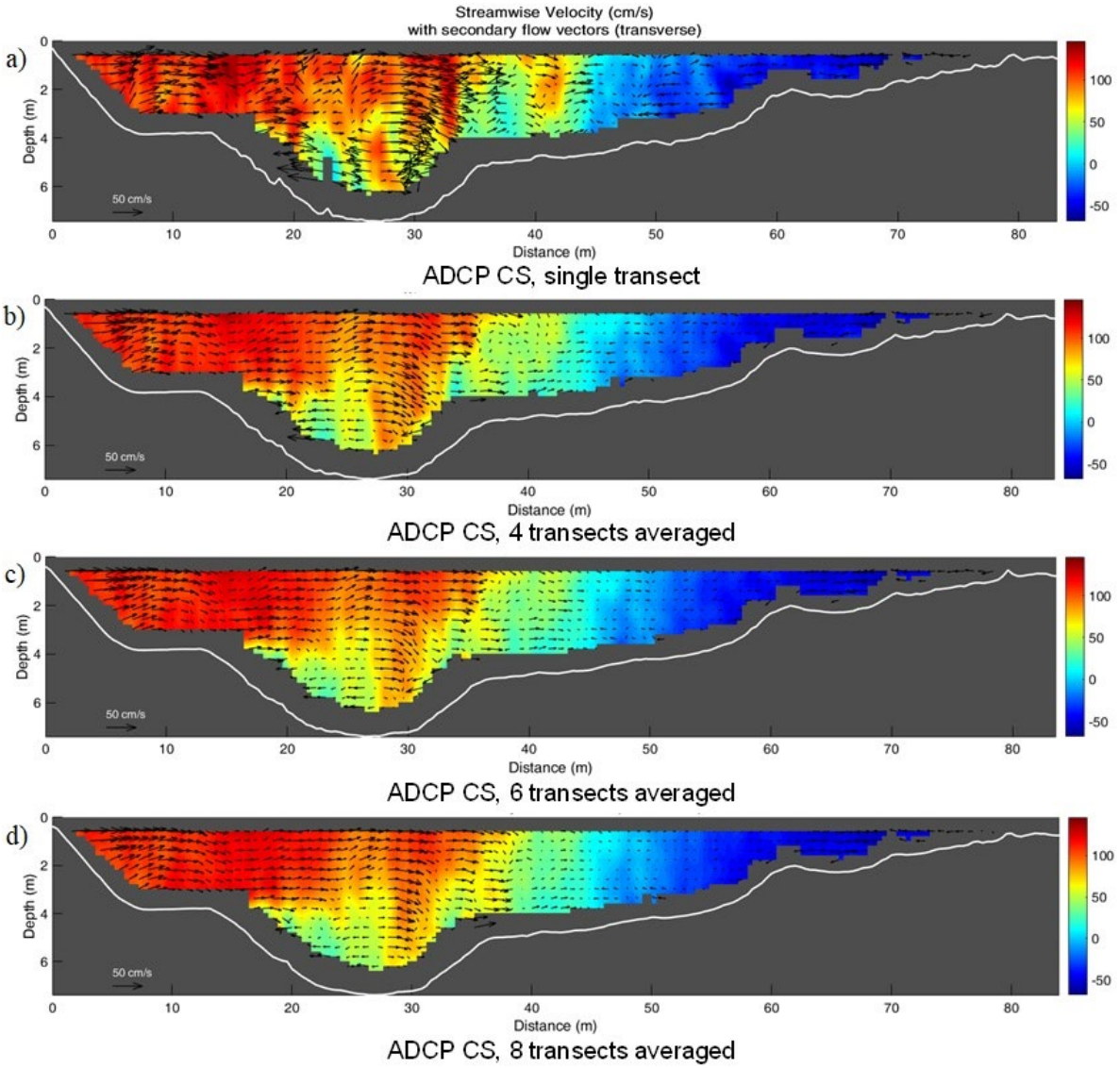

Figure 21: Effect of transect averaging about 50 m downstream of the turbine outlets for Q_T = 143 m^3/s (view in flow direction).

3.1.3.2 Numerical modelling

Model validation (Scenarios 1a and 1b)

For all scenarios, the simulated water surface elevations upstream and downstream of the HPP as well as the discharge distribution between the weir and turbines match with the measured surface elevations and turbine discharges, respectively, provided by the operator. For further validation, the simulated flow velocities at certain cross sections are compared with the results of the ADCP measurements for the same hydraulic conditions. Streamwise velocities as well as transversal flow vectors for a discharge of 402 m^3/s (scenario 1a) are compared in Figure 22. The exemplary cross section is located about 20 m upstream of the turbine inlets. In general, the simulated and measured flow fields match. It should be noted that for scenario 1a only two ADCP transects were measured and averaged during the post-processing. Hence, the agreement between measured and simulated velocities is only fair. The maximum simulated velocities reach about 0.8 m/s and are slightly lower than the measured velocities. The area of high velocities in front of the turbine inlets from 2 to about 40 m from the left riverbank agree very well with the observations. Consistently, both profiles show

significant transverse velocity components pointing towards the turbine inlets with a magnitude of approximately 0.8 m/s.

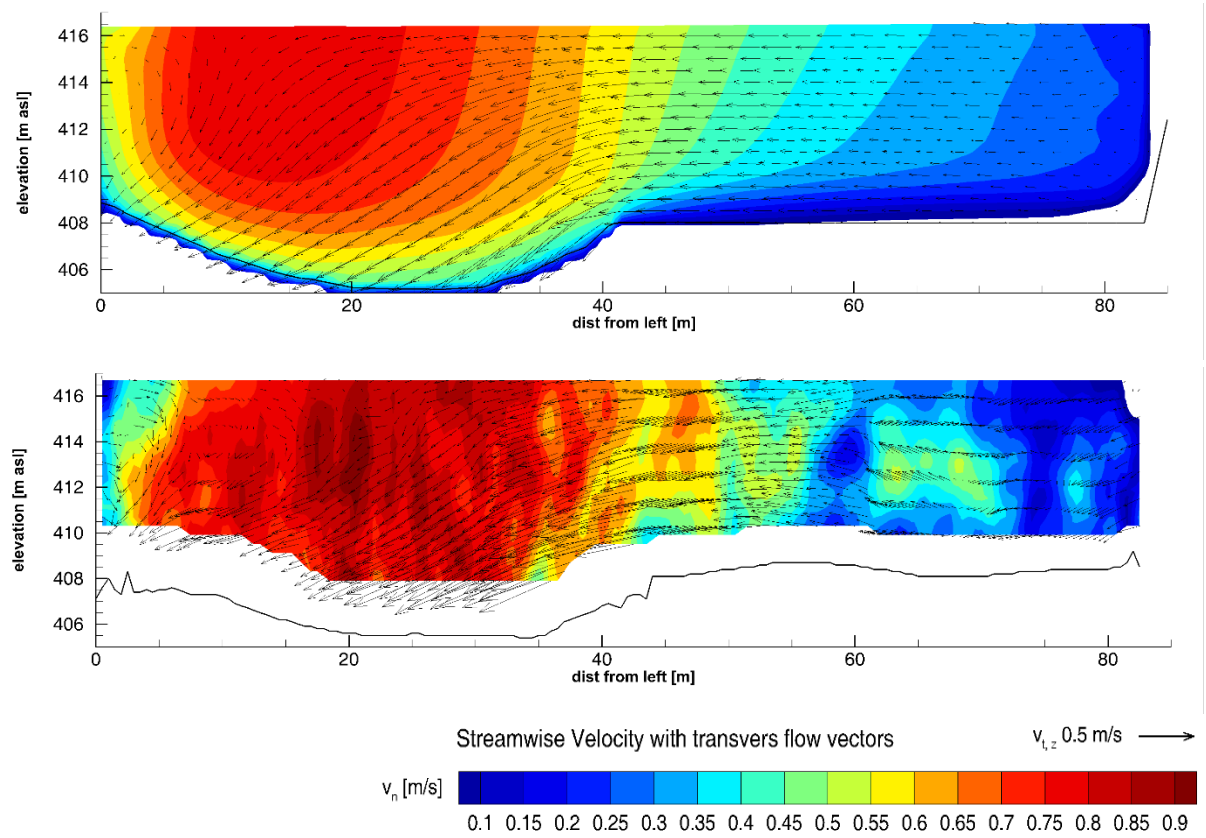

Figure 22: Comparison of the simulation results (top) with the ADCP measurements (bottom, average of two transects) for a discharge of 402 m³/s about 20 m upstream of the turbine inlets (view in flow direction).

Flow velocities for a discharge of 143 m³/s (scenario 1b) downstream of the turbine outlets are compared in Figure 23. For scenario 1b, 6 ADCP transects were averaged. Therefore, the flow velocities are more homogeneous and match well with the results of the simulations. In both cases, the maximum positive flow velocities in the left half of the cross section reach about 1.55 m/s. Due to the fact that the turbine runners are not included in the numerical model, it is not possible to fully capture the vorticity indicated by the significant vertical velocity components in the ADCP data (especially between 0 and about 35 m from the left riverbank). The regions showing negative streamwise velocities are almost identical in both plots with the maximum values of 0.55 m/s.

On the basis of comparison for scenarios 1a and 1b, it is concluded that the numerical 3D model is capable to simulate the major flow pattern upstream and downstream of the HPP (velocity magnitudes, flow directions, water surface elevations). So far, this is verified for conditions with turbine discharge only. Therefore, further ADCP measurements will be conducted for conditions with weir operation to also validate model scenarios with an Aare discharge of more than 450 m³/s.

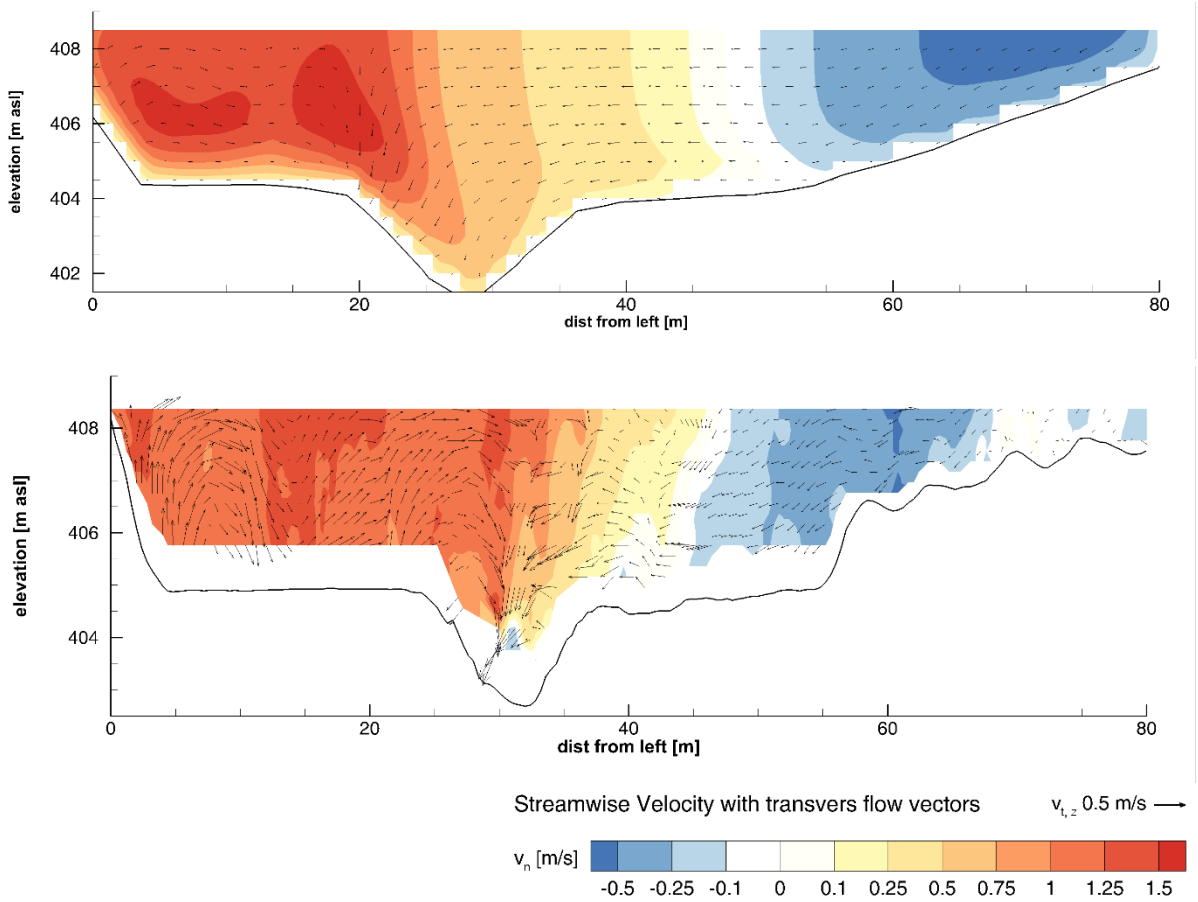

Figure 23: Comparison of the simulation results (top) with the ADCP measurements (bottom, average of 6 transects) for a discharge of 143 m³/s about 40 m downstream of the turbine outlets (view in flow direction).

Positioning of FGS

FGSs in the form of racks with either horizontally or vertically oriented bars are supposed to prevent migrating fish from swimming through the turbines and guide them along the screen axis to an alternative bypass and into the downstream reach. The FGSs are positioned with a certain horizontal angle $\alpha \leq 45°$ towards the approach flow in order to provide a ratio between the tangential v_t and normal v_n flow velocity components larger than one. This ratio is considered a suitable criterion to assess the potential guiding efficiency of a FGS. Furthermore, the normal flow velocities at the FGS should not exceed the maximum sustained swimming speed of the target fish species in order to prevent fish from being pressed against the FGS.

The numerical 3D model is a powerful tool in order to simulate normal and tangential flow velocities at any desired cross section of the computational domain for various discharges and operational conditions. A conceptual approach for the positioning of FGS using numerical 3D simulations was developed at VAW [6]. The advantage of the proposed procedure is that hydraulic conditions at potential FGS can be assessed without resolving the actual geometrical structure of the bars in detail. Such a detailed implementation would lead to an enormous number of very small computational cells (more than 50 Mio), which would make a practical model application at large-scale river power plants such as HPP Bannwil unfeasible.

For the purpose of planning future FGS at HPP Bannwil, the hydraulic conditions of two potential positions upstream of the turbine inlets have been investigated by means of 3D model simulations.

Locations of a FGS with an angle of α = 45 ° and a length of about 58 m as wells as another one with an angle of α = 37° and a length of about 80 m are shown in Figure 24. The latter promises a better ratio of tangential and normal velocities especially for the on-site conditions with the powerhouse being located at the inside of a river bend.

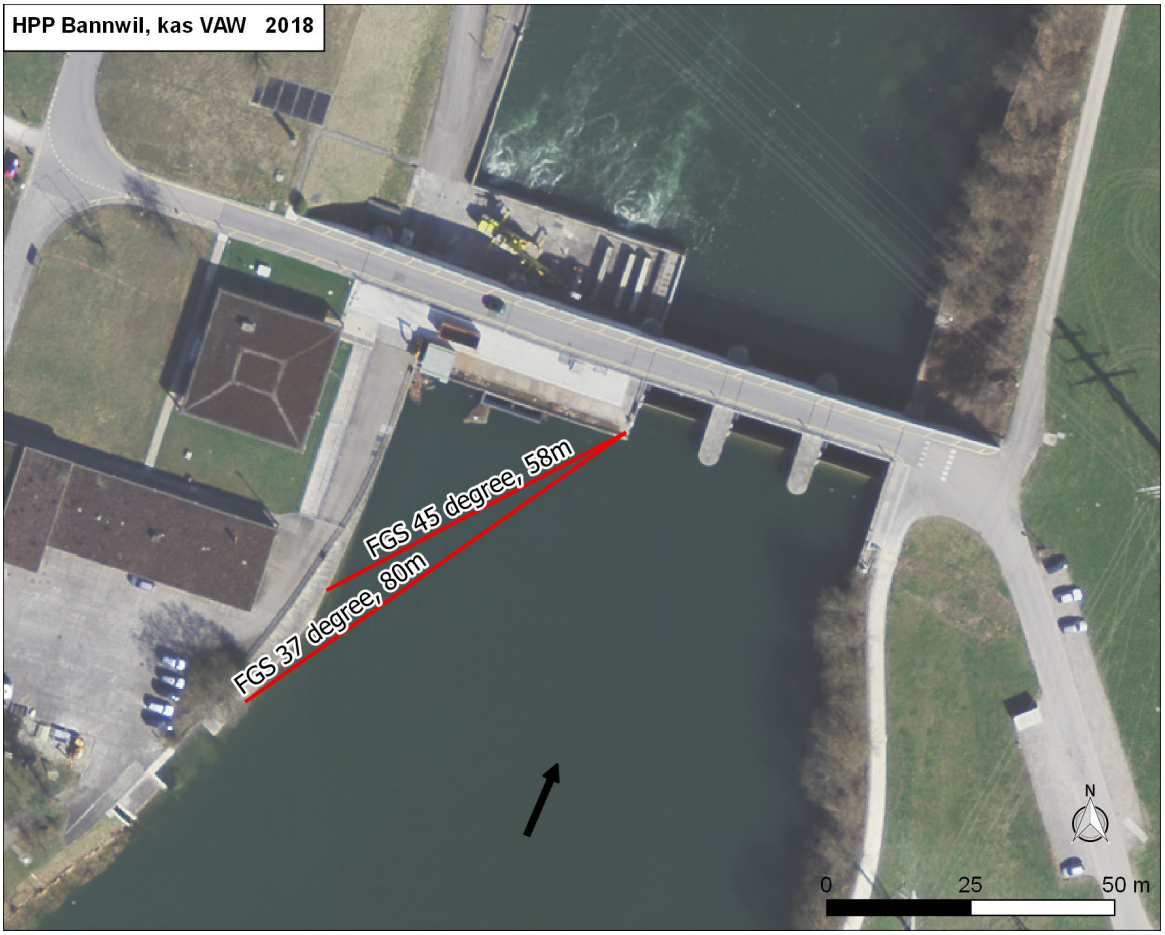

Figure 24: Potential positions of fish guidance structures upstream of the HPP Bannwil (background image: © 2018 swisstopo (JD 100041)).

As seen from Figure 25, the site-specific conditions at HPP Bannwil lead to quite high normal velocity components at the potential FGS positions. Apart from a small area close to the left riverbank near the water surface, v_n exceeds v_t at the considered locations. This holds for an angle of 45° as well as 37°. With respect to fish guidance efficiency, unfavourable conditions arise in front of the pillar between the powerhouse and weir field 1, where negative tangential velocities up to -0.8 m/s occur.

Scenario 1a, Q_T = 402 m³/s

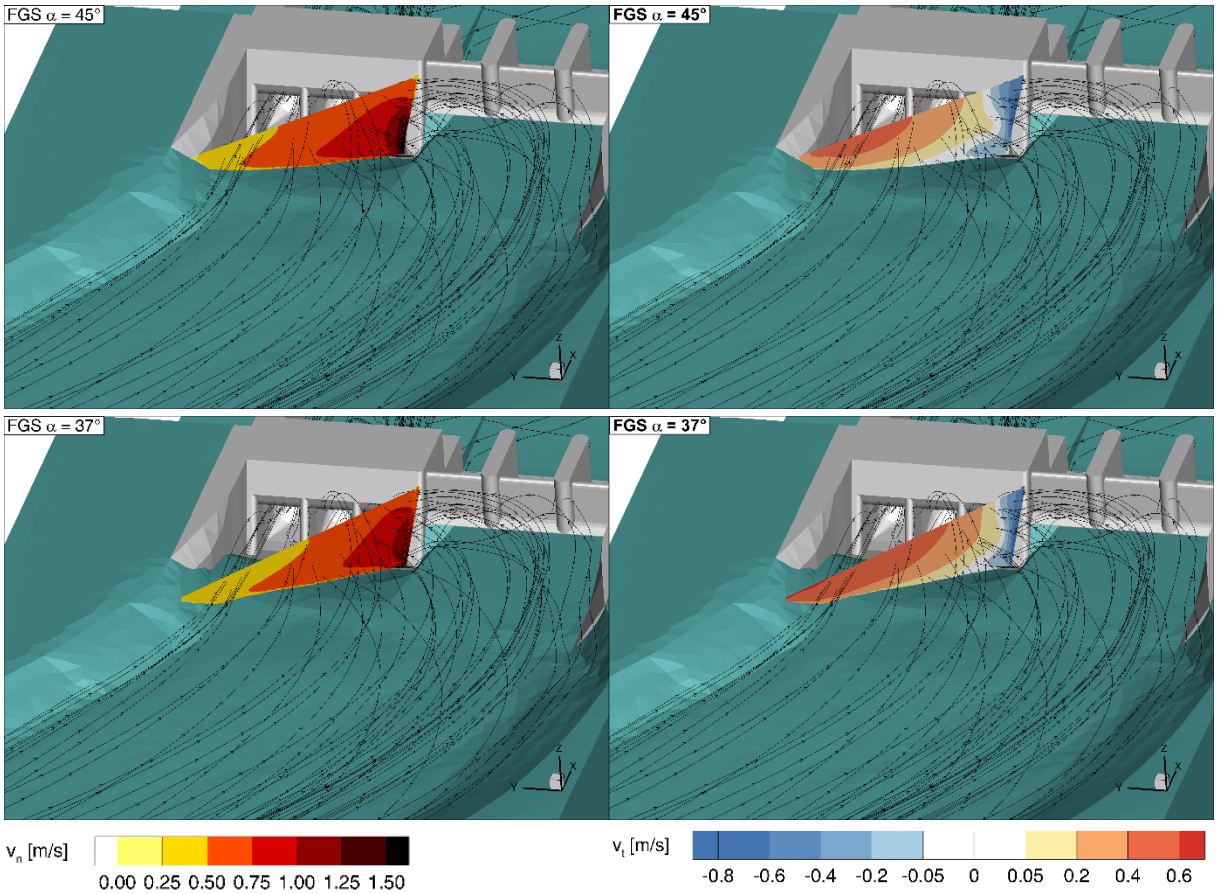

Figure 25: Normal (left) and tangential (right) flow velocities at potential FGS positions upstream of the turbine inlets for scenario 1a for FGS angled at 45° (top) and 37° (bottom).

For scenario 1b maximum v_n values of about 0.35 m/s are reached at an angle of 45 ° (Figure 26). Although normal velocities are generally lower compared to scenario 1a because of lower turbine discharge, the ratio v_t and v_n is smaller than unity for this case. Also negative tangential velocities increase, because only turbine 1 and 2 are in operation.

For both scenarios with turbine discharge only, the hydraulic conditions at the potential FGS position are rather unfavourable. The main reason is the location of the powerhouse on the inside of the river bend, which leads to a curved turbine admission flow at which the streamlines are almost perpendicular to the FGS over a wide range of the screen, both for turbine flow only (Figure 27, left) and combined turbine and weir flow (Figure 27, right). The detailed knowledge about the hydraulic conditions can also be used for positioning of a bypass. Since fish shall be guided along the screen, this would result in a bypass close to the pillar towards the weir. Again, the negative tangential velocities in this area might prevent such a bypass position. An improvement of the hydraulic conditions might be achieved by modification of the shape and/or upstream extent of the pillar. Another option would be the use of multiple guidance screens at different angles α to avoid perpendicular or even opposite admission flow close to the pillar. The 3D model can also be used for such an optimization process of the FGS positioning since modified structural components can be added to the model quite easily. Furthermore, also economical and structural aspects of such large FGS have to be considered. However, this is not subject of this investigation.

Scenario 1b, Q_T = 143 m³/s

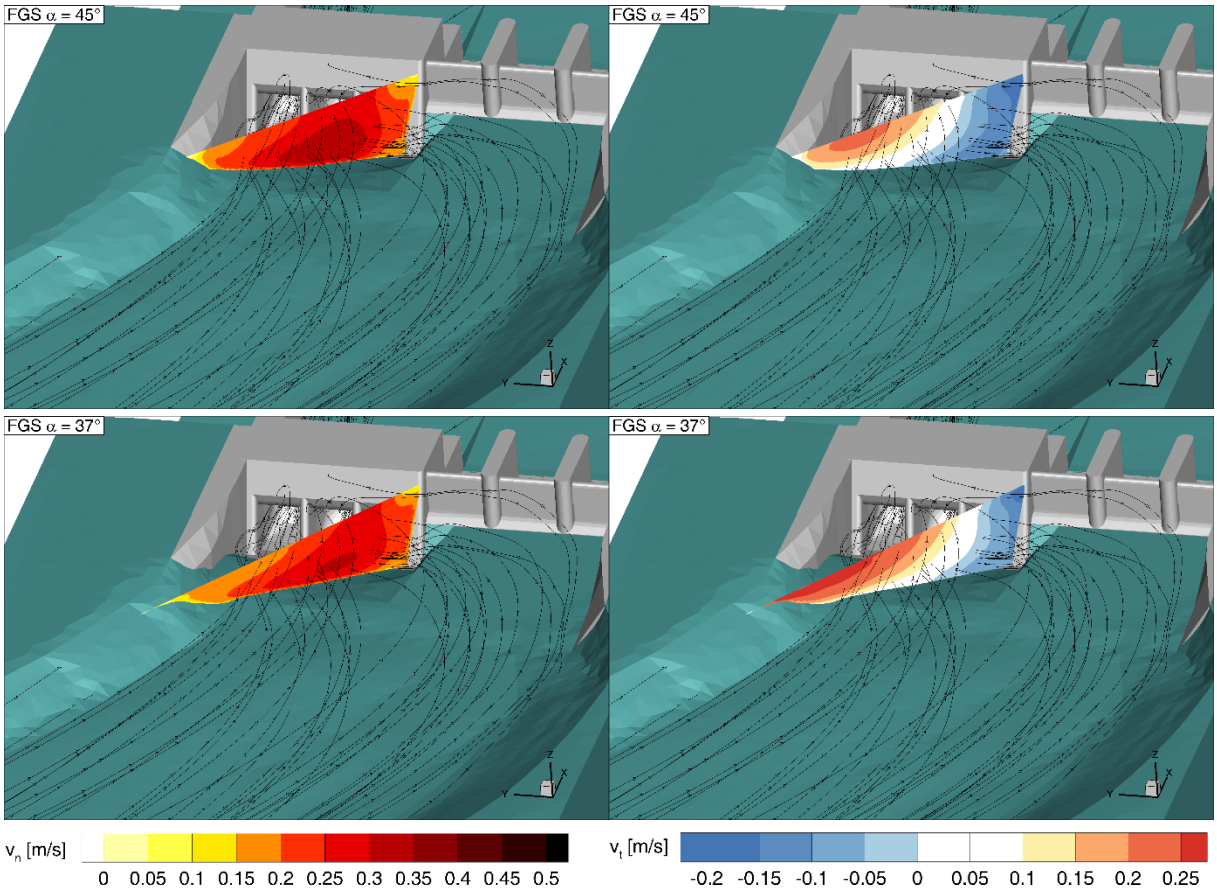

Figure 26: Normal (left) and tangential (right) flow velocities at potential FGS positions upstream of the turbine inlets for scenario 1b for FGS angled at 45° (top) and 37° (bottom).

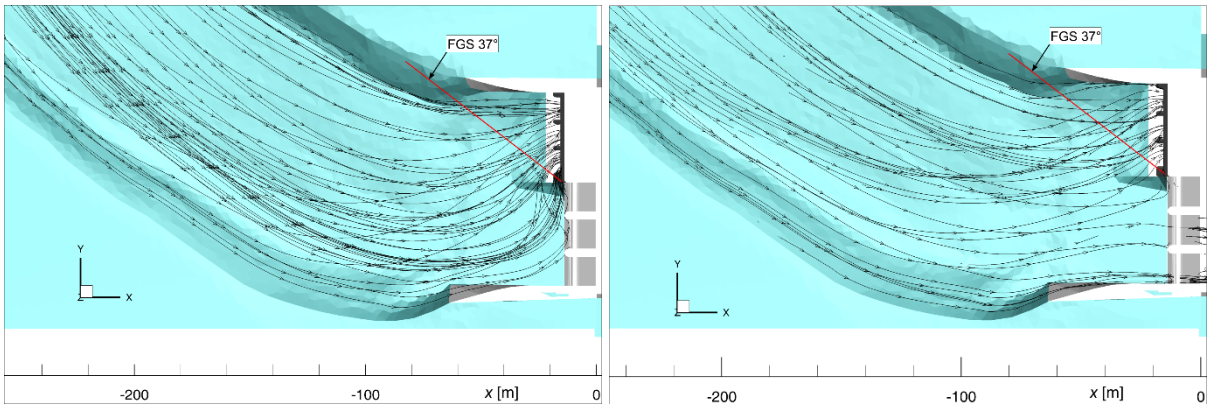

Figure 27: General turbine admission flow direction for turbine discharge only (left, scenario 1) and combined turbine and weir discharge (right, scenario 2).

In case of weir discharge, the hydraulic conditions along the screen are slightly improved due to more head-on approach flow, but the flow attack angle is still not favourable from a fish guidance perspective (Figure 27, right). The backwards tangential flow close to the pillar is reduced compared to scenario 1 (Figure 28). Nevertheless, normal velocities are even higher for scenario 2a because of an increased turbine discharge of 450 m³/s (design discharge). Especially for an angle of $\alpha = 45°$, v_n still exceeds v_t over a wide range of the FSG and v_n might be too high in view of the sustained swimming speed of the target fish species. In principle, weir operation could be a measure to provide better

hydraulic conditions at the FGS. However, weir discharge only occurs on about 42 days per year at HPP Bannwil (Figure 3). Furthermore, the large drop over the weir of up to 9 m as well as the hydraulic forces occurring in the stilling basin should be considered. The hydraulic conditions at the weir will be analysed subsequently.

Scenario 2a, Q_T = 450 m³/s, Q_W = 231 m³/s

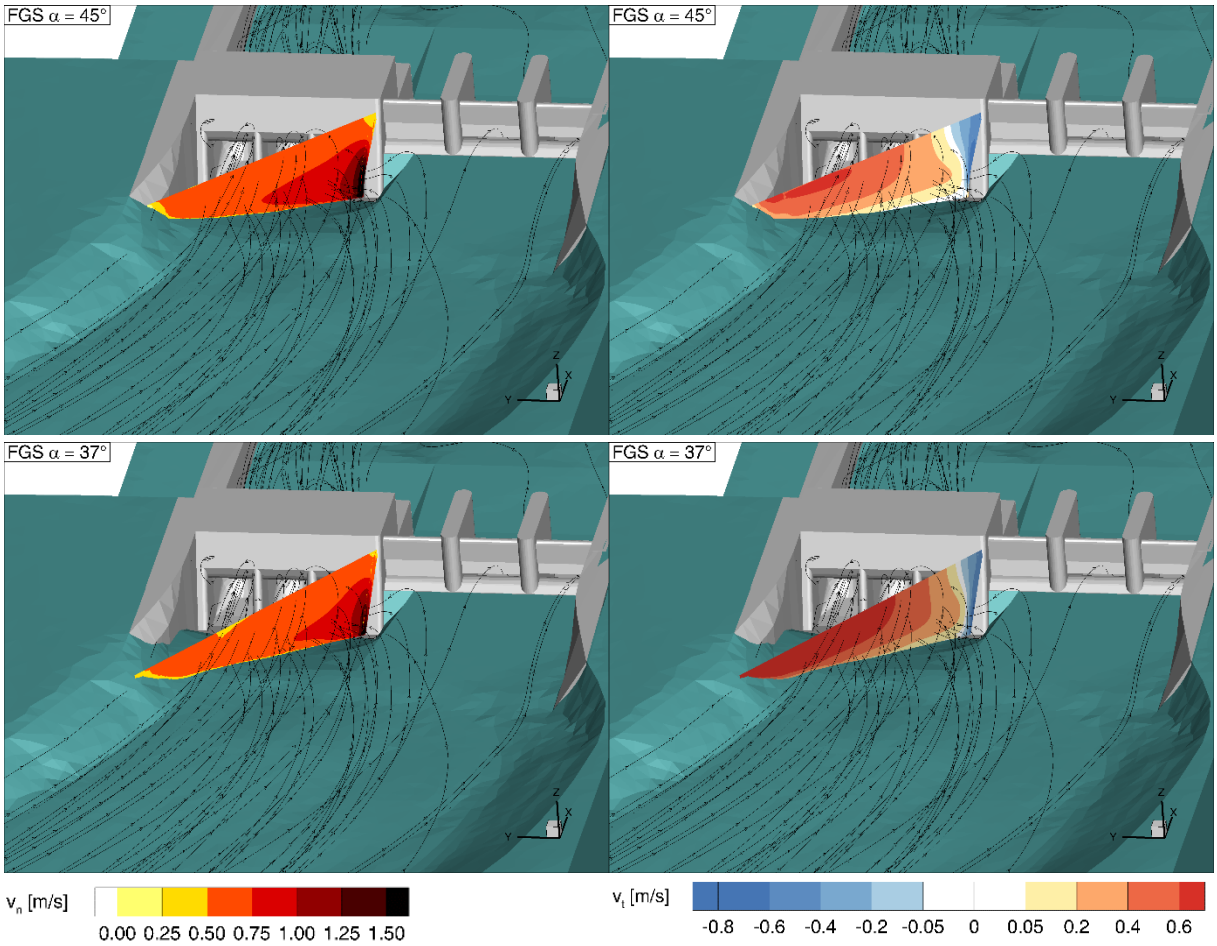

Figure 28: Normal (left) and tangential (right) flow velocities at potential FGF positions upstream of the turbine inlets for scenario 2a for FGS angled at 45° (top) and 37° (bottom).

Weir passage

During scenario 2a the gates of the weir fields (WF) 2 and 3 are open and 231 m³/s are released via the weir. This leads to flow velocities of up to 10 m/s at the weir crest (Figure 29). At the bottom of the stilling basin, velocities reach up to 7 m/s. The impact velocity at the baffle blocks at *x* = 9 m is about 5 m/s, which is a potential threat for fish migrating downstream via the weir. The vectors in the sectional plot of Figure 29 clearly show the roller in the basin with backwards circulation at a magnitude of up to 3 m/s close to the water surface.

During scenario 2b, overflow at all weir fields plus gate flow at WF 3 occur and 106 m³/s are released via the weir. The overflow jet reaches velocities of up to 10 m/s (Figure 30). At the bottom of the stilling basin, velocities reach up to 5 m/s. The impact velocity at the baffle blocks at x = 9 m is about 2 to 3 m/s. which might by a potential threat for fish migrating downstream via the weir. Similar to scenario 2a, the roller inside the basin occurs with a backward circulation at a magnitude of up to 2 m/s for this scenario.

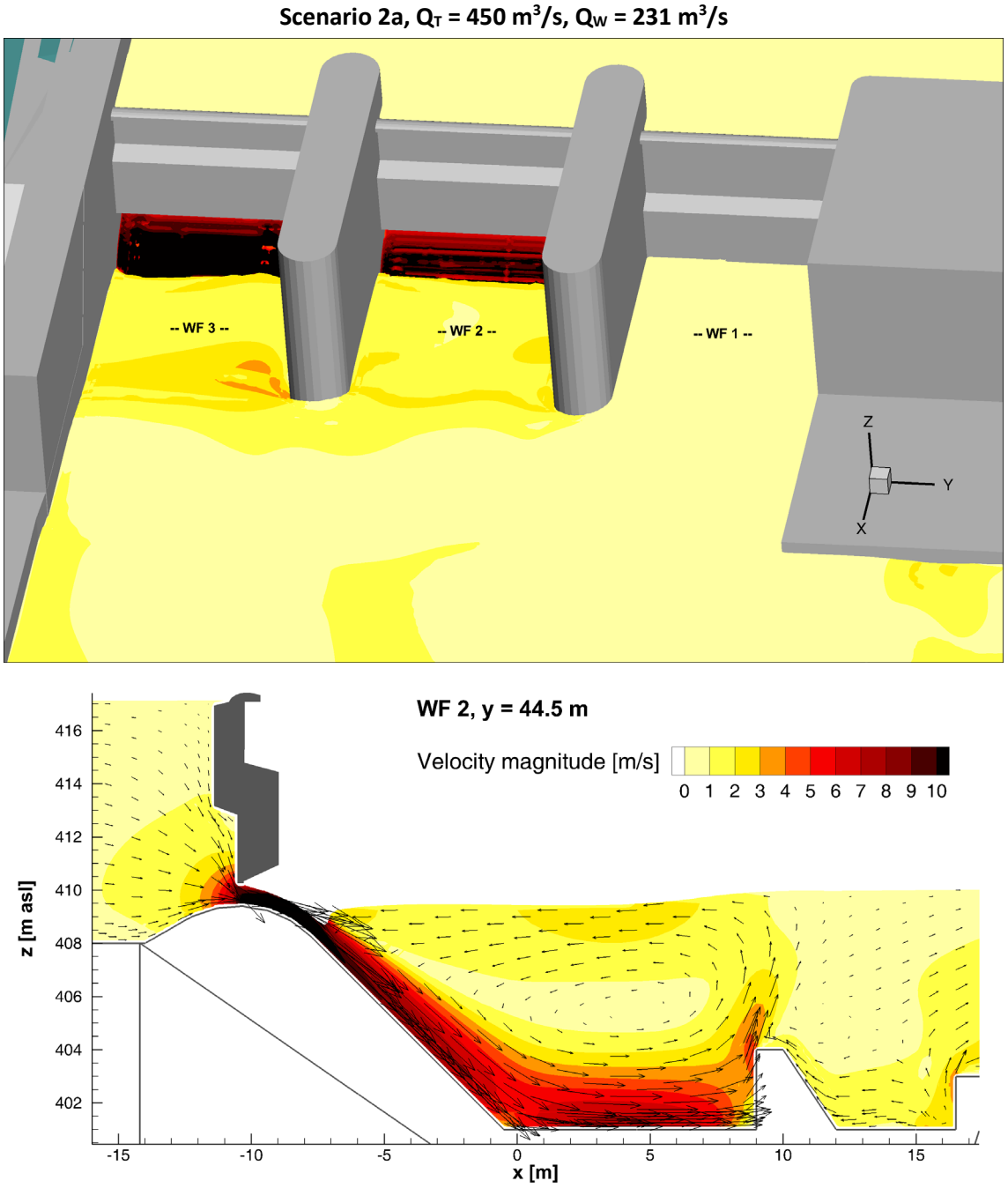

Figure 29: Velocity magnitudes at weir discharge for scenario 2a: Gate flow occurs at field 2 and 3, field 1 is closed. The depicted cross section is extracted at position y = 44.5 m in the middle of WF 2.

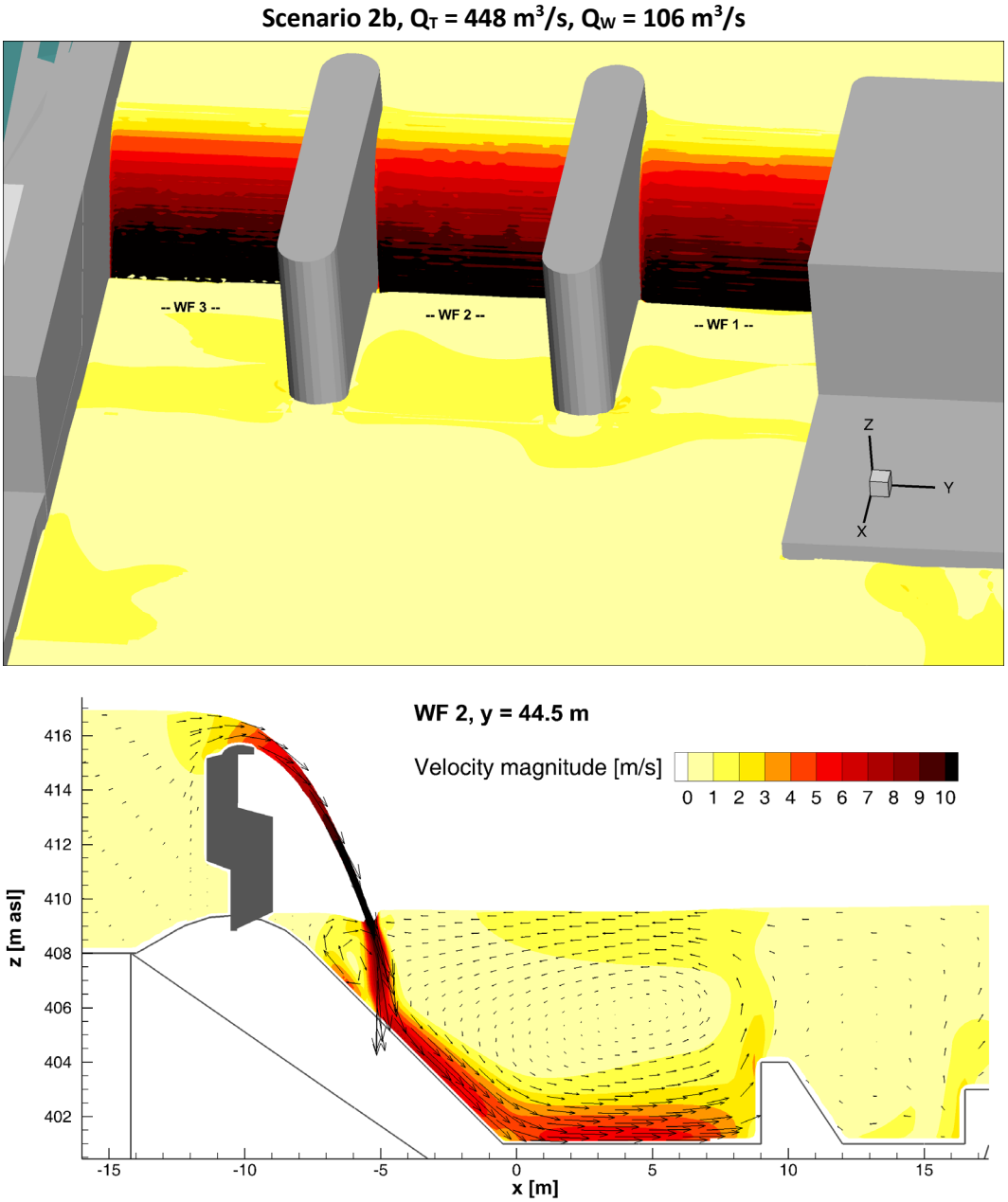

Figure 30: Velocity magnitudes at weir discharge for scenario 2b: Overflow occurs at WF 1, 2 and 3 plus gate flow at WF1. The depicted cross section is extracted at position y = 44.5 m in the middle of WF 2.

Discussion of the results for fish passage over the weir

[7] and [8] published considerable material dealing with Atlantic Salmon mortality at spillway passage. Passage through spillway may cause direct physical injury, increased exposure to predation, temperature change, atmospheric gas supersaturation, sub-lethal effects and/or stranding below the spillway. Neither large nor small fish can sustain impact velocity larger than 16 m/s when they fall in free-fall conditions. Above this critical flow velocity, significant damage occurs such as injuries to the gills, eyes and internal organs. The terminal velocities are approx. 16 m/s for fish in a 10 cm -13 cm size range and 58 m/s for fish in 60 cm. The smaller fish reach their terminal velocity at approx. 30.5 m fall height. At HPP Bannwil, the overflow velocities of up to 10 m/s (scenario 2b) are below the terminal velocities of small fish and hence no fish injuries is expected due to fall velocities. However, due to back-roll and possible atmospheric gas super saturation (>100%) in the stilling basin in both scenarios

2a and b, fish are exposed to predation and strike to baffle blocks and gas-bubble disease, respectively. The latter, i.e. the phenomenon of total dissolved gas super saturation (TDGS), has become of scientific interest mainly due to observations at the Columbia River (US), mainly at deep stilling basins of some 20 m depth where gas becomes dissolved. Exposure to TDGS can be fatal to fish and other aquatic organisms causing a so-called Gas Bubble Trauma (GBT) [9]. At Bannwil, TDGS is unlikely, however, as the hydrostatic pressure in the stilling basin is below critical values according to observation. It is also possible to model the phenomenon of air entrainment with the numerical 3D model, which could provide an estimate of the risk for GBT associated to downstream fish migration via weir discharge.

3.1.3.3 Fish monitoring

Hydro-acoustic analysis

The results of the data analysis show only little fish passage through the trash rack. 25 fishes were counted during the 5 runs. The highest number of fishes was recorded at position VI with 7 fishes. In addition during the continuous recording at position VI 49 fishes were detected. Figure 31 shows the number of detected fish and the registration time for all positions, while Figure 32 shows the length / frequency distribution of the detected fishes.

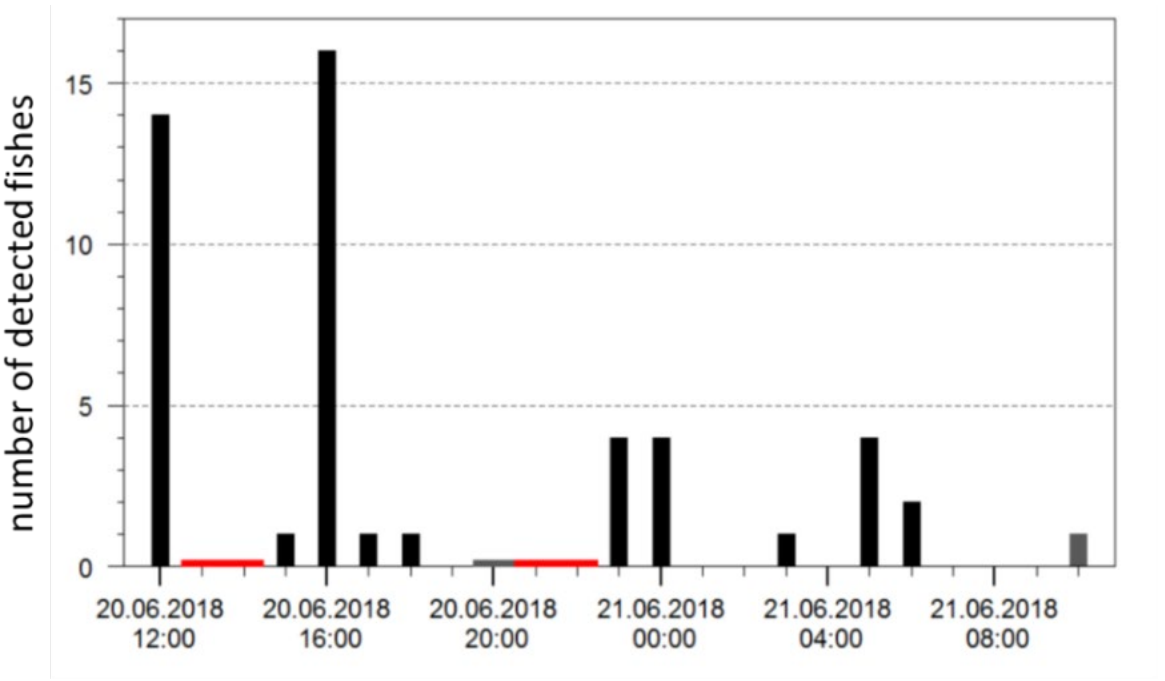

Figure 31: Number of detected fishes and time of registration for all 6 positions at HPP Bannwil intake trash rack. The red lines indicate data gaps.

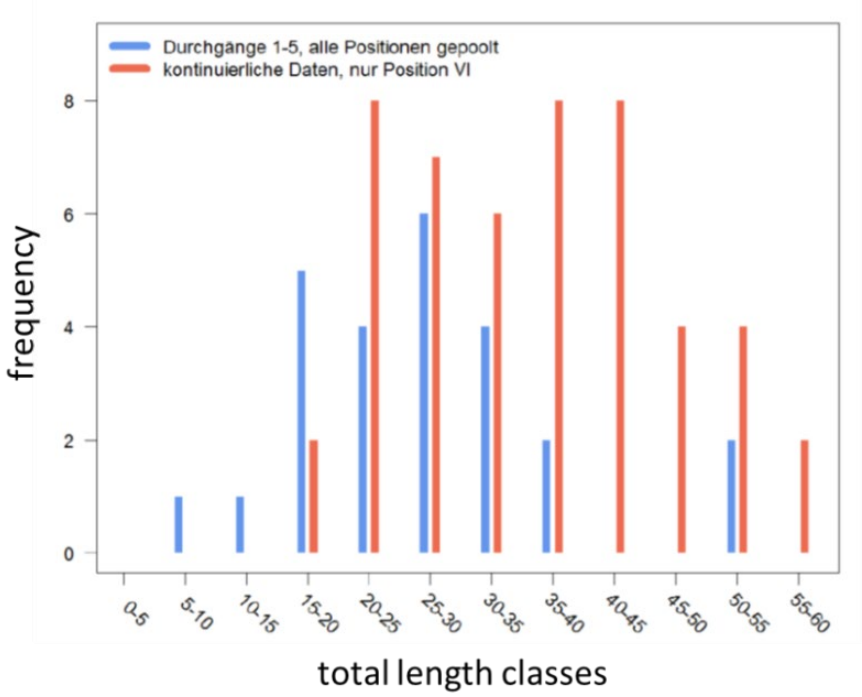

Figure 32: Total body length [cm] vs. frequency distribution of detected fishes at HPP Bannwil intake trash rack. Blue bars: pooled data for the 5 runs, red bar: continuous data, only position VI

The behaviour of fishes in front of the trash rack in terms of swimming depth is documented in Figure 33. The range of the observed fish swimming depth at position VI is between 2.3 and 14.5 m below the water surface. Individuals concentrate at depths between 4 and 8 m. However, during the 5 runs only few fishes were detected at this depth range.

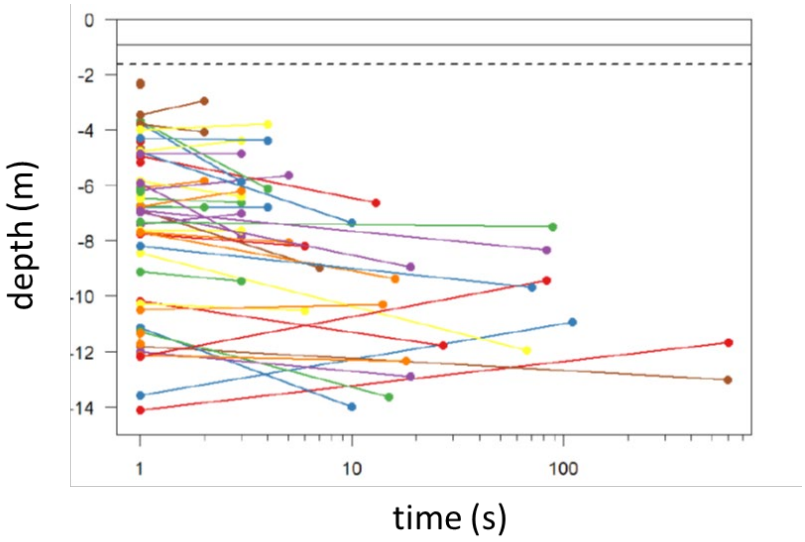

Figure 33: Swimming depth of all fishes registered during the continuous data analysis at position VI at HPP Bannwil intake trash rack (N=49). The colors serve only for a better identification of the individuals.

In summary, fish lengths ranged from 5 cm to 60 cm and individuals were detected at depths from 2.3 to 14.5 m below the water surface. The swimming motion was directed downwards in 70% and towards the concrete wall on the left riverbank in 55 % of the cases. The tracking of 6 individuals revealed two different kinds of behaviour: 3 passed through the sonar beam in a straight motion at

comparatively high speeds, whereas the remaining 3 stayed in the beam much longer, slowly moving up- and downwards in front of the left concrete wall. The distribution of fish locations is neither vertically nor horizontally homogeneous. Additional hydroacoustic observations would be interesting at another time of the year (e.g. in late autumn).

Radio telemetry analysis

Barbels were tagged on April 2 and December 17-18 in 2019. The length frequency histogram gives an overview about the 57 tagged barbels (Figure 34).

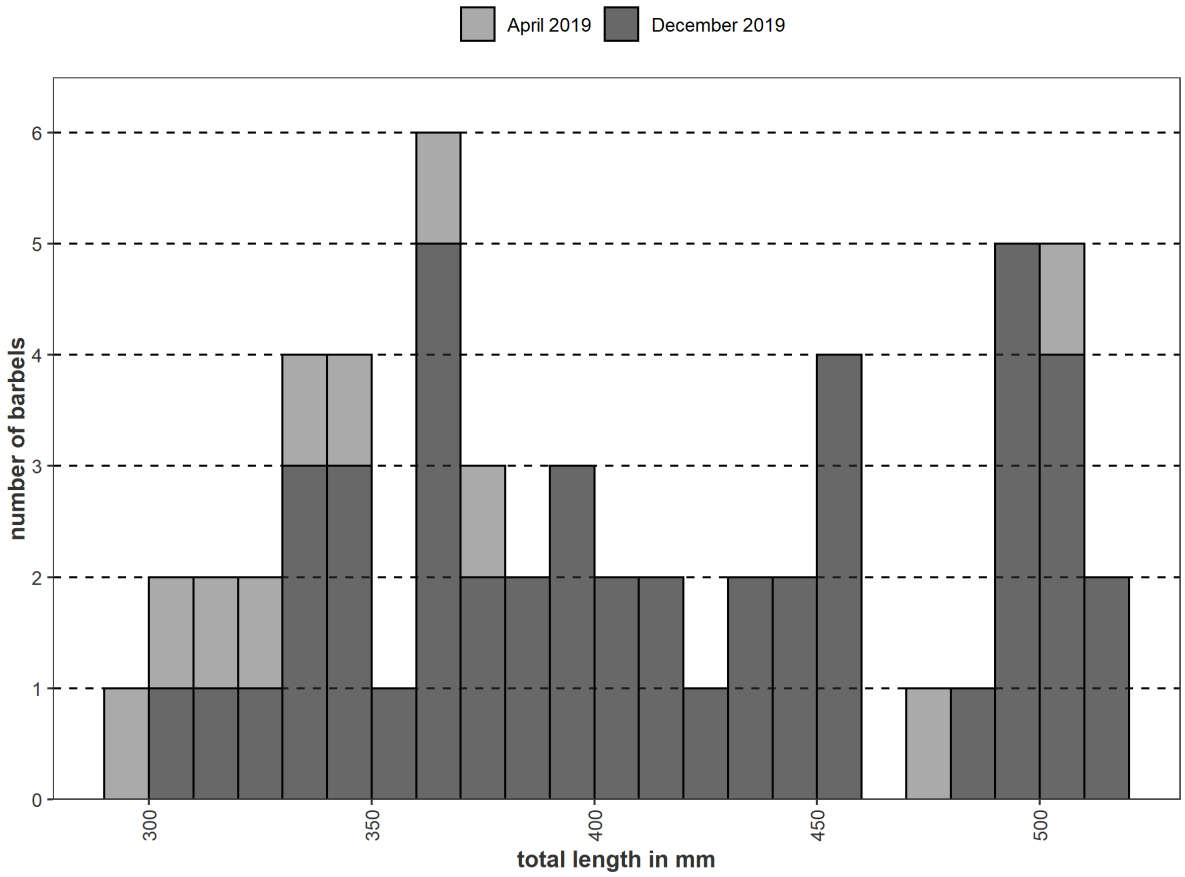

Figure 34: Length frequency histogram of the 57 barbels radio tagged in April and December 2019.

The length-weight relationship of these barbels is shown in Figure 35.

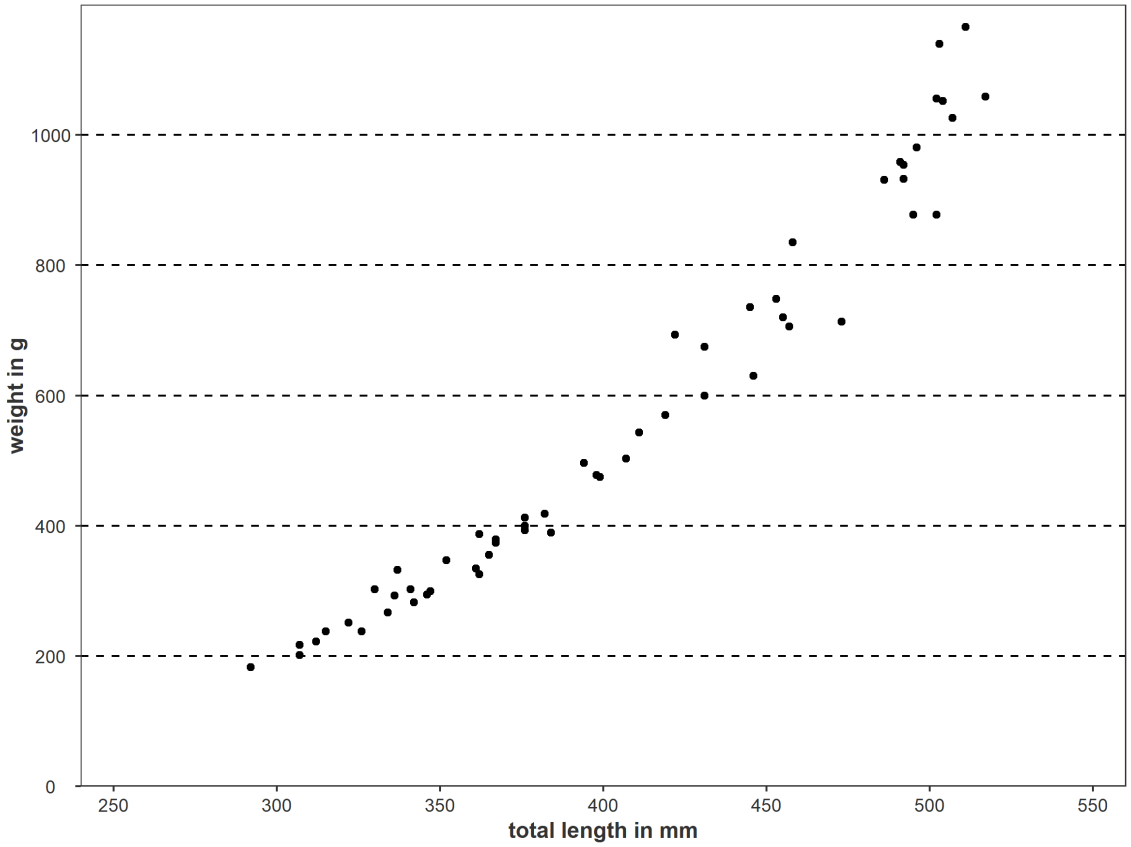

Figure 35: Length-weight relationship of the 57 tagged barbels.

In order to keep the tag/body mass ratio of 2%, fish with a minimal weight of 150 g were tagged with nano tags and fish of 400 g and 600 g weights were tagged with medium size transmitters and transmitters with pressure sensors, respectively.

10 barbels were tagged on April 2 2019. They were used in a preliminary test to make sure that the used transmitters were detectable in the forebay of the hydropower plant. Three individuals were never detected again. Three of them moved downstream of the hydropower plant. However, the migration corridor and the date of the descent were unknown because the radio telemetry installations could not be installed before November 2019. Four barbels stayed in the forebay and were detected during the manual tracking.

47 barbels were tagged on December 17/18 2019 and released upstream of the hydropower plant. The detection rate for these individuals was 100 %. They were either found during manual tracking or they were registered on the fixed telemetry stations.

After releasing 57 barbels (10+47), 31 individuals (54 %) did not migrate downstream, they stayed upstream of the hydropower plant till the end of the study period in August 2020. 23 individuals (40 %) passed the hydropower plant using one of the migration corridors described below.

Migration corridors for downstream migrating fish

***Unknown migration corridor*:** for three individuals the downstream migration corridor is not known. They all were tagged and released in April 2019 before the fixed antennas were installed at the hydropower plant.

***Fish ladder*:** none of the tagged individuals migrated through the fish ladder down to the tailrace area. However, two individuals used the fish ladder as a refuge (ID 63 in winter, ID 76 in summer) entering from the forebay. After a certain time, they left the fish ladder again in the upstream direction. These movements were detected by the PIT-Tag antennas.

***Spillway**:* Only one individual used the spillway as a migration corridor (ID 193 with 367 mm total length). The fish passed the spillway on December 24 at 2:49. The spillway was in operation since December 23 at 22:00. Therefore, the fish passed 4-5 hours after the spillway overflow started. The fish survived the passage and entered the fish ladder for refuge seeking over winter. On May 3 2020 the barbel left the fish pass and migrated in the downstream direction of the river where it was manually tracked.

Based on the analysis of the signal strength, the barbel used the spillway 2, the one in the middle (Figure 36). Immediately after the passage, the downstream YAGI antenna detected the fish in the tailwater. The subsequent tracking results confirmed the survival of the fish during the passage.

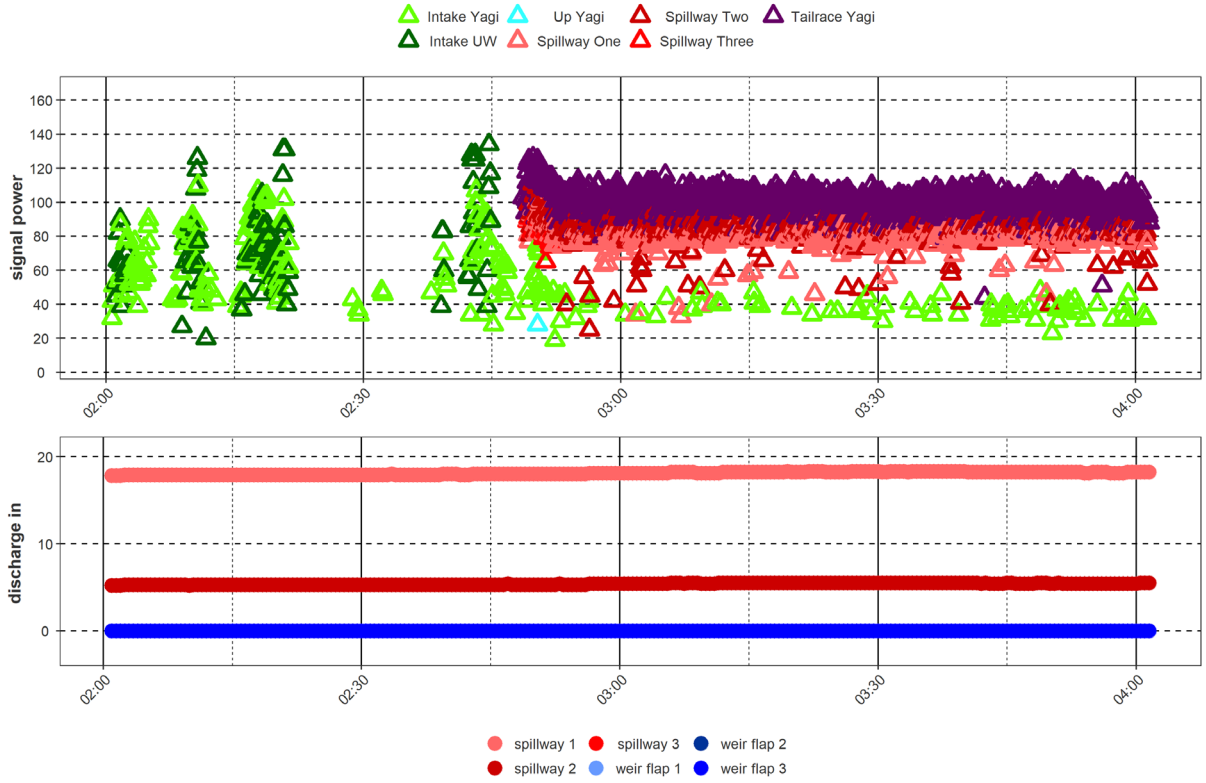

Figure 36: Spillway passage of barbel (ID 193).

Turbine passage: 19 individuals used the turbine passage for the downstream migration. Except one fish (ID 209, passage time 08:35), all the individuals passed the HPP at night (Table 3). Due to the antenna setup it was not possible to determine exactly which of the three turbines was used for the descent.

All downstream migrations happened within 28 days after release of the fish. However, 70 % of the individuals migrated downstream and passed the HPP within 2 days. On December 23, 4 days after the

release of the barbels in the forebay, spillway overflow happened for the first time (Figure 37). At this time, 14 individuals had already passed the hydropower dam by the turbines. The discharge over the spillway lasted 6 days. Only one barbel used the spillway passage during this period. But at the same time 3 individuals passed through the turbines despite the simultaneous overflow. 13 of the barbels survived the passage of the hydropower plant, 3 died during the turbine passage, and for 4 barbels the passage survival is uncertain.

Table 3: Hydropower passage of 20 downstream migrated barbels. Except ID 193, all individuals passed through the turbines.

barbel ID	Total length in mm	descent time	Passed time in hours after Release and start of the descent	survival after passage
30	431	17.12.2019 23:03	9	yes
67	382	18.12.2019 01:50	13	yes
68	407	18.12.2019 04:25	15	yes
208	307	18.12.2019 07:54	20	no
209	361	18.12.2019 08:35	16	yes
23	504	18.12.2019 22:31	6	yes
184	336	18.12.2019 23:36	7	yes
194	367	18.12.2019 23:00	7	uncertain
61	399	19.12.2019 00:01	7	yes
204	362	19.12.2019 01:00	36	no
187	362	19.12.2019 01:04	11	yes
205	322	19.13152.2019 01:05	11	yes
212	315	19.12.2019 03:45	16	yes
41	455	19.12.2019 05:38	36	yes
71	376	19.12.2019 23:00	57	uncertain
193	**367**	**24.12.2019 02:49**	**108**	**yes**
37	496	25.12.2019 01:15	157	yes
65	384	27.12.2019 01:00	225	uncertain
60	419	05.01.2020 04:42:38	420	no
43	517	15.01.2020 05:21	685	uncertain

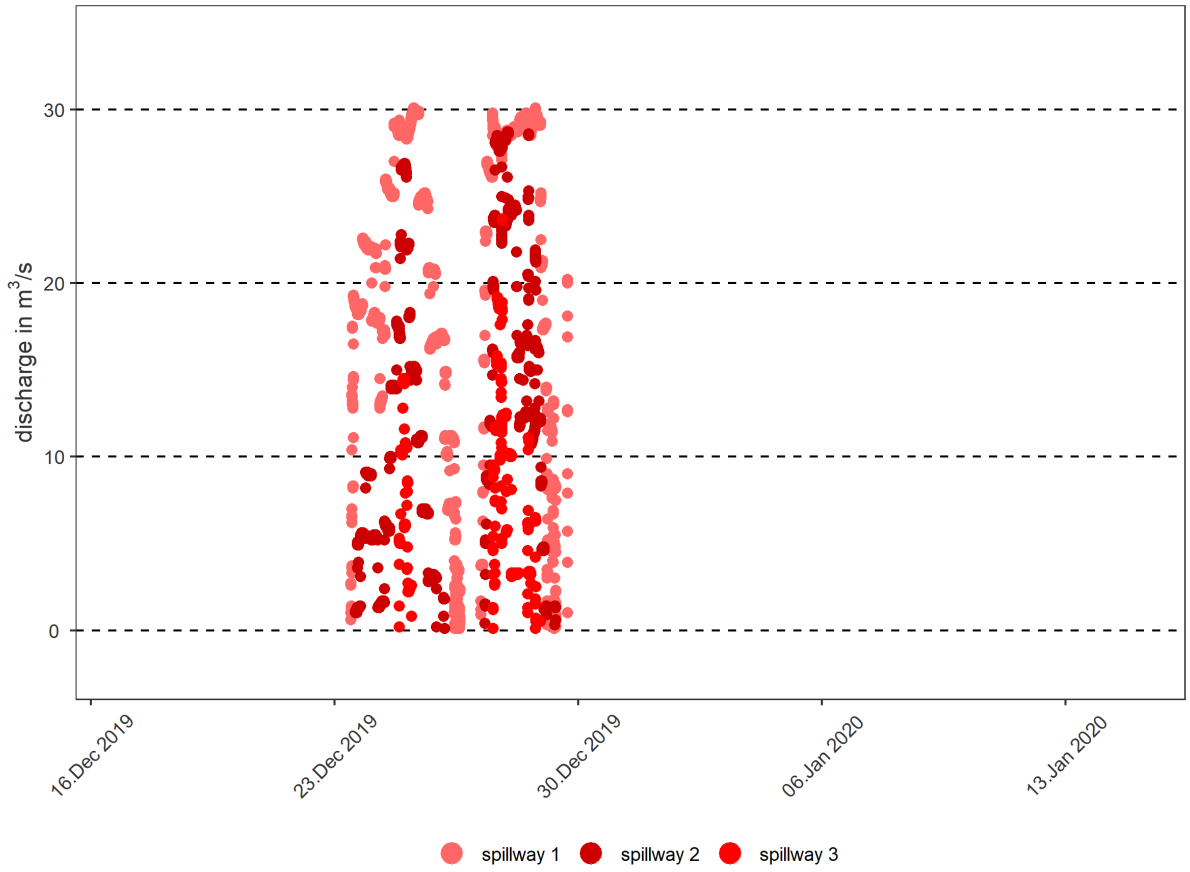

Figure 37: overflow on the spillway between December 16 2019 and January 15 2020.

The figure of the downstream migration of ID 23 shows the detections of the fish in the forebay between 22-22:30 o'clock (Figure 38). The barbel entered the turbine at 22:31 where it was immediately detected by the underwater antenna of the turbine exit. Subsequently the registration started on the tailrace YAGI antenna, where the fish was detected with a quite higher signal power than from the intake YAGI antenna. The plot shows exemplarily the depth use of the fish 15 minutes before the turbine passage. The barbel was mainly in a water depth between surface and 3 m. Before the turbine entrance the fish dove down to 7 m and left the turbine at a depth of 2 m. Therefore drastic barotrauma effects could have affected the barbel. However, the subsequent tracking during the next days and months confirmed the survival of the fish. This plot demonstrates how the downstream passages were analyzed for all the individuals.

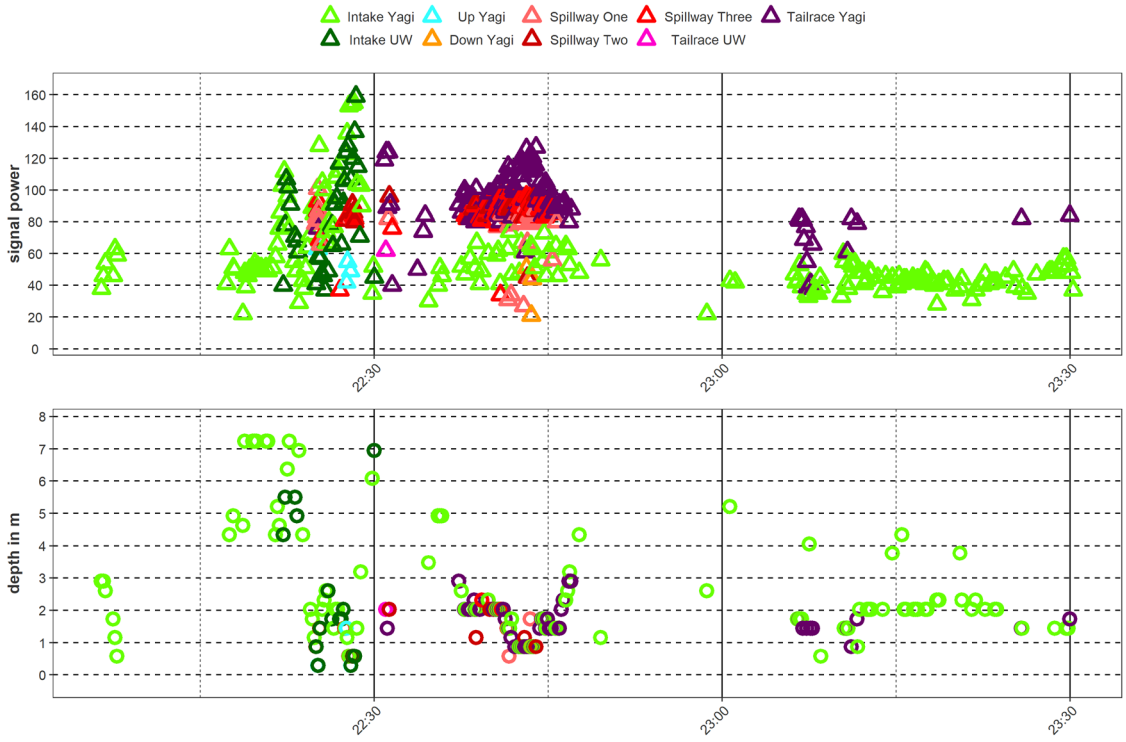

Figure 38: Downstream migration of the barbel with ID 23 (total length of 504 mm). The fish used the turbine as a downstream migration corridor and entered the turbine on December 18 2019 at 22:31(6 hours after release). At the time of descent, there was no overflow at the spillway.

The depth use of the barbel ID 41 between 01:30 and 02:30 are visible on the left side of the plot, registered by the Intake and Upstream Yagi antennas (Figure 39). The barbel used the water column between 0.5-14 m. The survival of the fish after the turbine passage is “likely”.

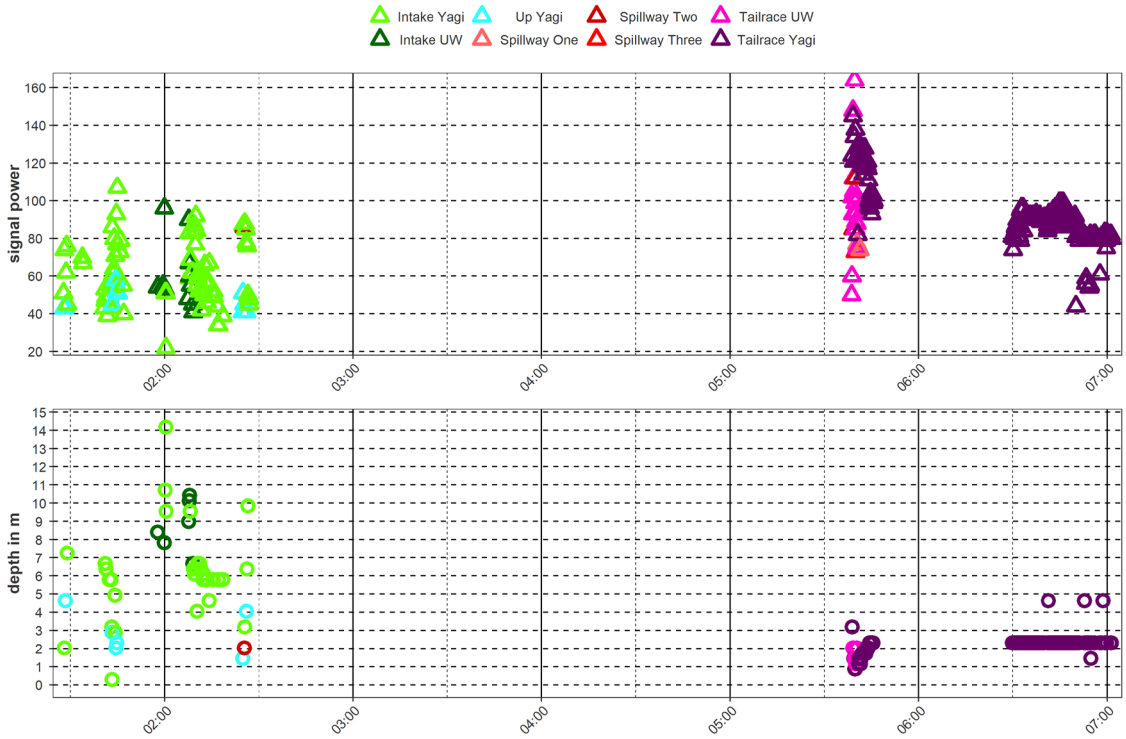

Figure 39: Downstream migration of barbel ID 41through the turbine on December 19 at 05:38:36.

The barbel (ID 204) was tagged with a nano tag and therefore no depth information is available. The spillway had no overflow at this time. Around 20:00, the fish was registered in the forebay. At 01:08:45 o'clock the barbel left the turbine (Figure 40). The analysis of the subsequent tracking patterns after the passage confirm that the fish did not survive the turbine passage.

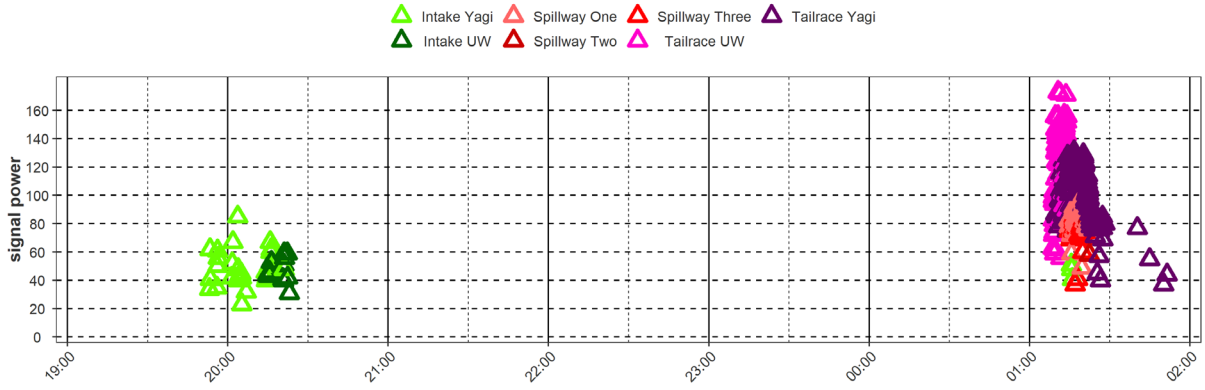

Figure 40: Downstream migration of barbel (ID 204) through the turbine on December 19 at 01:08:45.

The barbel (ID 60) was equipped with a transmitter with a beep interval of 2 s, but without depth sensors. The barbel spent a long time in the forebay prior to its descent and it might be interpreted as a searching pattern. There was no flow over the spillway at this time. At 04:42 the fish passed through the turbine (Figure 41). The fish did not survive the turbine passage.

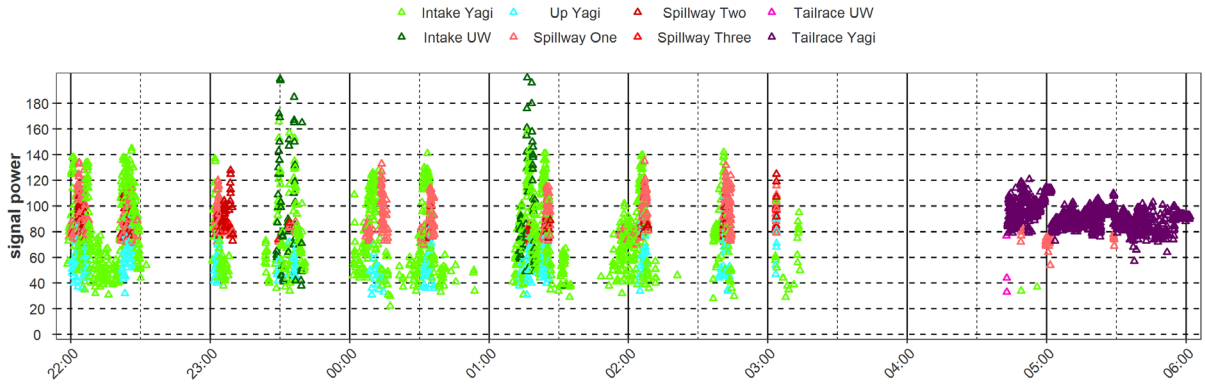

Figure 41: Downstream migration of barbel (ID 60) through the turbine on January 5 at 04:42:38.

Use of depth before the turbine passage

Barbels (ID 23, 30, 37 and 41) were using the deeper water column (> 4 m deep) excessively prior to the passage through the turbines. The fish with ID 30 only used the deeper areas. The sudden change in pressure at the end of the turbine could have negative effects on the survival. However, the fish survived the turbine passage. This is also true for the barbel with the ID 23, 37 and41. Unfortunately, we do not have depth profiles before and after the turbine passage for a fish that did not survive the passage. The effect of depth on mortality is greater on fishes that were acclimatized at deeper water depth [10] before the turbine passage. Therefore, an acclimation close to the surface before the turbine passage is less harmful to fishes than an acclimation in deep water.

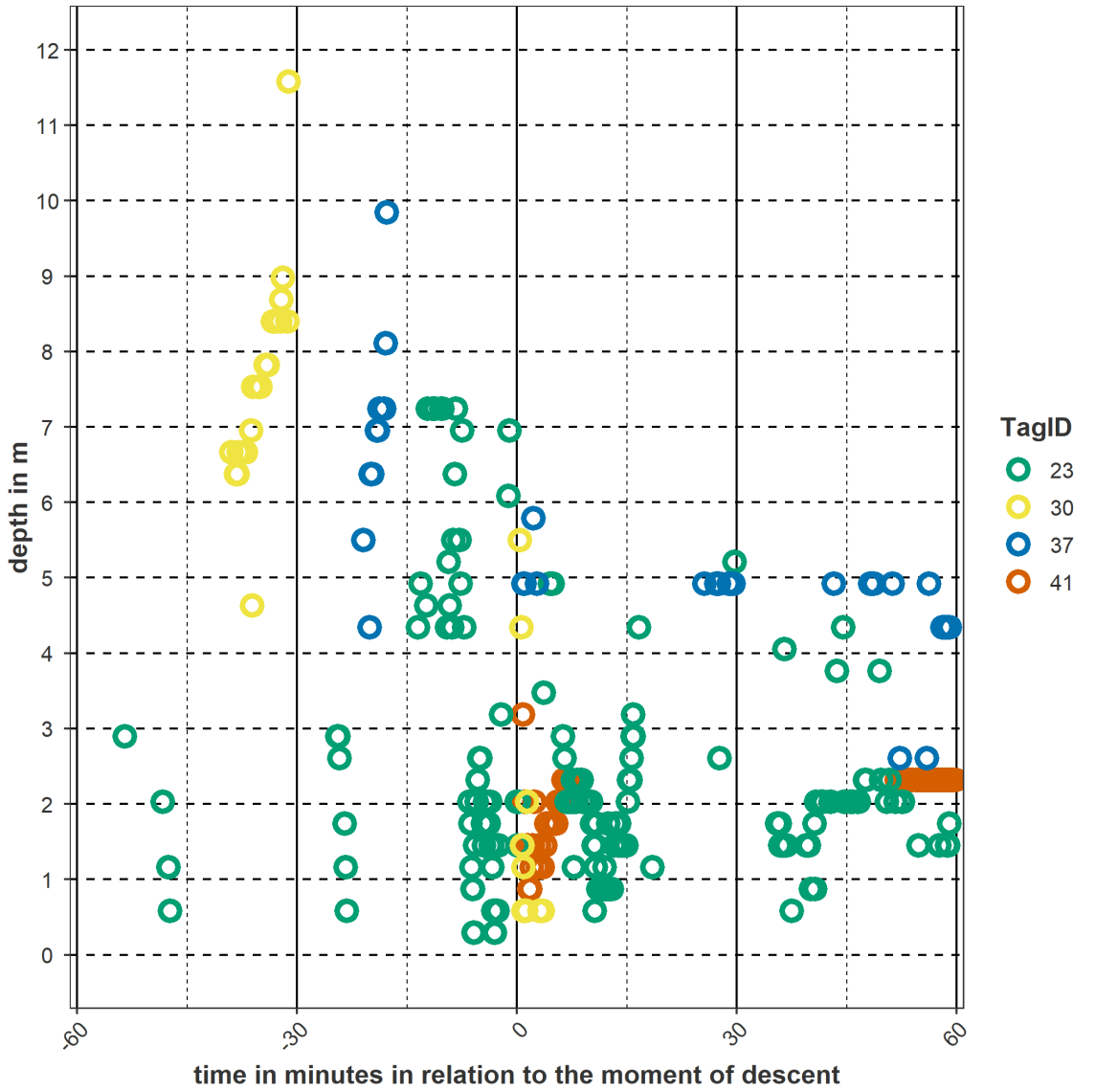

Figure 42: The use of depth for 4 barbels 60 minutes before the passage through the turbines and 60 minutes after the passage.

Distribution of tagged barbels in the Aare River

In order to quantify the distance of the area that a fish normally transverse during foraging, resting, reproduction and shelter seeking, the home ranges for the barbels were calculated [11]. The home range corresponds to the furthest upstream and downstream migration of an individual fish in the Aare River (Figure 43). Table 4 shows the appropriate home ranges and distances travelled from the HPP Bannwil. 44 individuals are included in the calculations (data from manual tracks). With a mean home range of 6.48 km, the chance is high that it expands at least over one hydropower plant in the Aare River. The distance between the HPPs Bannwil and Wynau is only 6.9 km. The barbel that migrated the longest distance downstream passed 3 HPPs and was manually tracked in the Aare River close to Olten.

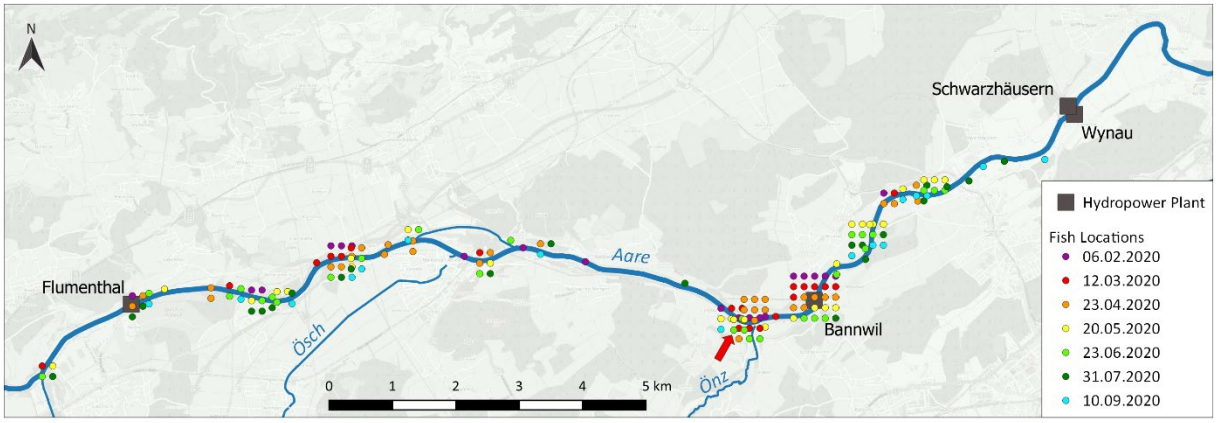

Figure 43: Distribution of the tagged barbels in the Aare River between Solothurn and Wynau. Red arrow: site of release. This map does not show all the manually tracked fishes. The individuals upstream of Solothurn (N=2) and downstream of Wynau (N=3) are not included.

Table 4: home range and migrated distances from the HPP Bannwil

	Min	Max	Mean	Std. Dev.
Home Range (km)	0.24	24.99	6.48	5.74
Max. Distance to Bannwil (km)	0.0002	23.77	6.37	6.10

Summary and suggestions for future radio tracking studies

The most important results of the study are summarized as:

- 40 % of the tagged fishes migrated downstream
- Downstream passage occured at night
- After the release of the tagged fish, downstream migrations happened within a few hours/days
- Only one barbel passed through the spillway. 19 fishes passed through the turbines.
- Fishes in front of the turbines used the range of available depth. They even had some preference for deeper places in the water column before they passed through the turbine.
- 12 of the barbels that passed the turbine survived. The survival rate is therefore at least 67 %. However, the survival for 4 individuals was uncertain. The estimated turbine passage survival rate is therefore between 67 – 84 %. This includes long time survival.
- The tagged barbels had a home range of 6.5 km. The migrations occurred in both directions, upstream and downstream. The longest migration distance was 25 km (downstream).
- None of the 19 used archival tags could be retrieved.

In order to gain a better understanding of downstream movements of fishes at hydropower plants the following recommendations are suggested:

- Prior to the installation of an antenna array on-site, field trials have to be carried out to establish reception ranges and noise detection problems. The noise can drastically fluctuate during the study period.
- Distribution of the tagging over several periods is recommended so that it will allow studying different discharge events and environmental conditions (water temperature, daylength) during the year. However, it is important that fishes are tagged and transferred during the active migration period.
- Tagging of a sufficient number of individuals. Because not all of the tagged fish migrated downstream, an appropriate detection of descending fishes is only-guaranteed by a reasonable number of tagged fishes. We therefore recommend to use at least 200 tagged individuals for downstream migration studies.
- The use of transmitters with depth sensors is very helpful and provides usable information. However, the tagging with pressure sensors is only feasible for larger fish (body mass > 600 g).
- Manual tracking is a valuable addition to the fixed telemetry stations. Manual tracking results help to interpret the downstream migrations at the automated fixed telemetry stations. Movement of manually tracked fishes gives a clue to their survival after passing a hydropower plant.

3.1.4 Conclusions & Outlook

We documented the current situation and investigated the efficiency of spill flow or water release as an operational measure at HPP Bannwil by means of field monitoring and 3-D numerical modelling in the area near the powerhouse and weir. The monitoring comprises:

- characterization of the flow field using ADCP
- 3D numerical simulation
- survey of the fish movements using ARIS Sonar and radiotelemetry techniques

Two field campaigns were conducted to measure river bathymetry and flow velocities around the HPP with discharges Q = 402 and 143 m^3/s using an ADCP. The ADCP data were used to construct the 3D numerical model of the HPP and calibrate and validate the model. The 3D numerical model was capable to simulate the major flow patterns upstream and downstream of the HPP (velocity magnitudes, flow directions, water surface elevations), and the simulated flow fields matched well with the measured data.

For the purpose of planning future FGS at HPP Bannwil, the hydraulic conditions of two potential positions upstream of the turbine inlets were investigated by means of the 3D model simulations. Locations of a FGS with an angle of α = 45 ° and a length of about 58 m as wells as another one with an angle of α = 37° and a length of about 80 m were studied. For both scenarios with turbine discharge only, the hydraulic conditions at the potential FGS position are rather unfavourable. It is recommended to use the 3D model for an optimization process since such FGS can be added to the model quite easily.

Spillway or weir passage as an operational measure was numerically studied for the different scenarios. The results indicate that the spillway velocities are lower than the critical impact velocities of small and large fish and hence no injury is expected. However, due to back-roll and potentially atmospheric gas supersaturation (>100%) in the stilling basin in both studied scenarios, fish can be exposed to predation and strike to baffle blocks and gas-bubble disease, respectively.

The fish monitoring study with hydro-acoustic technique provided fish behaviour data in front of the turbine intakes. However, the results do not allow to draw a general conclusion on fish behaviour in front of the turbine intake due to the low number of detected fish during the field campaign.

Radio telemetry provide excellent capabilities for studying the downstream migration of fishes. Enhanced understanding on turbine or spillway passage can be provided and related to existing discharge condition. The use of depth by the barbels in the forebay and in front of the turbine can be studied if transmitters with pressure sensors are used. Unfortunately, this is only possible for larger fish (total length > 42 cm). The use of archival tags could also be an advantage in future studies. However, there are specific problems with archival tags. None of our 19 archival tags could be retrieved and therefore valuable information was lost. Finally, the collected fish monitoring data and hydraulic data will be used to develop measures to improve downstream fish migration.

3.2 Turbine passage: Barotrauma Detection System measurements (TUT, SJE, BKW)

Dynamic pressure fluctuations experienced by fish during the turbine and spillway passages will be studied at HPP Bannwil using a Barotrauma Detection System (BDS) developed at TUT (Figure 44). The data will be analysed and the results will be provided to Voith (WP2) for BioPA model by TUT. VOITH will build a CFD model of turbines at HPP Bannwil, run the model and compare model results with the BDS results. The results will be used for WP 3.3. Furthermore, VOITH will use the same CFD-models and focus on different operating modes to evaluate the possibility of adapting the operation for certain time periods. Finally, the results from TUT and VOITH will be provided to TUM for fish turbine mortality assessment. SJE might help TUT for the field measurements and the analysis of BDS data.

3.2.1 Data

Data will be collected from the field campaign and literature. A complete list of the time series data collected by the sensors can be found in Table 5.

3.2.2 Methodology

In order to analyse the survival possibilities of fishes in hydroelectric turbines through swimming, we built in cooperation with the TUT Biorobotics Center “fish surrogates” that contain a plurality of underwater sensors. The device housing is made of a strong and durable polycarbonate, and the mechanical design of the entire device allows it to withstand and record turbine blade strike events. The electronics are equipped with three precision avionics-grade pressure sensors, which also measure the sensors temperature, and an inertial measurement unit that stores the absolute orientation, linear acceleration, rotation rate and magnetic field. The devices automatically calibrate themselves after turning on a reusable.

At a minimum, 30 data sets for each flow scenario should be recovered. This will take a minimum of one full 8-hour work day for each flow scenario. Based on previous BDS site investigations, it is recommended that one day be allocated for testing the injection system and training the on-site staff for deployment, recovery and quality control during the field work. Therefore, a minimum of 3 full workdays will be required at Bannwil to conduct the FITHydro BDS field work.

Table 5: Overview of the BDS text file data format. Each of the 27 columns corresponds to a different variable saved during turbine passage at 100 Hz (magnetometer 20 Hz), units given in parentheses.

Col 1	Col 2	Col 3	Col 4	Col 5	Col 6	Col 7	Col 8	Col 9
Timestamp (ms)	Pressure left (hPa)	Left temp (°C)	Pressure center (hPa)	Center temp (°C)	Pressure right (hPa)	Right temp (°C)	Euler angle X (deg.)	Euler angle Y (deg.)
Col 10	**Col 11**	**Col 12**	**Col 13**	**Col 14**	**Col 15**	**Col 16**	**Col 17**	**Col 18**
Euler angle Z (deg.)	Quat. X (-)	Quat. Y (-)	Quat. Z (-)	Quat. W (-)	Magnet. X (µT)	Magnet. Y (µT)	Magnet. Z (µT)	Dynamic linear accel. X (m/s²)
Col 19	**Col 20**	**Col 21**	**Col 22**	**Col 23**	**Col 24**	**Col 25**	**Col 26**	**Col 27**
Dynamic linear accel. Y (m/s²)	Dynamic linear accel. Z (m/s²)	Rate gyro X (rad/s)	Rate gyro Y (rad/s)	Rate gyro Z (rad/s)	Calibration status magnet. (0-3)	Calibration status accel. (0-3)	Calibration status gyro. (0-3)	Sum calibration status (0-9)

Fish undergo extreme conditions:

- Pressure rate of change of 100m water column in less than 1 sec
- Blade strike > 10 g acceleration
- Flow velocities of 10-20 m/s near turbine blade

Barotrauma Detection System (BDS) are capable of recording these extreme conditions:

- Span: +/- 5 bar (~50m of water level)
- Recording rate: configurable 100Hz / 250Hz (4096/1024 samples/recorded value)
- Absolute orientation of sensors to compare position during passage
- Inertial measurement unit: 3D linear acceleration, 3D body rotation rate, 3D magnetic field
- Temperature compensation of each individual pressure sensor
- Only barotrauma sensors with triple modular redundance (3x identical, independent pressure sensors)
- First barotrauma sensor with auto-levelling to reference atmospheric pressure (100 kPa)
- First barotrauma sensor capable of directly measuring pressure gradients (shear) as well as pressure magnitudes
- Length/diameter: 14.5cm/4cm
- Housing materials: Polycarbonate (tube body) / Polyoxymethylene (end caps)
- Impact tested up to 3000 g

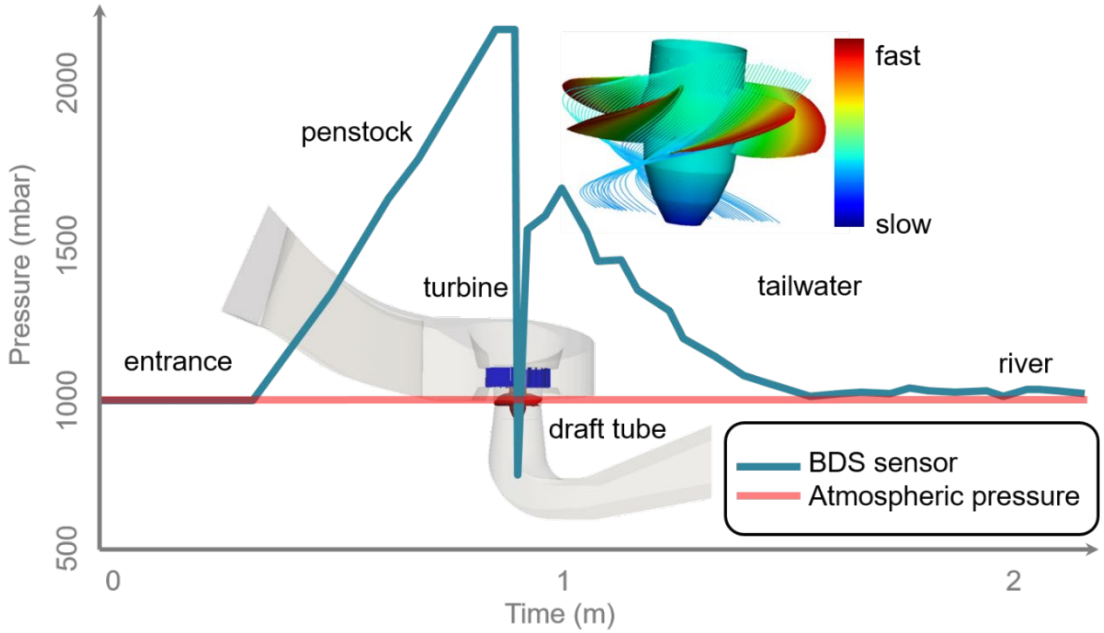

Figure 44: Barotrauma Detection System (BDS) and illustration of the multiple regions in which pressure changes occur that fish experience during turbine passage (vertical Kaplan).

3.2.3 Results

The results of the BDS are a statistical analysis of the time series data for each of the sensor modes (e.g. pressure, acceleration, etc.). The following parameters are calculated for each individual measurement: min, max, mean, median, standard deviation, Q1, Q3 and the number of blade strikes. These statistical parameters are then aggregated according to the flow scenario (full or half-load) and injection location (low, mid, high) into ensembles representing the distributions of each parameters. In this way, each hydropower plant can be compared using a set of reproducible, statistically-derived parameters. For example, if the number of blade strikes differs between flow scenarios but only significantly between two different injection heights, it is possible to “drill down” into the data by comparing the ensemble statistics to gain insight into the physical environment during passage and suggest corrective measures such as installing fish avoidance targeted at a particular location. The results of the study at Bannwil HPP are presented in Section 3.3.

3.2.4 Conclusions

See section 3.3.

3.3 Turbine passage: BioPA modelling (VOITH, BKW)

To analyse the fish passage through a turbine, Voith Hydro set up a CFD model of the turbine passage at HPP Bannwil. Different operating conditions were simulated to evaluate the possibility of adapting the operation for a certain period. In a second step the results are also compared with BDS measurement results, see chapter 3.2. The results are used in WP 3.3. Furthermore, all results from TUT and VOITH are also provided to TUM for fish turbine mortality assessment.

3.3.1 Data

With the help of the operating characteristics of the last 6 years, it was possible to determine in which operating points the turbines of Bannwil HPP were frequently operated and thus more relevant for the analyses of the impact on the fish population [12]. The operating data consists of 15-minute measured

values of the flow, generator power and the corresponding opening angle of the wicket gate. Figure 45 shows the flow duration curve in 2017. Comparing between the years reveals that the machines alternate to have a similar number of operating hours in a multi-year perspective. In 2017, the turbine of unit 2 had the highest operating time with 8760h.

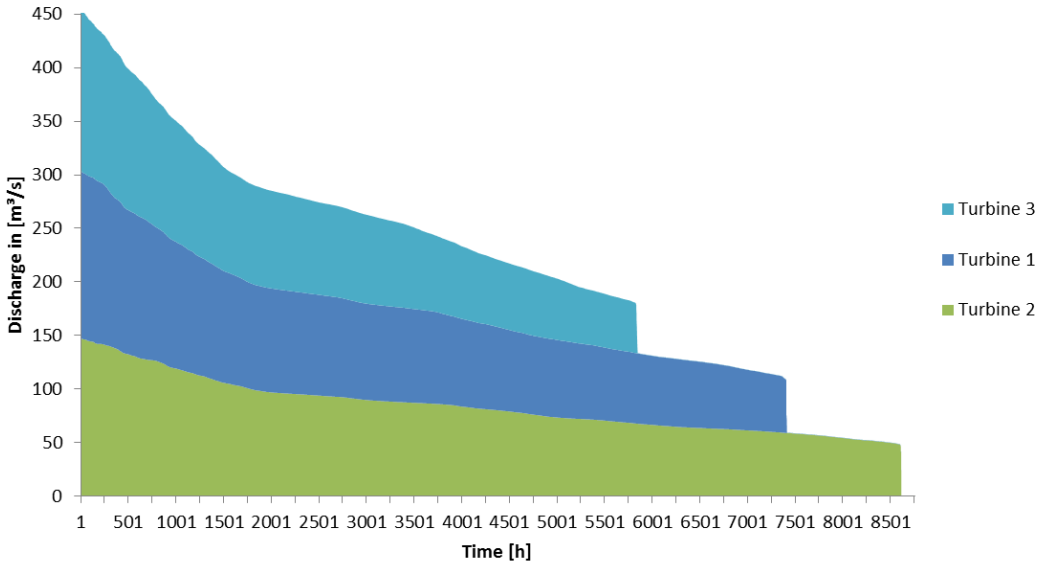

Figure 45: Annual discharge of Bannwil in 2017 according to the three machine units.

The power plant operation of the simultaneously operated turbines results in the annual load duration curve shown in Figure 46. It is visible that either all 3 turbines or 2 turbines are running simultaneously over the year. Each unit has about the same discharge, which is important to determine the tailwater level and estimate the fish passage of the entire system.

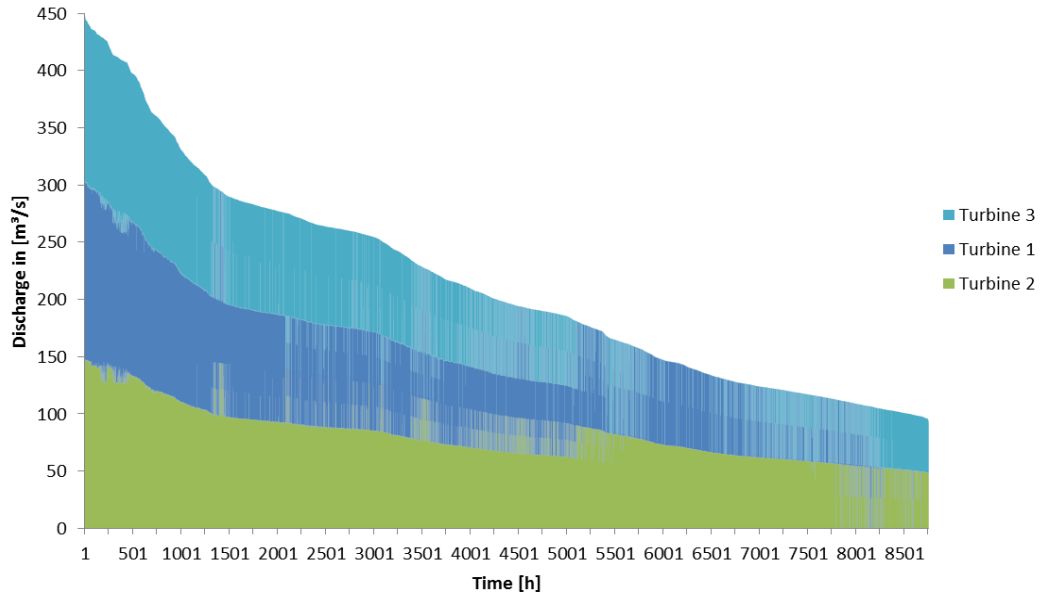

Figure 46: Annual Load Duration Curve (simultaneous).

The hill-chart of the turbines is shown in Figure 47, runner opening angle, wicket gate opening angle and efficiency are normalized to 100%.

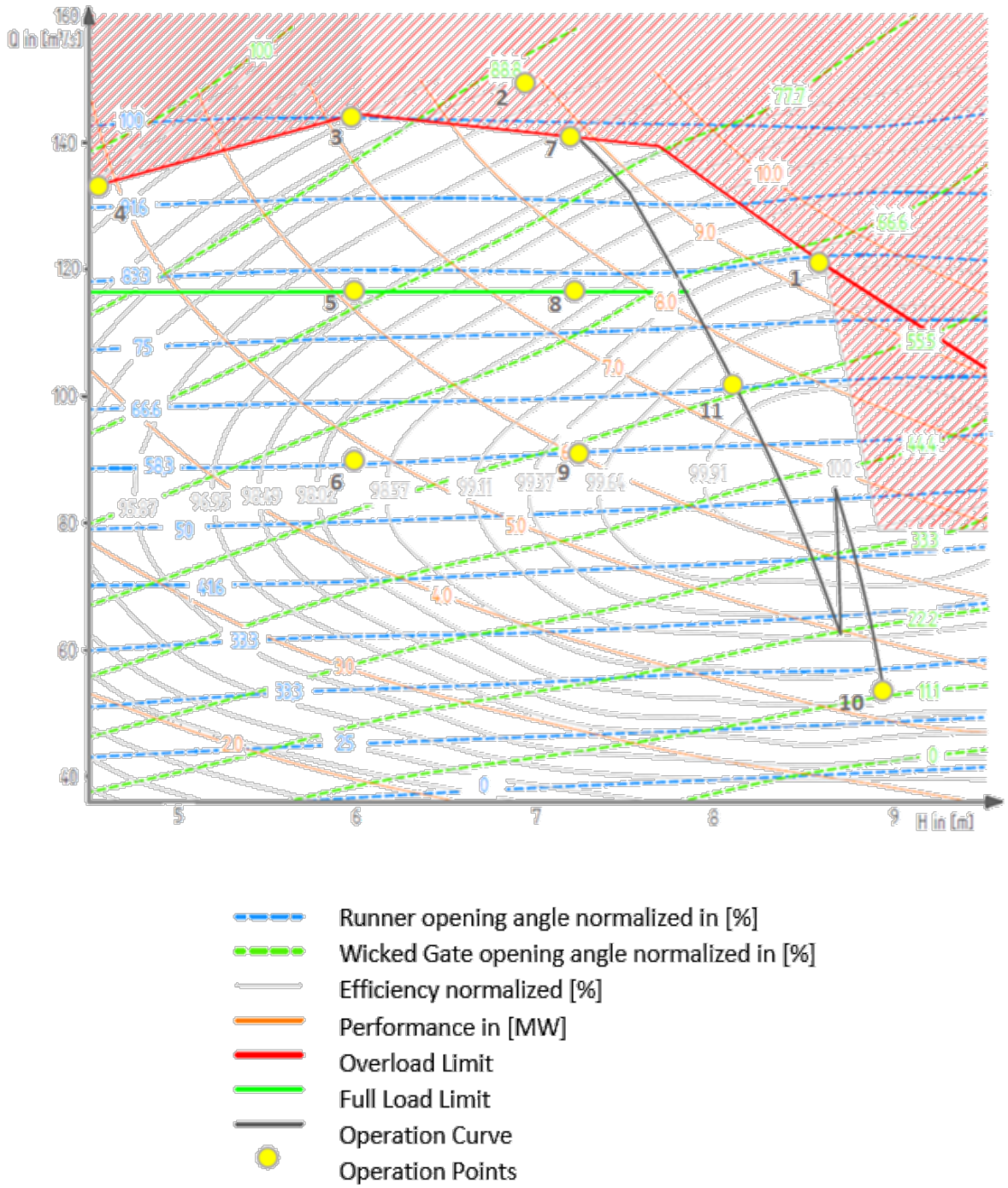

Figure 47: Normalized Hill Chart of Bannwil HPP.

The operation curve is shown in grey (Figure 47). The full load limit is marked in green, as well as the initial overload limit in red. For all illustrated operating points CFD simulations have been performed.

The investigated operating points are listed below:

Load case	Head [m]	Discharge [m³/s]	Wicket Gate Angle [%]	Runner Angle [%]
t01	8.65	122	79	82
t02	6.95	150	92	100
t03	6	144	94	98
t04	4	133	98	92
t05	6	116.5	87	79
t06	6	90	78	58
t07	7.2	142	88	97
t08	7.2	116.5	82	79
t09	7.2	90	74	58
t10	8.8	68	58	28
t11	8.2	100	74	64
t12	7.0	102	78	67
t13	4.5	90	85	59
t14	8.6	140	84	95

3.3.2 Methodology

To evaluate the influence of the turbine passage on the fish a biological performance assessment (BioPA) developed by Pacific Northwest National Laboratory (PNNL) is used. The analysis is based on a CFD simulation of the turbine assuming that a fish pathway follows a streamline through the turbine. The information of stressor exposure, including pressure, strike, shear and turbulence can be extracted from the streamlines and leads to an exposure probability based on the total amount of streamlines applied. To obtain a measure of injury risk, the estimated exposure to the stressors during turbine passage is related to the fish response to them. The so-called dose response value is multiplied with the exposure probability at that stress level, obtained from the exposure estimate. Integrating these risks over all values of the stressor variable yields to the BioPA score (Figure 48). The BioPA score is high when the risk of passage injury is low. Richmond et al. describe in detail how the baseline BioPA score for the existing turbine unit at Priest Rapids was calculated [13]. It is understood that the score does not, at this time, represent a passage-survival estimate. The score should only be used to estimate the relative risk of one design compared to another. A scenario (a specific design and operating point) receiving a higher score than another scenario can be considered to have a lower injury risk to passing fish. The absolute risk cannot be reliably quantified at the present time.

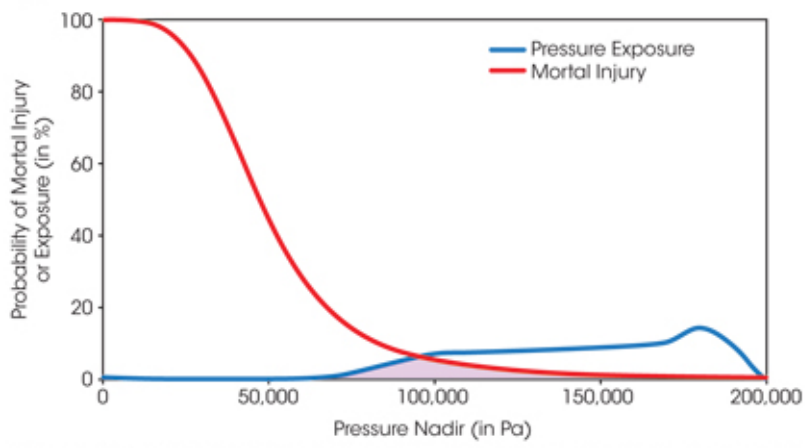

$$P_{Mortality} = \int (P_e \cdot P_m)\, dx$$

P_e=exposure probability of stressor

P_m=exposure mortality of fish

Figure 48: BioPA probability distribution and dose- response of pressure Nadir [13].

As the BioPA considers both fish response to a given stress level and exposure probability, the results provide additional insight into evaluating the size of the affected region within the turbine. For example, a geometry that produces a lower pressure within a small region of the water passage may have a negligible influence on the calculated risk of injuries through pressure. Developing an alternate turbine geometry that addresses the low-pressure region may result in higher component costs and lower turbine performance, without impacting the expected fish survival rate. The BioPA provides a systematic way to evaluate trade-offs associated with various hydraulic solutions.

Application on test case Bannwil

As a basis for the modelling of the HPP Bannwil the 3D-CAD geometry in Figure 49 was created based on the drawings of the power plant, which were kindly made available by BKW. Unfortunately, the geometry of the runner renewed in 1996 by Escher Wyss could not be made available in the original. For the studies a runner geometry from Voith Hydro, which was designed for a similar operating range and an equivalent specific speed, was used. Significant for the later simulation are in particular the wicket gate section, the runner and the draft tube. The inlet area of the power plant was also modelled to investigate its effect on the fish passage.

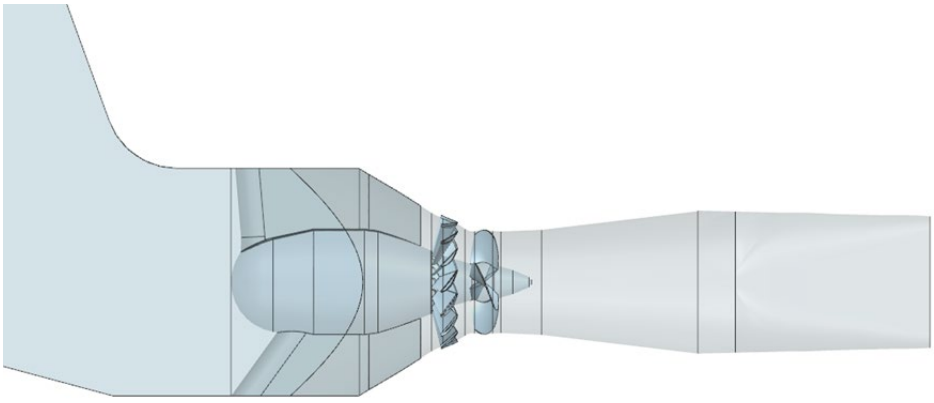

Figure 49: CAD Model of the Bulb Turbine in Bannwil

The CFD calculations for this study are stationary and calculated with the k-ω SST turbulence model. The whole 360°-machine was modelled, and simulations were performed at prototype size. The inflow condition was set to be mass flow and flow direction. The pressure level at the outlet is set to a constant pressure. The mesh generation of wicket gate, runner and draft tube was done with a Voith in-house tool, the inlet region was meshed with ANSYS ICEM. The results of the CFD were then analysed by extracting the required stressor variables from the streamlines and further post-processed by using the available dose response data of salmon in BioPA. For the analysis of the streamlines an ANSYS CFX macro was created to simplify the process compared to the Tecplot post-processing routine used in BioPA. Comparisons of results showed no significant difference in the results [14]. In the following the post-processing routine is described in more detail.

Creating the streamlines

Starting the evaluation process, the first step is to create streamlines within the flow field, which assumes that the fish floats through the turbine as a buoyant body. The number of streamlines can be determined variably by the user. However, the streamlines should be densly distributed to roughly correspond to the size of the fish to be examined. This covers all areas where the fish possibly could swim through. A sensitivity study showed that a streamline number of 5000 is sufficient for this case.

The streamlines are a standard post-processing object from CFX which describes the path that a particle with no mass takes through the fluid domain. „The path is calculated using a Runge-Kutta method of vector variable integration with variable time step control." [10, Chap. 10.4]

BioPA uses the program Tecplot for this step. Again, streamlines are created throughout all domains. The variable of the turbulent kinetic energy is directly taken over from the CFD simulation results. The pressure and the shear strain rate are calculated within Tecplot. To achieve the same results as in BioPA, the formulas are identical. The key benefit of the new routine is that the variables can be automatically created internally in CFX regardless of turbine type and orientation.

To make the data of the streamlines usable for the program, each streamline is represented as a sequence of points with X, Y, Z.-coordinates. The extreme values of the variables presented below, as well as the velocities in each direction are written in a large matrix and exported into a file. This contains all the basic information needed in the further process.

Pressure

As the pressure at the outlet of the turbine domain is set to 0 as a default for stationary CFD, the atmospheric pressure p_{atm} and the hydrostatic pressure p_{stat} must be included. The static pressure at each point of the turbine results from the density, the gravitational constant and the height difference of the respective point to the tailwater surface.

The following applies for the pressure:

$$P_{abs} = P_{CFD} + P_{atm} + P_{stat}$$

$$P_{stat} = \rho \cdot g \cdot (Z_{maxOutlet} - Z)$$

Turbulent Kinetic Energy

The turbulent kinetic energy is automatically part of the result file of Ansys CFX. The turbulent kinetic energy is defined from Ansys CFX. Ansys calculates the turbulent kinetic energy with the turbulent intensity I_{def} set to 5%. U_s, limits the speed to 0.01 m/s by the result of 0 for the turbulent kinetic energy, if there is an initial zero velocity . U_{IG} is the estimated velocity at the beginning. U_ω, is the product of the simulation average length scale and the rotation rate. “This term is designed to produce a suitable velocity scale for rotating domains.” [10, Chapter 3.2.10.1]

The turbulent kinetic energy yields [15]:

$$TKE = \frac{3}{2}\left(I_{def}\max(U_s|U_{IG}|U_w)\right)^2$$

Shear Strain Rate

The shear strain rate is the change in deformation over time. With the strain rate tensor in each direction:

$$SSR = \sqrt{2\cdot\left(\left(\frac{\partial U_x}{\partial_x}\right)^2+\left(\frac{\partial U_y}{\partial_y}\right)^2+\left(\frac{\partial U_z}{\partial_z}\right)^2\right)+\left(\frac{\partial U_x}{\partial_y}+\frac{\partial U_y}{\partial_{yx}}\right)^2+\left(\frac{\partial U_x}{\partial_z}+\frac{\partial U_z}{\partial_x}\right)^2+\left(\frac{\partial U_y}{\partial_z}+\frac{\partial U_z}{\partial_y}\right)^2}$$

Strike

To approximate the thickness of the blade leading edge a geometrical approach is chosen. It is defined by the diameter of the smallest possible circle within the leading edge at several cylindrically arranged cuts through the runner blade. In BioPA the cuts are made parrallel throughout the blade. The runner must then be placed in a defined position. The advantage of circular cuts is the independency of the coordinate system.

The created data files of the streamlines and blade thicknesses are now combined. The location of each streamline just above the leading edge of the blade is determined and the velocity information is extracted there. The points can be seen in Figure 50. The colouring describes the speed. In this case approximately from 5 m/s (blue) up to 25 m/s (red). The velocity increases with radius, i.e. with distance from the turbine axis.

The blade thickness is based on the radial streamline position at the blade leading edge and calculated by interpolation.

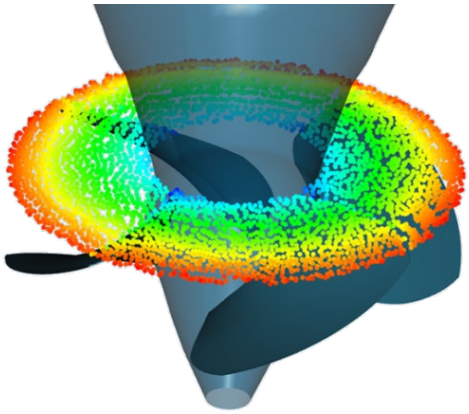

Figure 50: Intensity Distribution.

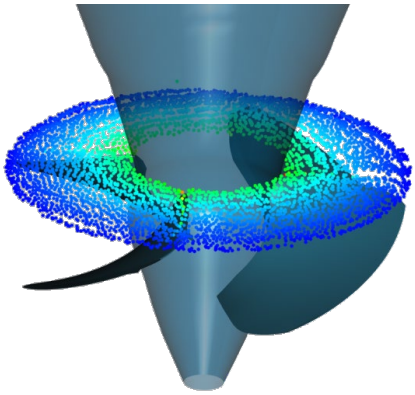

Figure 51: Strike Probability Distribution.

The probability of hitting the blade is calculated. The basis for this is the strike equation below, which is extended by a term which also includes the blade thickness. With the sum of the ratios of fish length *l*, speed *V* and the entrance edge thickness T_b, in relation to the velocity in axial direction, the number of revolutions *n* and the number of blades *N*, the probability of an impact is:

$$P_{Strike} = n \cdot \frac{N}{60} \cdot \left(\frac{l}{V} + \frac{T_b}{V_{axial}}\right)$$

The probability of strike is shown in Figure 51. It ranges from about 2% (blue) at the shroud to 15% (green) at the hub.

The ratio of leading edge thickness to the fish length and the impact velocity of the fish on the blade are important parameters for the strike evaluation. The difference of the tangential speed of the fish and the peripheral velocity of the blade gives the intensity of the impact. The velocity of the rotating blade in (tangential direction) at each diameter is calculated using:

$$v_{tangBlade} = 2 \cdot \pi \cdot r_x \cdot \frac{n}{360}$$

The tangential velocity of the flow is the scalar product of the unit vector in tangential blade direction and the flow velocity in the XY plane.

$$v_{Intensity} = abs(v_{tangBlade} - v_{tangFlow})$$

To calculate the survival probability of the strike itself, additionally to the blade thickness and the intensity, the biological data is needed. The biological data gives the mortality rate of the fish as a function of the ratio of fish length to blade thickness, which becomes valid at the critical speed shown in Figure 52.

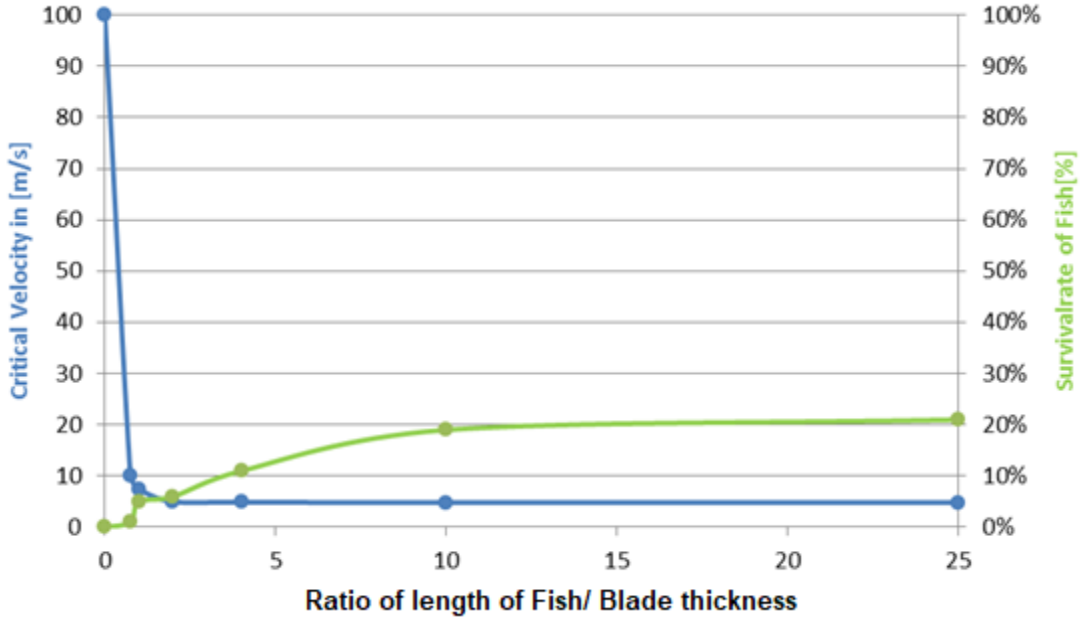

Figure 52: Blade Strike Mortality Curve for salmon [16].

The blade thicknesses and the calculated intensity as well as the ratio of fish length to blade thickness are used to derive the survival rate.

The following cases are distinguished:

1. If the speed at the blade (intensity of impact) is below the associated critical speed v_{crit}, the fish will survive:

$$P_{Survival} = 1 \quad \text{for } v_{Intensity} \leq v_{crit}$$

2. If the speed on the blade (intensity of the impact) is above the associated critical speed v_{crit}, the survival rate is calculated with:

$$P_{Survival} = 1 + m_r * \left(v_{Intensity} - v_{crit}\right) \quad \text{for } v_{Intensity} \geq v_{crit}$$

A passage through a gap region, will be scored with 0% survival.

3.3.3 Results

In the following results of the analysis of the Bannwil test case are presented. Further information on the work can be found in [17] and [19]. All presented results are based on the dose-response data for salmon, which is available from literature. All stressors are rated equally for now. The influence of entering location, fish size, acclimation depth, fish orientation and the impact of different operating points are investigated

Influence of entering location

The influence on the survival probability of the fish based on the entering location was investigated by looking at three passage locations as illustrated in Figure 53. The locations are chosen reflecting the same area at hub, middle and shroud and used to analyze the influence of different operating conditions on the main stressors.

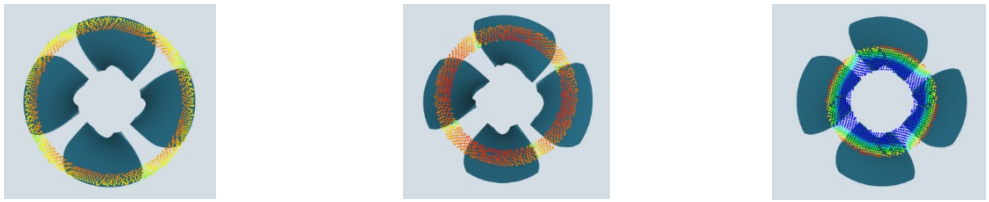

Figure 53: Variation of passage location colored by strike survival ratio from low (blue) to high (red).

The results presented in Figure 54 show representative operating points at similar head and different discharge for the Bannwil power plant. For the overload operating point t02, the pressure stressor has a dominant influence, due to high flow rates and therefore lower pressures, especially in the gap regions at hub and shroud. For the operation close to the optimum t12, better overall flow conditions are present in the turbine, which decreases the negative impact of pressure. Strike is becoming more relevant and shows lower survival ratios in the middle region and at the shroud region. This is due to the higher impact velocities at the outer sections. The results show, that the passage location has a significant influence on survival and that a passage in the middle is favorable regarding pressure and

shear influences and a passage close to the hub is favorable especially regarding strike, due to low impact velocities.

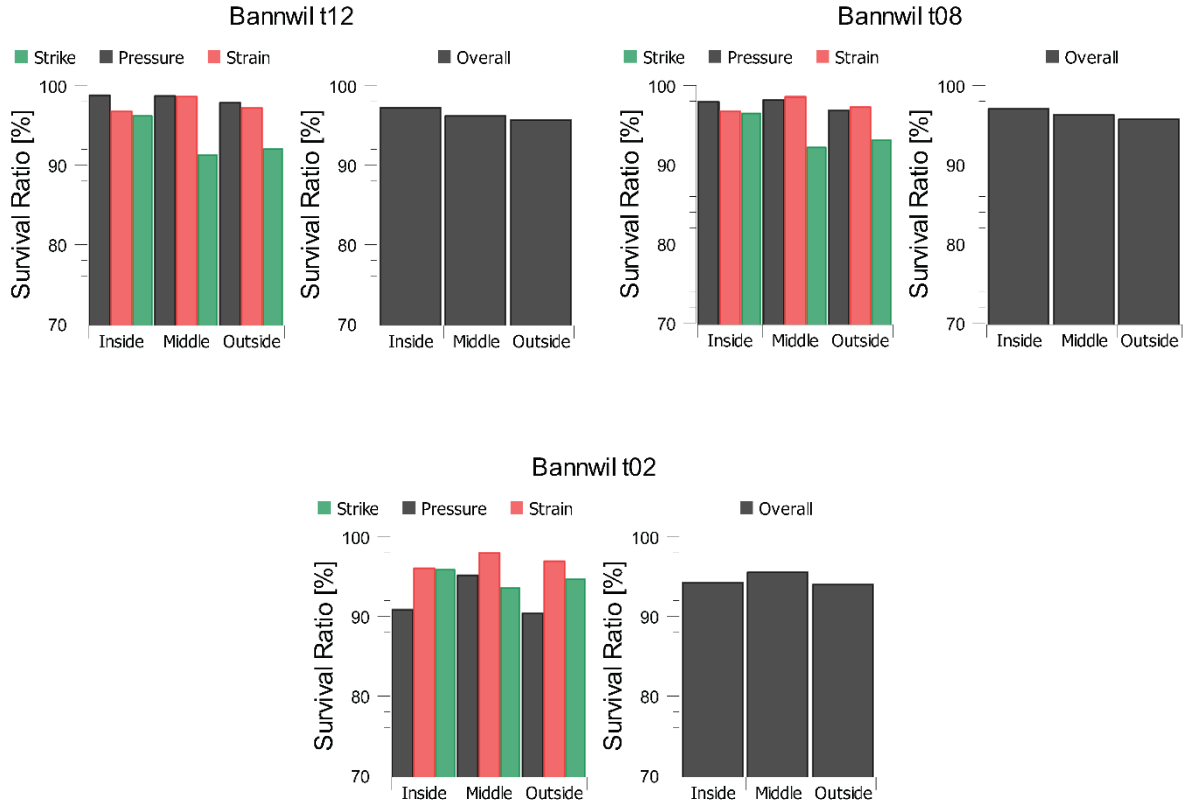

Figure 54: Bannwil HPP - Variation of passage location [18].

Fish length

For the evaluation of the strike the fish length is set to a standard value of 10 cm. This corresponds to a young migrating salmon. The consideration of the survival probability for larger fish at the example of operating point t02 is presented in the following.

The formula for calculating the probability of a fish hitting the runner blades depends on the length of the fish and on the relation of fish size to the blade thickness. An increase in mortality rate is expected with increasing fish length. Figure 55 presents the exposure probability and the strike survival ratio depending on the size of the fish. In future other relevant fish species can be investigated if biological data is available. Fish tests at the test case Obernach [19] showed that the strike modelling tends to underrate the survival rate. Experimental tests in the Oak Ridge laboratory [20] indicated that tail strikes hardly ever lead to damage to the fish. Besides the sensitivity of certain body regions also the orientation of the fish in relation to the runner is reducing the accountable length. Using 2/3 of the fish length as active length leads to a good agreement with the test results. In the results presented for the Bannwil project the full length was used for the analysis. The strike values for a 10 cm fish therefore rather reflect the effect of strike on a 15 cm fish.

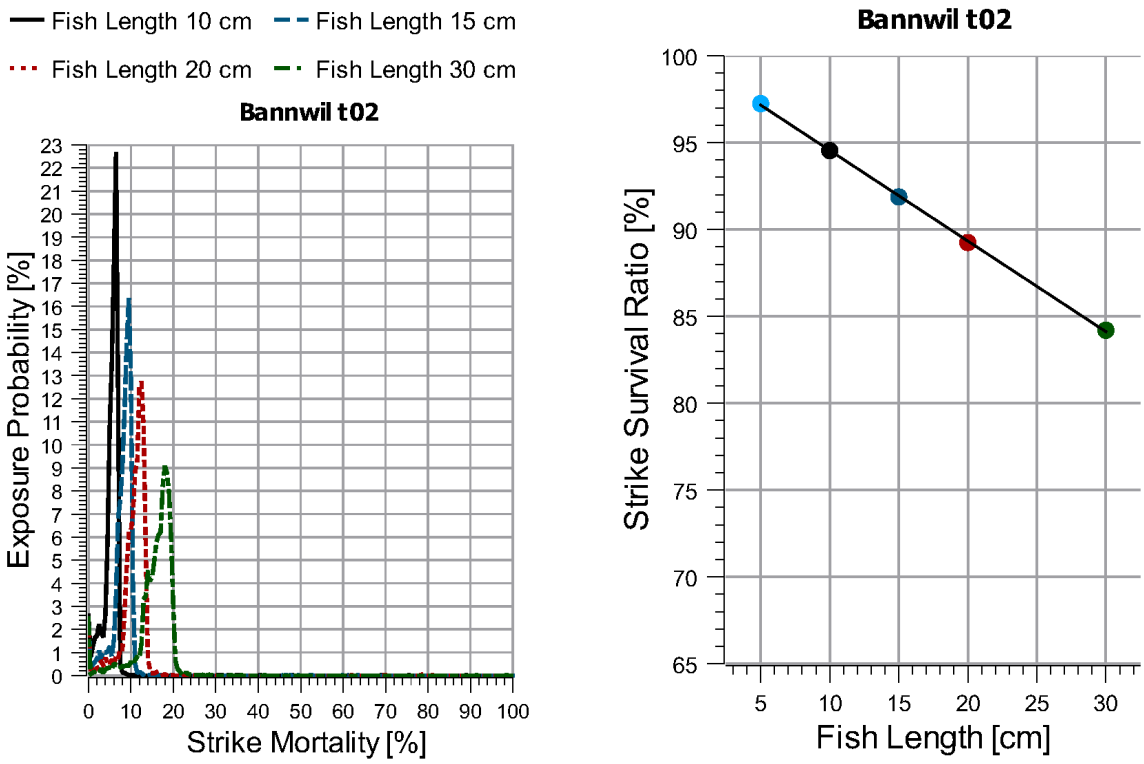

Figure 55: Sensitivity fish length.

Modelling of fish speed and orientation

The standard BioPA modelling assumes that the fish follows a streamline as non-buoyant body. As introduced in Figure 56, the impact of fish swimming velocity and positioning to the flow direction can be covered in an extended strike formula.

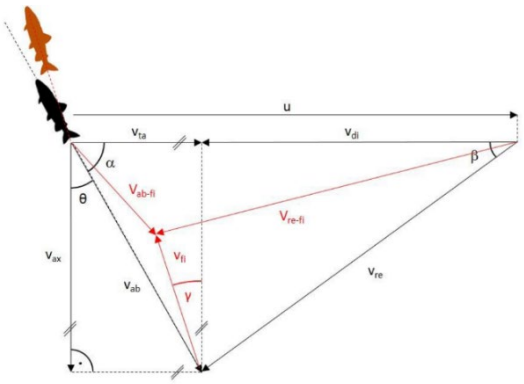

$$p = n \cdot z \left[\frac{v_{di+fi} \cdot l_{fi}}{u} \cdot \left(\frac{cos(\gamma)}{v_{ax-fi}} + \frac{sin(\gamma)}{v_{di+fi}} \right) + \frac{t}{v_{ax-fi}} \right]$$

$$v_{ax-fi} = v_{ax} - v_{fi} \cdot \cos(\gamma)$$

$$v_{di+fi} = v_{di} + v_{fi} \cdot \sin(\gamma)$$

n = rotational speed

z = number of blades
u = circumferential velocity
v = velocity
l = fish length
t = entrance edge thickness

Figure 56: Velocity triangle and strike formula including fish velocity and orientation [21].

The swim speed of a fish is time dependent, as the fish can keep a relatively high speed only for a short time. Typical flow velocities during turbine passage are rather low in the intake region and accelerates towards the guide vanes with velocities increasing rapidly above more than 2 m/s, which most fish can't swim against for a longer period of time. It's expected that most fish have only limited capabilities to control or influence turbine passage trajectories in close vicinity of the turbine. However, a change of position in the intake section is possible for most species. A principle study was performed to evaluate the influence of an active swimming fish on the strike score. The results are presented in Figure 57. The fish swimming against the main flow increases the passage time through the turbine and therefore the probability of a collision with the runner blades. At the same time the impact velocities increases slightly, so that the overall risk of a strike injury increases. In most operating conditions flow velocities are significantly higher and fish most likely won't swim for a long time against the flow. Consequently, the potential influence of swimming speed is rather low on survival rates.

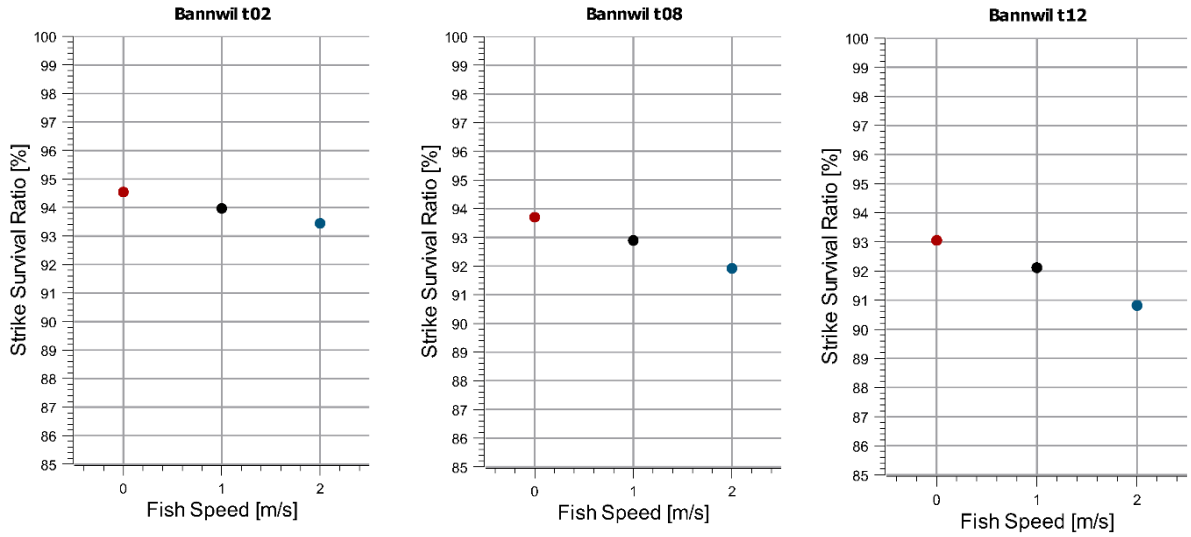

Figure 57: Influence of fish swimming speed on strike.

Another aspect is the orientation of the fish in relation to the blade. For the strike modelling based on von Raben, it is assumed that the fish is oriented with the flow. Using the extended formula in Figure 56, variations of the orientation can be taken into account. Figure 58 shows the results for full load operation t02, a medium load condition t08 and an operation close to the optimum t12.

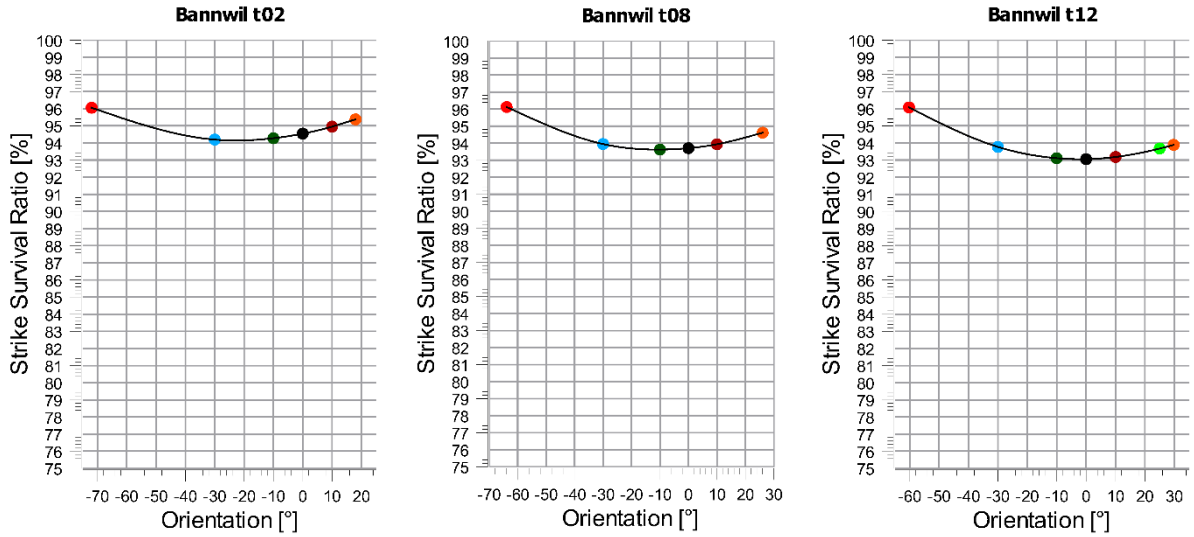

Figure 58: Influence of fish orientation on strike

The orientation is measured relative to the absolute flow direction, which is indicated with 0°. A range from a radial to an axial orientation was taken into account. The fish orientation leads to a tolerance of 1-2% in the fish passage assessment. Having the fish aligned with the flow direction, provides a conservative approach and is close to the worst case scenario.

Influence of Operating Points

The evaluation of individual load cases regarding advanced fish passage helps to identify individual damage mechanisms and to evaluate them. To rate a whole power plant, however, this consideration is not sufficient. It requires the evaluation of a complete set of operating points to create a better understanding of which parameters affect the fish passage through the turbine of an entire power plant. Therefore, the operating points were selected and each simulated with a 360°-CFD model. All evaluations are made using the CFX post-processing tool. The fish survival rate score is calculated using the BioPA Excel Sheet. The survival rate score is then converted into a "traffic light" scoring system from 1 to 10. Where 10 is the best score and corresponds to the BioPA score of 100. The scoring of 1 corresponds to 70 in BioPA .

This standardization is intended to prevent the performance scores from being confused with absolute survival rates and to give a better overview.

The results are interpolated 3-dimensionally over the head and the discharge flow to get iso-curves for a characteristic evaluation diagram. The fish passage hill-chart shows iso-lines indicating the fish passage score. The characteristic diagram reads like a typical hill-chart.

Pressure

Regarding the sensitivity related to the occurring minimum pressure, the acclimation depth of the fish entering the turbine as illustrated in Figure 59 plays an important role. A good understanding on how certain fish species acclimatize is crucial for the judgment of barotrauma. One can argue if the applicable head has a direct influence on the acclimation depth. Depending on the size of the dam and the depth of the backwater a significant influence of the acclimation depth is possible, depending on the behaviour of the fish species and the amount of time spent in deeper water levels.

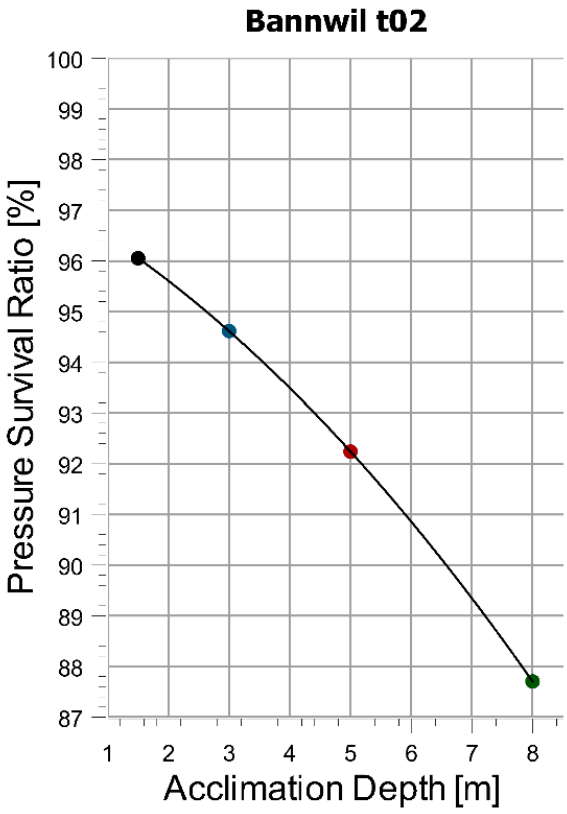

Figure 59: Sensitivity acclimation depth.

For the further analysis an acclimation depth of 5m is assumed. In Figure 60, the resulting fish passage hill-chart regarding barotrauma is presented. It turns out that the probability of survival decreases in all cases towards higher discharges. It is clear that flow conditions around the runner have a major impact on the pressure rating. Regions of low pressure occur mostly close to the runner blade. In order to determine the tail water level a constant head water level was used. Naturally at higher heads the tail water is fairly low, which leads to lower overall pressure levels in the runner and therefore a higher barotrauma risk.

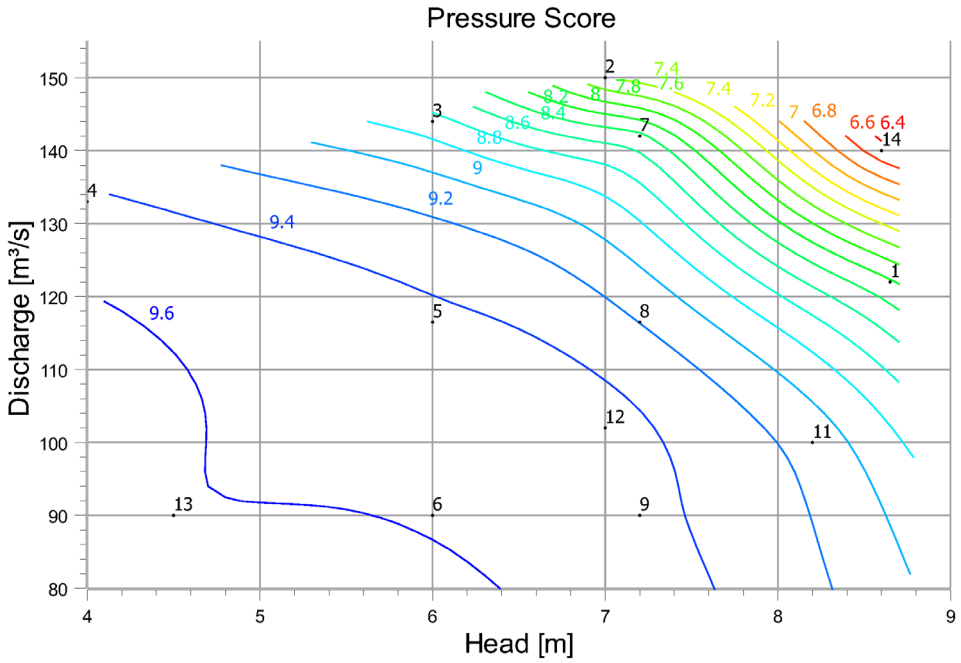

Figure 60: Fish Passage Hill Chart of Pressure.

Turbulent Kinetic Energy

In Figure 61, the fish passage score of the stressor turbulent kinetic energy is presented. In addition to the scores on the iso-lines they are coloured by the score value. It can be seen that the best score is in the optimum operation of the turbine. However, the scoring is overall very high, which shows that the influence of turbulence on the fish survival at the turbine passage is low. Secondary effects like predations caused by disorientation are not captured, as these effects are highly site dependent. Both for fish and for the turbine, a flow without vortex and flow separation is most favourable.

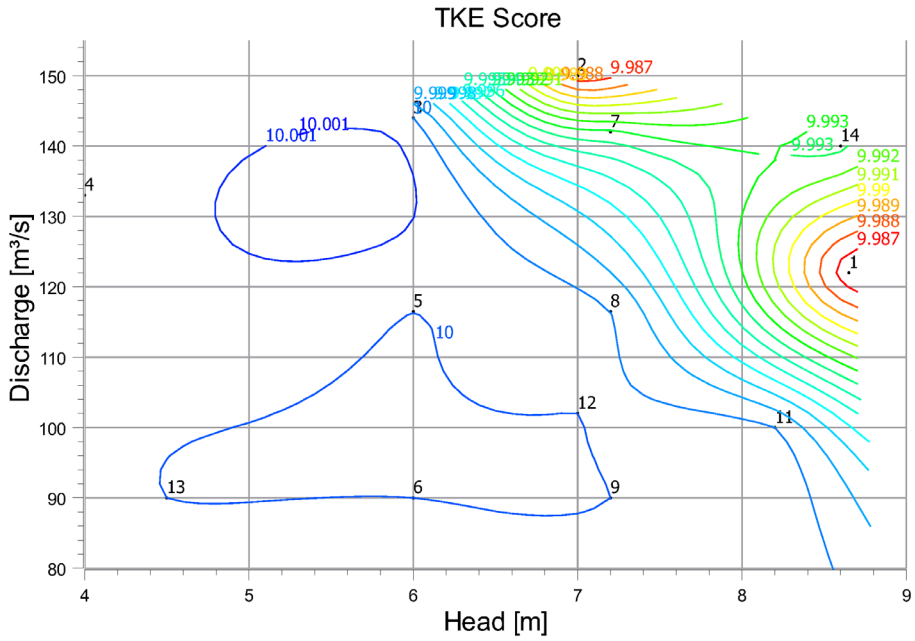

Figure 61: Fish Passage Hill Chart of TKE.

Shear Stress

The shear stress score is shown in Figure 62. Overall, the score is very high and the impact on fish therefore low. The critical points for shear are at the leading edges of the blades. The influence of the shear stressor increases, for example if the orientation of inflow angle deviates from the blade angle.

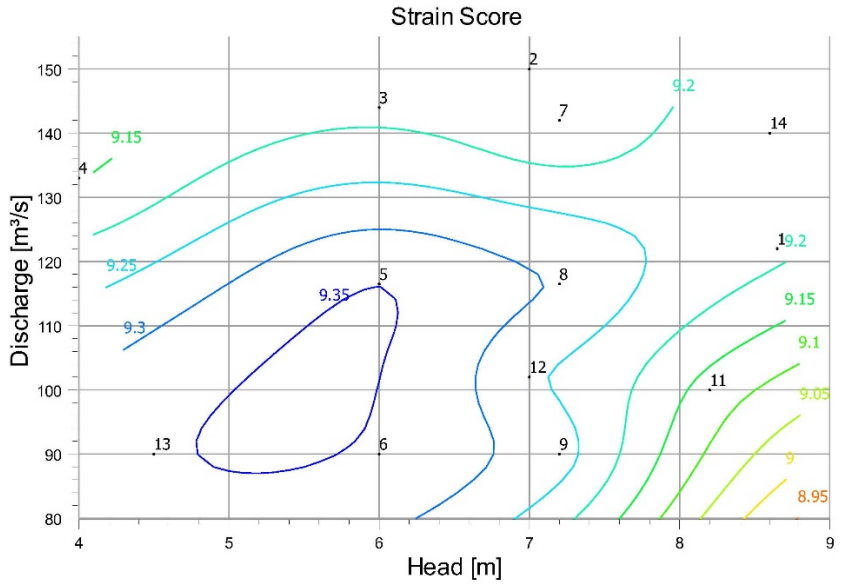

Figure 62: Fish Passage Hill Chart of Shear Stress.

Strike

The strike score is peaking at high heads and large volume flows. However, the fish passage score has a rather small range of variation. For smaller heads the lower flow velocity leads to a higher risk of a hit. For smaller blade openings the same effect is valid. Hits with the blade leading edge are recognized in this model but no secondary hits on the blade (Figure 63).

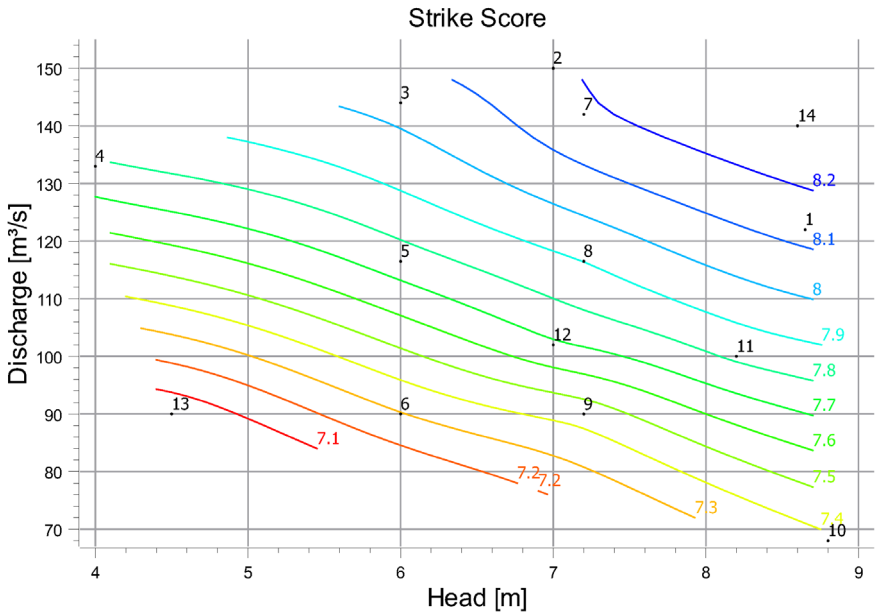

Figure 63: Fish Passage Hill Chart of Strike.

Combined Results

The Hill charts show that individual stressors behave differently. For now the results are equally averaged and shown in Figure 64. However, this doesn't account for specific influences of turbine size, rotational speed of the runner and above all the fish species. A specific weighting of the stressors seems to be necessary. For example, if pressure sensitivity plays only a minor role for a fish species, the stressor should get a smaller weighting factor.

With the operating data of the power plant and the representative operating points an "average fish passage friendliness" can be estimated.

For this consideration, the operating data of the power plant of the year 2017 is linked with the average fish passage score. The fish passage rating was calculated based on a representative operating condition based on the operating data of all 3 machines. The corresponding fish friendliness score for the power plant Bannwil is then calculated to be around 9.0 considering an acclimation depth of 5 m.

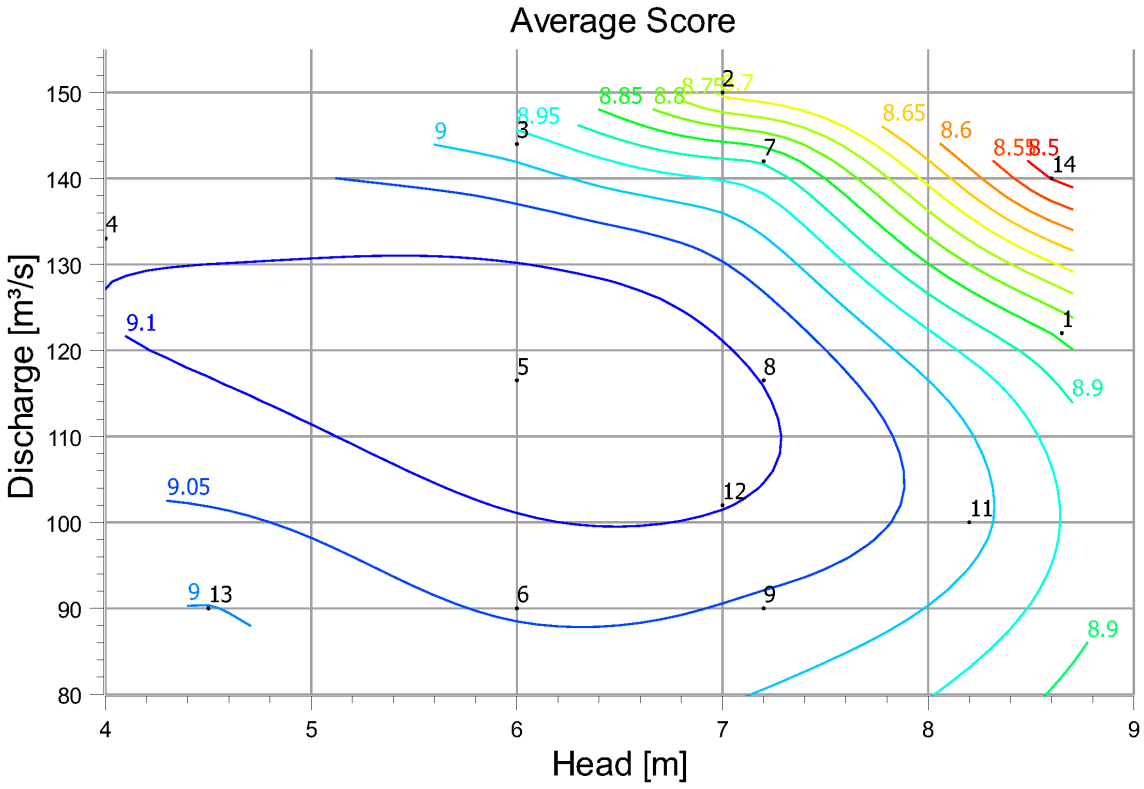

Figure 64: Combined Fish Passage Hill Chart for 5 m Acclimation Depth.

Comparison of BDS with CFD results

The results of the sensor fish test at the Bannwil site were analysed and compared to the CFD results. A detail overview can be found in FIThydro Deliverable 3.1 [19].

3.3.4 Conclusions

These results indicate the great potential of the CFD based turbine passage assessment. It is possible to include the turbine operation in the assessment and to generate improved operating schemes. The

fish passage hill charts show how the operating condition (head and discharge) have different effects for the relevant stressors. Also the influence of fish size, entering location and fish orientation was evaluated. If and how the swimming speed is a reasonable input to the fish survival modelling, requires still further investigation on fish behaviour in close vicinity of the turbine. For the pressure stressor the acclimation depth of the fish is an important variable. For the strike evaluation the definition of the effective fish length is crucial. The evaluation of the turbulent kinetic energy did not deliver meaningful results and should be neglected for future applications.

The CFD results are reliable for main operating conditions, while for extreme operating conditions transient calculations might become necessary. So far the evaluation of the results assumes that the fish follows a streamline. Additionally the evaluation is still restricted to the biological response data available in literature. To rate all species relevant in the Aare river, the dose response data needs to be generated with laboratory tests or adapted by expert assessment. The post processing on streamlines is a statistical approach, which seems most promising to obtain a representative result, with acceptable effort. Potential movement of fish during turbine passage is still an open topic and difficult to assess. The BioPA assessment is a relative approach and does not deliver absolute survival rates for now. Future investigations will focus on the weighting of the different stressors based on machine boundaries on the one hand and on the other hand on biological data depending on the fish species.

4 Reference

[1] WinRiver II, Software User's Guide. Teledyne RD Instruments 2018.

[2] Flow Science, Inc., 2016, FLOW-3D User Manual, Release 11.2.3, USA 2016.

[3] Marty, G. D., Summerfelt, R. C. (1986). Pathways and mechanisms for expulsion of surgically implanted dummy transmitters from channel catfish. Transactions of the American Fisheries Society 115:577-589.

[4] R Core Team (2020). R: A language and environment for statistical computing. R Foundation for Statistical Computing, Vienna, Austria.

[5] U.S. Geological Survey, Streamgaging, Fact Sheet 2005-3131 (2007). https://hydroacoustics.usgs.gov/.

[6] Feigenwinter, L., Vetsch, D.F., Kammerer, S., Kriewitz, C.R., Boes, R.M. (2019). Conceptual approach for positioning of fish guidance structures using CFD and expert knowledge. *Sustainability*, 11(6), 1646; https://doi.org/10.3390/su11061646.

[7] Ruggles C.P. (1980). A review of the downstream migration of Atlantic salmon. Canadian technical report of fisheries and aquatic sciences No. 952.

[8] Ruggles, C.P., Murray, D.G. (1983). A review of fish response to spillways. Canadian technical report of fisheries and aquatic sciences No. 1172.

[9] Fidler, L.E. (1988). Gas Bubble Trauma in Fish. University of British Columbia. doi: 10.14288/1.0097966.

[10] Richmond, M.C, Serkowski J.A, Ebner L. L, Sick M., Brown R. S, Carlson, T. J. (2014). Quantifying barotrauma risk to juvenile fish during hydro-turbine passage. Fish Res 154:152–164.

[11] Burt, W.H. (1943). Territoriality and home range concepts as applied to mammals. Journal of Mammalogy 24:346–352.

[12] BKW Energie AG: Power plant drawings and operational data.

[13] Richmond, C. (2014). Computational Tools to Assess Turbine Biological Performance, Hydro Review Volume 6.

[14] Jäger, S. (2018). Investigation of the fish passage through Bulb Turbines by means of flow simulation.

[15] ANSYS CFX Help, CFX-Solver Theory Guide, (2009).

[16] Crew, A.V., Keatley, B.E., Phelps, A.M. (2017). Literature review: Fish mortality risks and international regulations associated with downstream passage through hydroelectric facilities. Can. Tech. Rep. Fish. Aquat. Sci. 3207: iv + 47 p.

[17] Jäger, S. (2018). Investigation of the fish passage through Bulb Turbines by means of flow simulation.

[18] Stoltz U., Geiger F., Thutan J.A. (2020). Influence of operation modes and fish behavior on fish passage through turbines, IAHR 2020 - 30th Symposium on Hydraulic Machinery and Systems, Lausanne.

[19] Geiger F., Stoltz U. (2019). FIThydro – Guidelines for Mortality Modelling Fishfriendly Innovative Technologies for Hydropower Deliverable 3.1.

[20] Bevelhimer, M.S. (2017) An Overview of Experimental Efforts to understand the Mechanisms of Fish Injury and Mortality caused by Hydropower Turbine Blade Strike, Oak Ridge National Laboratory, 2017.

[21] Geiger F. (2018). Fish Mortality Rate during Turbine Passage – Generalized Runner Blade Strike Probability Modelling *12th International Symposium on Ecohydraulics* Tokyo Japan.